

# MONTPARNASSE

Daylight-Driven Parametric Optimization of  
High-Rise Envelopes:  
Application to the Recladding of  
Tour Montparnasse in Paris





**POLITECNICO**  
MILANO 1863

**School of Architecture, Urban Planning and Construction Engineering**

Master of Science Building and Architectural Engineering

**Daylight-Driven Parametric Optimization of High-Rise Envelopes:  
Application to the Recladding of Tour Montparnasse in Paris**

**Supervisor:**

Prof. Gabriele Masera

**Authors:**

Ozlem Akin

Ecem Irem Kilinc

# Abstract

This thesis applies performance-based design principles to reimagine the Tour Montparnasse, Paris's most disputed skyscraper since its completion in the 1970s. The tower's dark brown façade has long been criticized for clashing with the urban context, while offering poor daylight conditions, excessive glare, and technical inefficiencies. These challenges established the building as a relevant case study for exploring façade retrofitting strategies.

The research began with shoebox simulations to evaluate daylight performance across various façade arrangements, including horizontal, vertical, and angled configurations. Metrics such as Spatial Daylight Autonomy (sDA) and Annual Sunlight Exposure (ASE) guided the assessment. Results demonstrated that angled systems achieved superior daylight distribution and glare control. Building on this, the Wallacei evolutionary algorithm was employed to optimize façade angles, with the tower segmented into sections to balance precision with feasibility.

The optimization produced three façade typologies that successfully integrated environmental performance and architectural expression. From these, one design was developed further with detailed drawings and constructability studies. Integration with Schüco systems confirmed that parametric variation could be translated into modular, industrially feasible solutions.

The findings underline the potential of combining simulation-based evaluation with evolutionary optimization to retrofit high-rise buildings. Beyond improving environmental performance, the proposed design offers renewed architectural identity and enhanced social acceptance. By transforming the Montparnasse Tower into a responsive, sustainable landmark, this research demonstrates how computational workflows can bridge performance, design quality, and construction feasibility—providing a replicable framework for the sustainable renewal of urban skyscrapers.

Keywords: daylight performance, shoebox simulations, genetic algorithms, façade optimization, Tour Montparnasse, sustainable retrofitting

# Sintesi

Questa tesi applica i principi del design basato sulle prestazioni per ripensare la Tour Montparnasse, il grattacielo più discusso di Parigi sin dal suo completamento negli anni '70. La facciata marrone scuro della torre è stata a lungo criticata per il contrasto con il contesto urbano, offrendo al contempo scarse condizioni di luce naturale, eccessivo abbagliamento e inefficienze tecniche. Queste criticità hanno reso l'edificio un caso di studio rilevante per l'esplorazione di strategie di riqualificazione delle facciate.

La ricerca è iniziata con simulazioni semplificate per valutare le prestazioni luminose di diverse configurazioni di facciata, comprese quelle orizzontali, verticali e inclinate. Le metriche di riferimento, come la Spatial Daylight Autonomy (sDA) e l'Annual Sunlight Exposure (ASE), hanno guidato la valutazione. I risultati hanno dimostrato che i sistemi inclinati garantiscono la migliore distribuzione della luce diurna e il controllo dell'abbagliamento. Successivamente, è stato utilizzato l'algoritmo evolutivo Wallacei per ottimizzare gli angoli delle facciate, segmentando la torre in sezioni al fine di conciliare precisione e fattibilità.

L'ottimizzazione ha prodotto tre tipologie di facciata che integrano con successo prestazioni ambientali ed espressione architettonica. Una di queste è stata sviluppata ulteriormente attraverso disegni dettagliati e studi di costruttibilità. L'integrazione con i sistemi Schüco ha confermato che la variazione parametrica può essere tradotta in soluzioni modulari e industrialmente realizzabili.

I risultati sottolineano il potenziale della combinazione tra simulazioni prestazionali e ottimizzazione evolutiva per la riqualificazione dei grattacieli. Oltre a migliorare le prestazioni ambientali, il progetto proposto offre una nuova identità architettonica e una maggiore accettazione sociale. La trasformazione della Tour Montparnasse in un punto di riferimento sostenibile dimostra come i flussi di lavoro computazionali possano unire prestazioni, qualità architettonica e fattibilità costruttiva, fornendo un modello replicabile per il rinnovamento sostenibile degli edifici alti in contesti urbani contemporanei.

Parole chiave: prestazioni della luce diurna; simulazioni semplificate; algoritmi genetici; ottimizzazione delle facciate; torre montparnasse; riqualificazione sostenibile

# Acknowledgements

We sincerely thank Prof. Gabriele Masera for his invaluable guidance and support throughout this thesis. His expertise and constructive feedback were essential in advancing our research and enhancing the quality of this work.

We are equally grateful to our families, whose patience and encouragement sustained us, and to our friends, whose motivation and support accompanied us throughout this academic journey. Their presence was vital in overcoming challenges and bringing this study to completion.

Finally, we extend our gratitude to all who contributed directly or indirectly to this research.

*Tez sürecinde yol gösterici desteğini esirgemeyen Prof. Gabriele Masera'ya en içten teşekkürlerimizi sunarız. Onun uzmanlığı ve yapıcı geri bildirimleri, araştırmamızın gelişmesine ve çalışmamızın niteliğine önemli katkılar sağlamıştır.*

*Bu süreçte sabır ve teşvikleriyle en büyük desteği veren ailelerimize ve bizlere sürekli moral ve motivasyon sağlayan arkadaşlarımıza da derin bir teşekkür borçluyuz. Onların varlığı, karşılaşılan zorlukların aşılmasında ve bu çalışmanın tamamlanmasında belirleyici olmuştur.*

*Son olarak, bu araştırmaya doğrudan ya da dolaylı katkıda bulunan herkese şükranlarımızı sunarız.*

# Table of content

.....CHAPTER I	
<b>1.Introduction</b>	2
1.1. Aim and Scope of the Study	2
1.2. Research Methodology	2
1.3. Work Flow	2
.....CHAPTER II	
<b>2.Development of Skyscrapers</b>	6
2.1. Background of Skyscrapers Worldwide	7
2.2. The Evolution of Skyscrapers in Europe	8
2.3. The Evolution of Skyscrapers in Paris	9
2.3.1. Early Visions of High-Rise Architecture (1900–1940)	9
2.3.2. Post-War Reconstruction and the Rise of Modernist Skyscrapers (1950–1970)	9
2.3.3. La Défense: The Skyscraper District (1960–1990)	10
2.3.4. A Shift Toward Sustainability (2000–Present)	10
2.3.5. Montparnasse Tower: A Catalyst for Debate	11
2.4. Tour Montparnasse	11
2.4.1. Building Problematics	12
2.4.2. Lack of Integration with the City	12
2.4.3. Aesthetic Criticism	13
2.4.4. Asbestos Problem	13
.....CHAPTER III	
<b>3.Simulation Studies</b>	16
3.1. Modeling and Simulation Process	17
3.2. Environmental Analyses (Using Ladybug in Grasshopper)	17
3.2.1 Direct Sun Hours	17
3.2.2. Sunpath Analysis	18
3.2.3. Solar Radiation	19
3.2.4. Wind Velocity and Direction	19
3.2.5. Temperature Analysis	20
3.2.6. Shadow Analysis	21
.....CHAPTER IV	
<b>4.Case Studies</b>	24
4.1. BBVA Bancomer Operations Center	25
4.2. Manhattan Loft Gardens	26
4.3. Shenzhen Zhongzhou Holdings Financial Center	27
4.4. Modular Design: Beijing Greenland Center	28

---

## CHAPTER V

<b>5. Daylight Analysis</b>	30
5.1 Introduction	31
5.2 Daylight Metrics and Performance Indicators	32
5.3 Computational Workflow in Grasshopper	32
5.3.1 Input Parameters and Geometry Setup	33
5.3.2 Glazing and Shading Definition	33
5.3.3 Climate and Weather Data	34
5.3.4 Simulation Grids and Model Assembly	34
5.3.5 Visualization and Results	35
5.4 Shoebox Test and Facade Experiments	36
5.4.1 Base Analysis - Original Facade	36
5.4.2 Vertical Fins	37
5.4.3 Overhangs	37
5.4.4 Overhangs + Vertical Fins	38
5.4.5 Symmetric and Asymmetric vertical + Horizontal Shading Combination	38
5.4.6 Brise-Soleil System	39
5.4.7 SOM Manhattan Garden Reference	39
5.4.8 Angled Facade Modules	40
5.5 Summary of Daylight Analysis	42
5.6 Transition to Parametric Module Development	43
5.7 Grasshopper Parametric Implementation	44

---

## CHAPTER VI

<b>6. Multiobject Optimization - Wallacei</b>	46
6.1 Optimization Workflow	47
6.2 Why Wallacei was selected	49
6.3 Introduction to Wallacei	50
6.4 Transition from Shoebox to Optimize Modules	53
6.4.1 Integration with Daylight Simulation	54
6.5 Subdivision Strategy for High-Rise Optimization	55
6.6 Evolutionary Outcomes	56
6.7 Implementation of the Optimization	58
6.7.1 Defined Variables	58
6.8 Results	59
6.9 Discussion	60
Summary	61

---

## CHAPTER VII

<b>7. Facade Opteneering</b>	63
7.1. Introduction	64
7.2. Design Limitations	65

7.2.1 Glazing Height Ratio and Distance from Façade	66
7.2.1.1. Case S1-1 (South-East, 45th Floor)	66
7.2.1.2. Case S5-1 (South-East, 5th Floor)	68
7.2.1.3. Case N1-1 (North-West, 45th Floor)	69
7.2.1.4. Case N5-1 (North-West, 5th Floor)	70
7.2.2. Spacing Between the Modules	72
7.3. S1-1 (South-East, 45th Floor)	73
7.3.1.Regular Façade	74
7.3.1.1 F01 Scenario: Baseline from Optimization	74
7.3.1.2 F02 Scenario:Distance between Modules and F02 Generations	74
7.3.1.3 Façade Development	76
7.3.2. Random Façade	77
7.3.2.1 F03 Scenario: Randomization	77
7.3.2.2 Façade Development	79
7.3.3.Wave Façade	80
7.3.3.1 F04 Scenario : Variable Glazing Height	80
7.3.3.2 F05 Scenario: Flexible Range and F05 Generations	81
7.3.3.3 Façade Development	82
7.4. S5-1 (South-West, 5th Floor)	83
7.4.1.Regular Façade	83
7.4.1.1.F01 Scenario: Baseline from Optimization	83
7.4.1.2 F02 Scenario:Distance between Modules and F02 Generations	84
7.4.1.3 Facade Development	86
7.4.2. Random Façade	87
7.4.2.1 F03 Scenario: Randomization	87
7.4.2.2 Façade Development	88
7.4.3.Wave Façade	88
7.4.3.1 F04 Scenario : Variable Glazing Height	88
7.4.3.2 F05 Scenario: Flexible Range and F05 Generations	89
7.4.3.3 Façade Development	90
7.5. N1-1 (North-East, 45th Floor)& N5-1 (North-East 5th Floor)	91
7.5.1.Regular Façade	92
7.5.1.1.F01 Scenario: Baseline from Optimization	92
7.5.1.2 F02 Scenario:Distance between Modules and F02 Generations	93
7.5.1.3 Façade Development	96
7.5.2. Random Façade	97
7.5.2.1 F03 Scenario: Randomization	97
7.3.2.2 Façade Development	97
7.5.3.Wave Façade	98
7.5.3.1 F04 Scenario : Variable Glazing Height	98
7.5.3.2 F05 Scenario: Flexible Range and F05 Generations	99
7.5.3.3 Façade Development	100
7.6. Comparative Evaluation	101

7.6.1. Structural Integration	101
7.6.2. Facade Typologies	105
7.7. Selection of Wave Façade Typology	106

.....**CHAPTER VIII**

<b>8. System Integration for Tour Montparnasse Façade Retrofit</b>	108
8.1 Introduction	109
8.2 Office Floor Plan Integration	109
8.3. Schüco Parametric System Overview	110
8.4. Adaptation to tour Montparnasse	112
8.5. Conclusion	115

.....**CHAPTER IX**

<b>9. Conclusions and Recommendations</b>	117
9.1. General Discussion	118
9.2. Advantages and Limitations	118
9.3. Future Development	119
9.4. Final Remark	119

.....**CHAPTER X**

<b>10. References and List of Figures</b>	120
References	121
List of Figures	123

# ***CHAPTER I***

Introduction

## **1. Introduction**

### **1.1 Aim and Scope of the Study**

The main objective of this research examines how performance-oriented parametric design techniques enable the transformation of an outdated high-rise exterior into an adaptable sustainable architectural framework. The Montparnasse Tower in Paris became the research focus because it needs improvement in both operational performance and visual appeal. The tower received criticism after its construction because its dark brown glazing creates uncomfortable daylight conditions while making the building unpopular with the public. The research aims to create a new façade design which will enhance environmental performance while solving problems related to visual comfort and architectural identity and contextual integration.

### **1.2 Research Methodology**

The research methodology in this thesis combines computational simulation with evolutionary optimization techniques. The research started with shoebox models to evaluate different façade arrangements and shading systems. Angled module is selected as their most effective solution which led to further development based on the Schüco Parametric Façade system with its hybrid opaque-transparent module arrangement. The research team performed daylight simulations through Grasshopper using Honeybee while Wallacei executed multi-objective genetic algorithms for optimization. The evaluation of performance relied on LEED standard-compliant Spatial Daylight Autonomy (sDA) and Annual Sunlight Exposure (ASE) daylight metrics.

### **1.3 Workflow**

The research and design process of this thesis followed a sequential workflow which started with background research and ended with the optimized façade design. The research started by studying skyscraper history and Montparnasse Tower development while analyzing its changing public perception since its construction. The research phase enabled researchers to recognize essential architectural problems together with environmental issues and functional requirements.

The research moved forward to create design objectives and investigate new façade solutions based on previous research findings. The Schüco Parametric Façade and other precedents and technological references guided the development of an adaptive system which combined environmental performance with architectural design goals.

At this stage, case studies were conducted through shoebox simulations to expand case studies by testing various façade designs under various daylighting scenarios. . The experiments demonstrated that angled modules delivered the best results which led to further development through the combination of transparent and opaque elements for achieving solar protection and visual comfort. Once the effectiveness of the angled form was established, the Schüco Parametric Façade was adopted as a reference framework to ground the proposed system within an industrially feasible context.

Wallacei's evolutionary algorithm served as the last stage of the process to optimize the façade design. The tower received façade group division to handle orientation-based requirements while maintaining workable computational processing. The optimization process generated various design alternatives which researchers transformed into three typologies named Regular, Random and Wave to evaluate their performance and architectural quality. The optimized façade system achieved sustainability goals and construction feasibility and architectural identity integration to create a responsive landmark that unites with its Parisian context.

The investigation began with shoebox simulations that tested the daylight performance of façade modules. To capture different boundary conditions, representative cases were taken from several orientations and vertical zones of the tower. Wallacei results were then narrowed by applying design limits on distance from façade, window height ratio, and module spacing. From these filtered options three typologies emerged—Regular, Random, and Wave which were first studied at the shoebox scale and later applied to entire façade sections. This step made it possible to compare local daylight effects with larger architectural outcomes, while keeping the results consistent with design feasibility.

In the following stage, the focus shifted to the system integration of these strategies for the retrofit of Tour Montparnasse. The analysis looked at how daylight quality influences the placement of functions across the floorplate, leading to a spatial hierarchy aligned with international standards. At the same time, the Schüco Parametric System was examined as a precedent that demonstrates modular design, digital workflows, and prefabricated construction. Its logic was adapted to the tower through anchoring details at slab edges, layered assemblies around columns, and the addition of a secondary glazing line on the interior. These adjustments improved acoustic comfort and maintenance access while ensuring technical compatibility. To avoid excessive cantilevering, the façade units were restricted to a maximum projection of 0.65 m, which preserved usable interior space and kept structural stresses within acceptable limits. Taken together, these steps resulted in a retrofit strategy that connects environmental performance with architectural quality and practical buildability.

**Research & Design  
Methodology**

**Research Framework**

- *Project Scope*  
*Retrofitting (Tour Montparnasse)*
- *Building Typology*  
*High-rise, office tower*

**Case Studies**

- *Facade Precedents*  
*Retrofitting (Tour Montparnasse)*
- *Material Systems*  
*High-rise, office tower*
- *Sustainable Strategies*  
*Daylight control, thermal comfort*

- *Direct Sunhours*
- *Sunpath*
- *Solar Radiation Studies*
- *Shadow*

**Environmental Analysis**

- *Façade*  
*Angled modules*  
*Parametric*
- *Parametric*  
*Distance*  
*height ratio*

**Computational**

### **Performance Analysis**

- **Daylight Simulation**  
Honeybee (sDA, ASE evaluation)  
Scenario Testing (ASE 10%/15%/20%)
- **Multi-object Optimization**  
Wallacei evolutionary runs
- **Performance Indicators**  
LEED daylighting thresholds  
Comfort + constructability limits

### **Final Design Iterations**

- Integration of results & comparisons
- Merging performance with design
- Final retrofit façade proposal

### **Initial Geometry Definition**

opaque-transparent

script in Grasshopper

### **Parameterization**

from facade, window  
ratio, tilt angle

### **Generational Design**

- **Design Limitations**  
Visual Comfort, Maintenance construction, architectural design
- **Module Generation**  
S1-1, S5-1, N1-1, N5-1
- **Façade Generation**  
Regular, Random, Wave
- **Comparison**

### **Façade Opteneering**

# ***CHAPTER II***

## Development of Skyscrapers

## 2.1. Background of Skyscrapers

The development of skyscrapers has occurred through continuous advancements in structural and mechanical systems and technological and economic progress. The high-rise building design emerged during the late 19th century in New York and Chicago because of expanding office requirements. The initial high-rise buildings depended on heavy masonry walls for structural support which needed powerful foundation systems. The development of steam-powered drilling machines during the 1830s made it possible to construct these deep foundations.

Architects created iron and steel frame structures to meet expanding requirements for rentable space and natural illumination which enabled them to construct buildings with thinner walls and larger windows. The Home Insurance Building in Chicago from 1885 stands as the world's initial skyscraper because its steel frame structure enabled builders to construct taller buildings with reduced material weight. The Monadnock Building from 1891 in Chicago (Figure 2.2) represented the final example of load-bearing masonry construction before steel framing became the standard for high-rise buildings. The availability of mass-produced steel through Henry Bessemer's 1856 invention enabled the transition to steel construction at affordable costs. The combination of elevator technology with improved fire safety and ventilation systems enabled the construction of taller buildings. The Chrysler Building (1930) and Empire State Building (1931) (Figure 2.3) became two of the most famous skyscrapers when they surpassed 300 meters in height.

The International Style emerged after World War II because European architects who studied at the Bauhaus school brought their design principles to the United States. The architectural style of Mies van der Rohe's Lake Shore Drive apartments (1951) and the Seagram Building (1958) showcased the International Style through their use of functional design and minimalistic clean lines. The 1960s brought about advanced structural systems including diagrids and mega frames and high-strength concrete tubes which allowed architects to create flexible and innovative building designs.



Figure 2.1.1 - Home Insurance Building, Chicago, Postcard, 1912



Figure 2.1.2 - Monadnock Building, Chicago, Postcard, 1912.



Figure 2.1.3 - Empire State Building, NY by Boyah Georgiev Creative, 2023

Building technology advancements during recent times have led to the development of high-performance façades with natural ventilation systems and responsive skins which enhance both energy efficiency and adaptability of skyscrapers. The current generation of skyscrapers uses smart materials and automated systems and advanced construction materials to achieve new heights in design and operational performance.

## 2.2. The Evolution Of Skyscrapers In Europe

European cities made them hesitant to construct tall buildings which American cities had already adopted as progress indicators. European skyscraper development followed a different path than what occurred in the United States. The historic urban structures of cities started constructing buildings above 100 meters only during the 1950s because they needed to update their cities and provide more office and residential areas after World War II.

Paris and Frankfurt and London have become major skyscraper development hubs for office buildings in Europe. The majority of high-rise buildings constructed during the 20th century consisted of office towers which reached maximum heights below 150 meters. The 21st century brought about a substantial growth of residential and mixed-use skyscrapers which now span between 150-250 meters in height.

European construction of supertall buildings has started but their height remains lower than other global regions since only a few reach beyond 250 meters. European skyscrapers maintain their unique character through their ability to blend with historic urban settings even though they reach limited heights. The general view of Frankfurt skyscrapers presented in Figure 2.4 demonstrates how modern towers exist alongside traditional architectural elements in the city. European developers now build mixed-use buildings as standard practice for their tall structures because these designs meet the requirements of densely populated cities for adaptable multi-purpose areas.

The CityLife development in Milan showcases European skyscraper design trends through its eco-friendly towers created by Zaha Hadid and other architects. European



Figure 2.2: Frankfurt cityscape showing integration of modern skyscrapers with historic urban fabric (Igor Flak, 2019).

tower designs incorporate double-skin systems as façade technology to achieve daylight control and energy efficiency while reducing environmental effects.

European skyscraper development occurred through a slow process of tall building acceptance because of the dense urban environment and extensive architectural history of the continent. The current development path of skyscrapers in Europe centers on sustainable design and functional buildings with performance-based architecture. European skyscrapers achieve their unique status through their combination of modern technology with cultural understanding which creates valuable examples for upcoming high-rise retrofit projects and sustainable urban development initiatives.

## 2.3. The Evolution Of Skyscrapers In Paris

### 2.3.1. Early Visions of High-Rise Architecture (1900–1940)

The development of skyscrapers in Paris started during the first years of the twentieth century. In 1903, Auguste Perret introduced modern reinforced concrete to Paris with the Rue Franklin building. This project laid the groundwork for high-rise design in the city by blending engineering progress with architectural elegance.. Perret presented his concept of a skyscraper ring around the city in 1905. The design aimed to create a new skyline for Paris through its integration with the existing horizontal urban design while creating public and commercial areas at street level. The American skyscraper model focused on vertical dominance but Perret designed his structures to respect Parisian architectural heritage (see Figure 2.3.1).

### 2.3.2. Post-War Reconstruction and the Rise of Modernist Skyscrapers (1950–1970)

The post-war reconstruction period brought fast urban development to Paris which led to the construction of its first major skyscrapers during the 1950s and 1960s. The expanding economy and increasing population of Paris required more compact urban development which made high-rise buildings an essential solu-

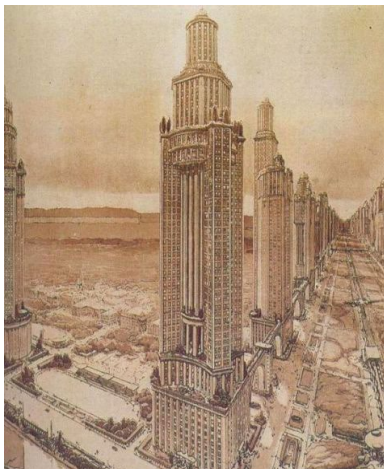


Figure 2.3.1 - L'Avenue des Maisons-Tours. Auguste Perret. Perspectiva de Jacques Lambert, L'illustration, 12 de agosto de 1922. Bibliothèque Forney, Paris (Abram,1994, p. 321)



Figure 2.3.2 - Quecq d'Henripret, Jacques. "Tour Montparnasse, Paris (15th arrondissement), general view." 1980. Mémoire. Ministry of Culture.



Figure 2.3.3 - Panorama of La Défense, seen from the Henri IV Pavilion in Saint-Germain-en-Laye (photo: R. Brunet, July 2010)

tion. The Montparnasse Tower became a notable construction of this time when it finished its construction in 1973. The building reached a height of 210 meters which made it the tallest structure in Paris during that time. The Montparnasse Tower received negative feedback because its modernist design created an unflattering impact on the traditional Parisian skyline. The negative public reaction toward skyscrapers led to new urban planning rules which restricted high-rise buildings in central Paris while creating special zones for tall buildings. (see Figure 2.3.2).

### 2.3.3. La Défense: The Skyscraper District (1960–1990)

La Défense established itself as Paris's business center which enabled the city to develop contemporary high-rise buildings while safeguarding its traditional central area. The CNIT building started the development of La Défense in 1958 before the construction of multiple office buildings and cultural facilities and shopping centers. The Grande Arche (1989) and Tour First (1974) represent the key architectural developments of Parisian modernization during this time. The vertical development plan at La Défense demonstrated how skyscrapers could be concentrated in particular areas to solve urban density problems while protecting Parisian cultural values and architectural beauty. (see Figure 2.3.3).

### 2.3.4. A Shift Toward Sustainability (2000–Present)

The early 21st century brought back skyscraper development in Paris through technological progress and environmental sustainability initiatives. The city expanded its vertical growth through new developments which occurred in Boulogne-Billancourt and Issy-les-Moulineaux and Saint-Denis. Modern skyscrapers in Paris now demonstrates a dedicated approach to designing buildings that follow ecological and bioclimatic principles.

The Duo Towers (Figure 2.3.4) demonstrate how environmental responsibility can



Figure 2.3.4. - Halbe, Roland. Photograph of Tours Duo



Figure 2.3.5.1- Henry, Steven. Photograph of Tour Montparnasse. Skyscraper Center



Figure 2.3.5.2 - Montparnasse Tower from the Tossan slab

be integrated into high-rise construction through their sustainable design features. The towers use state-of-the-art energy recovery systems and photovoltaic panels and green terraces to establish a sustainable urban design pattern. The Hekla Tower at La Défense showcases Jean Nouvel's design through its combination of advanced shading systems and renewable power generation and its focus on maintaining excellent indoor environmental conditions.

### **2.3.5. Montparnasse Tower: A Catalyst for Debate**

The Montparnasse Tower (Figures 2.3.5.1 and 2.3.5.2) remains a significant architectural landmark in Paris although people have consistently shown disapproval toward it. The modernist design of the building triggered widespread public dialogue about skyscrapers' compatibility with Paris's established architectural heritage. The building undergoes current renovation work which focuses on improving energy performance and visual integration because modern urban architecture places these elements at the forefront.

## **2.4. Tour Montparnasse**

The Montparnasse Tower stands in the 15th arrondissement of Paris. The building reaches 210 meters to become one of the tallest office buildings in Paris. The building contains 59 floors which serve as office space for its main purpose. The Montparnasse Tower construction spanned ten years from 1969 to 1973 through multiple design revisions.

The Tower is part of a specific moment in French urban and economic history and is part of a larger operation to redevelop Montparnasse station which, in the 1950s, saw its traffic increase tenfold. The construction took place at the site of an abandoned train station which is located near the Montparnasse train station. The building received strong criticism after its 1970s completion because its design clashed with the traditional Parisian skyline. The city of Paris established a height restriction in 1977 which prohibited buildings above 32 meters (12 stories) to protect architectural unity and reduce public opposition stemming from the unpopular Tour Montparnasse skyscraper which reached 210 meters. The height restriction operated from 1977 until 2010 when Paris modified the rules to permit buildings up to 180 meters for offices and 50 meters for residential use.

The Tour Maine Montparnasse Real Estate Complex (EITMM) contains the high-rise Tower and the sports center and shopping center and CIT Tower and Building D which functions as an office building. The complex has parking facilities located underground. The total floor space of this complex reaches 187,000 m<sup>2</sup>.

The Montparnasse Tower presents a basic rectangular prism design with a simple functional exterior design. The building design includes efficient floor arrangements which create adaptable office spaces that fulfill different business requirements. The Tower functions as a major office center which houses 450 businesses across 52 floors within

90,000 m<sup>2</sup> of space. The Tower functions as a major office building but it also operates as a tourist and recreational center. The building features a separate gourmet restaurant and bar and event space which operate independently from the office areas to preserve work and leisure zones. The building extends across six underground levels and reaches a total floor area of 120,000 m<sup>2</sup>. The building's vertical movement depends on 25 passenger elevators and three freight elevators.

### 2.4.1. Building Problematics

The Montparnasse Tower represents the conflict between contemporary urban development and the traditional character of Paris. The structure failed to meet its purpose as a modern symbol because it faces multiple problems with its design and environmental and health.

### 2.4.2. Lack of Integration with the City

The Montparnasse Tower faces ongoing criticism because it fails to match the architectural style of Parisian urban development. The tower stands as an independent structure which creates an urban island effect because its massive size does not match the surrounding Haussmannian buildings.



Figure 2.4.2 :The Montparnasse Tower (left) with the Panthéon in the foreground. The image illustrates how the tower disrupts the historic Parisian skyline, overshadowing iconic landmarks. Photograph by Etienne Laurent / Getty.

The tower creates a sense of separation from Paris because it stands out in the skyline while blocking views of famous landmarks including the Eiffel Tower and Les Invalides. The tower's large size creates a visual obstruction that disrupts the historic city view as shown in Figure 2.4.1.2 which shows the Panthéon in the foreground. The tower stands

out as “un-Parisian” and “anti-Parisian” according to Colin Marshall in his 2023 article A Defense of the Ugliest Building in Paris because it creates a dark foreign atmosphere within its 19th-century setting. The tower has created a widespread belief that it breaks both the architectural sequence and the symbolic essence of Paris.

### **2.4.3. Aesthetic Criticism**

The Montparnasse Tower generates urban controversy because of its unappealing design which clashes with Parisian architectural traditions. The building’s “nicotine-colored” exterior and functional slab design create an aesthetic conflict with Paris’ traditional classical appearance. The design of the building follows economic efficiency principles which critics believe represents modernization that damages cultural and aesthetic heritage. The tower received criticism because it resembled an American skyscraper according to Saul Bellow who stated it looked like a Chicago building that ended up on a Parisian street corner.

The architectural community has presented multiple complex views about the building. Architect Michel Holley and Claude Parent identified specific design elements which set the tower apart from typical American glass-box skyscrapers through its oval shape and its side indentations.

### **2.4.4. Asbestos Problem**

The Montparnasse Tower revealed its asbestos contamination in 2005 because this toxic substance leads to dangerous health problems including cancer. The maintenance and repair operations at the building produced dangerous asbestos dust which exceeded legal safety limits by 20 times. The discovery of asbestos contamination led to major health problems and legal issues which forced some businesses to leave their offices. The asbestos removal process started in 2009 after a three-year delay during which the building operated normally. The asbestos removal process at the building reached 90% completion by 2012. The ongoing health risks at the tower maintain its negative reputation because they demonstrate dangerous conditions and create a negative public perception of the structure.



# Why Tour Montparnasse must be reimagined in 2025?

*Tour Montparnasse, a symbol of its time, now faces challenges that have rendered it outdated and disconnected from contemporary needs. The need for renovation stems from its inability to align with the expectations of functionality, aesthetics, and sustainability in today's world.*



## Existing Challenges



### **Poor Daylight Performance**

*Insufficient daylight penetration and excessive glare due to the building's dark brown façade and lack of adaptive shading strategies, resulting in uncomfortable interior environments.*



### **Outdated Aesthetic**

*The façade is dark, monolithic, and has long been criticized for its incompatibility with the Parisian skyline.*



### **Limited Functionality**

*Interior spaces are rigid and fail to meet the needs of modern urban dwellers, particularly in terms of flexibility and visual comfort.*



### **Lost of Identitiy**

*Once a vibrant center for artists, the area has become lifeless and disconnected from its creative roots.*



# Design Parameters



## **Environmental Factors:**

*Shading & Glazing Systems: Shoebox simulations demonstrated that optimized façade systems ensure optimal daylight performance, reduce glare, and improve energy efficiency.*

*Natural Ventilation: Optimized façade openings to enhance airflow and indoor comfort.*



## **Aesthetic Approaches:**

*Refined Façade Design: A solution that improves public perception and achieves a lighter architectural expression.*

*Contextual Sensitivity: A design that softens the imposing character of the tower.*



## **Spatial Needs**

*Artistic Revival: Art studios to restore the area's creative identity and vibrancy.*



## **Materials and Technology:**

*High-Performance Façade Systems (Schüco): Adopted after shoebox case studies and genetic algorithm optimization demonstrated superior daylight results and overall comfort.*

*Sustainable Construction: Long-term durability and reduced material waste through advanced façade technology.*

# ***CHAPTER III***

## Environmental Analysis



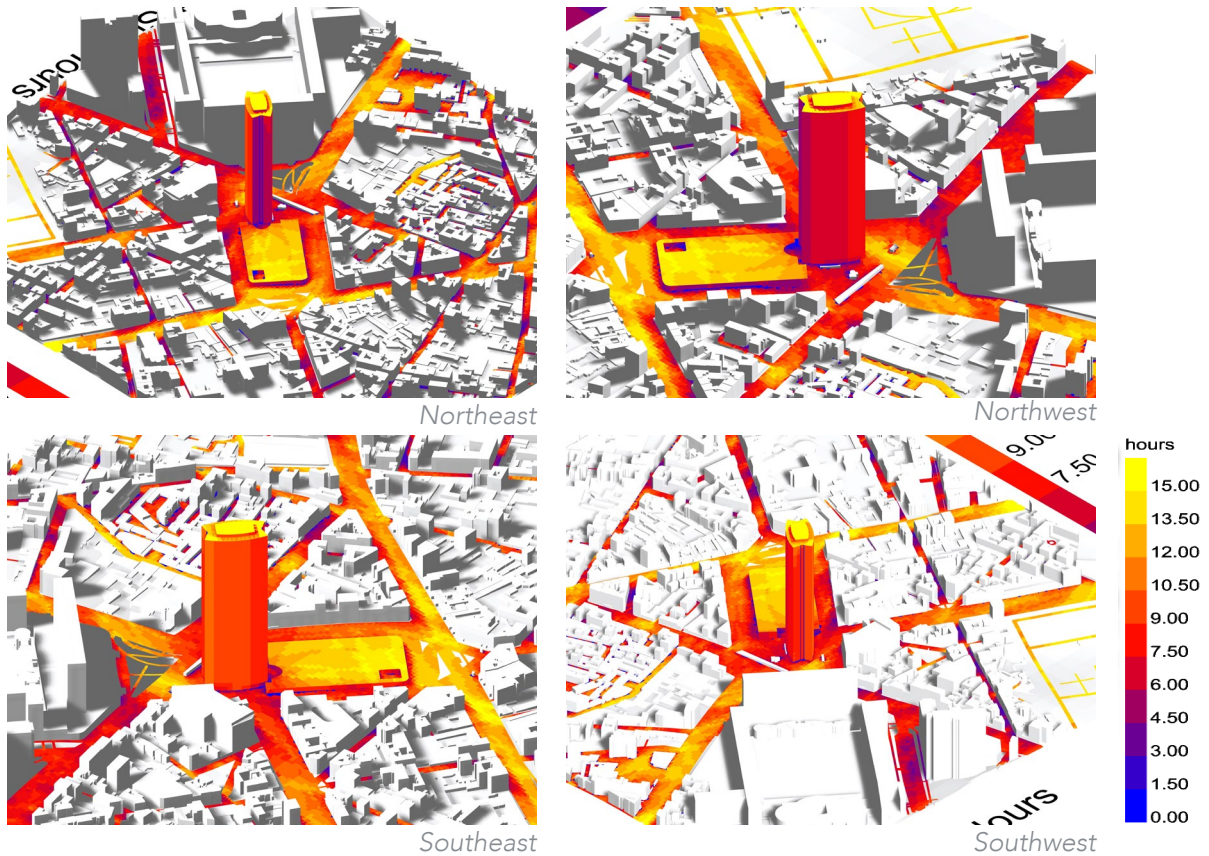


Figure 3.2.1. Direct Sun Hours analysis across different façades of Tour Montparnasse using Ladybug in Grasshopper.

The analysis revealed that the Southeast orientation of the tower faces the most severe overheating and glare problems. The subsequent design work concentrated on developing solutions for the conditions found on this specific façade.

### 3.2.2. Sunpath Analysis

The Sun Path analysis (Figure 3.2.2) examined the position and movement of the sun throughout the year, revealing clear seasonal variations in solar incidence angles.

The tower façades experience high sun angles during summer months but receive lower sun angles during winter thus allowing deeper sunlight penetration inside buildings. The Southeast orientation received the most solar radiation during summer months according to the analysis. The Northwest façade received minimal exposure to sunlight during the study period.

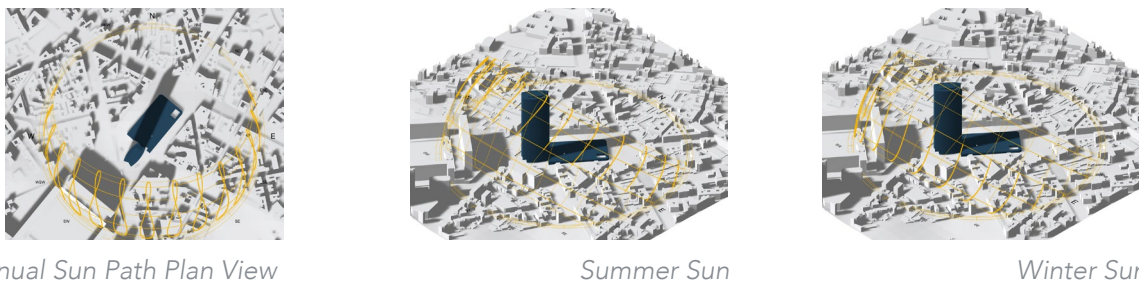


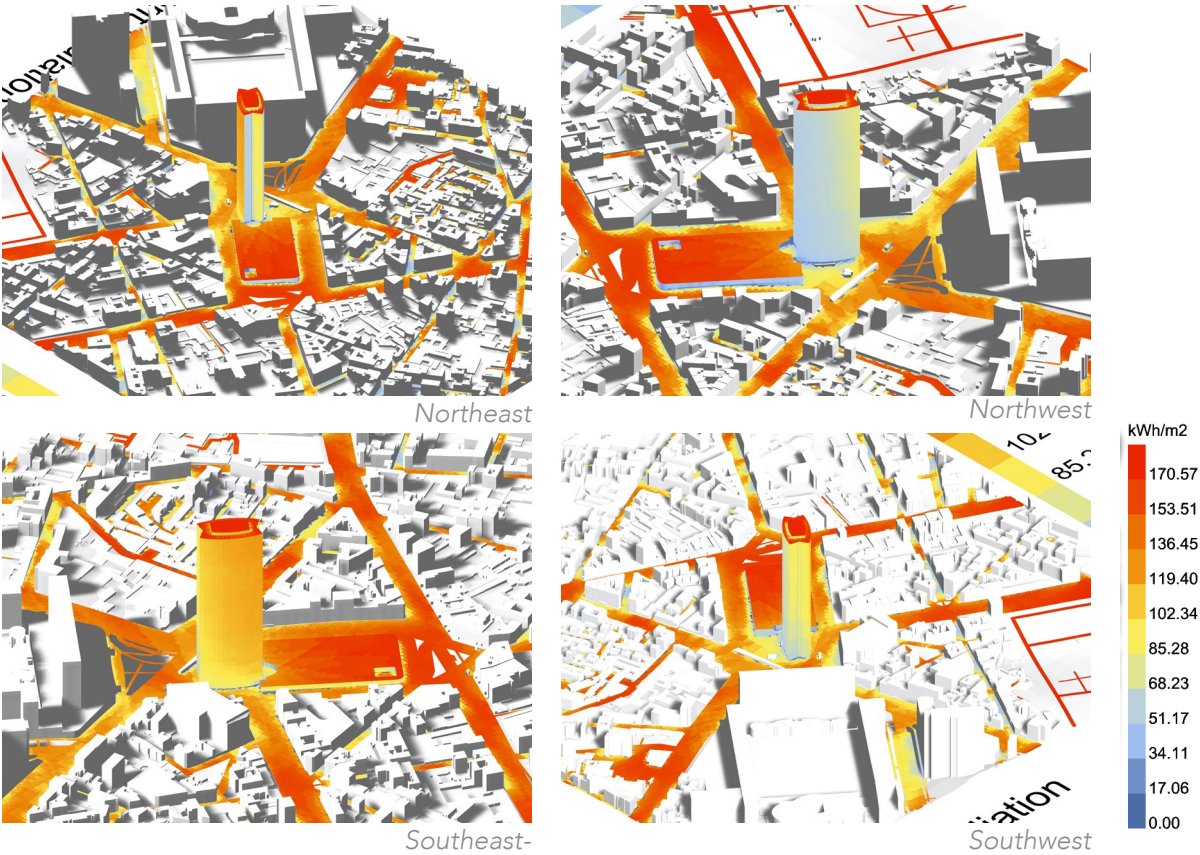
Figure 3.2.2. Sunpath diagrams for Tour Montparnasse, illustrating annual, summer, and winter sun positions.

The analysis required the Southeast façade to become the primary focus for daylight strategy testing because of its unique orientation characteristics.

The study demonstrated that using inclined façade designs presents a viable architectural solution to control both glare and heat buildup. The angled design would block direct summer sunlight while allowing wintertime low-angle rays to enter the building for better illumination.

### 3.2.3. Solar Radiation

The solar radiation analysis (Figure 3.2.3) measured the amount of solar energy that reaches the building façades of Tour Montparnasse through kWh/m<sup>2</sup> units. The Southeast façade received the most solar radiation which made it the most important orientation for analysis. The Northwest façade received significantly less solar radiation than the other sides of the building. The analysis of solar exposure between the two tower sides proved that specific façade solutions need to be developed for each orientation.



3.2.3 Solar radiation analysis of Tour Montparnasse façades, showing annual radiation distribution in kWh/m<sup>2</sup>.

### 3.2.4. Wind Velocity and Direction

The map shows how Paris experiences wind speed changes from 0 to 18 m/s during the entire year. Most of the year displays minimal wind activity through blue coloration yet winter months occasionally produce strong gusts which show up as yellow to red

shades. The research shows Paris experiences constant low wind speeds throughout twelve months without significant changes between seasons. The city experiences

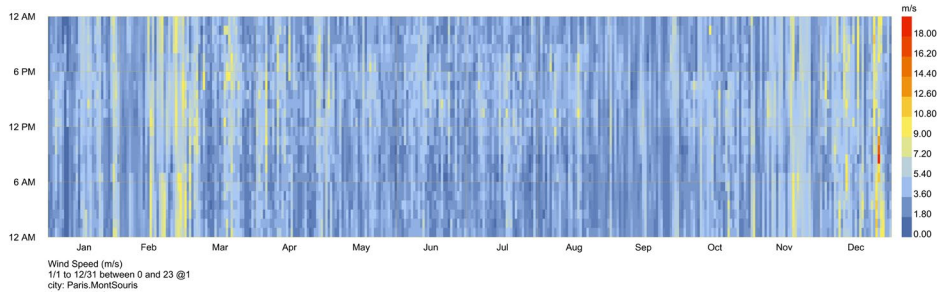


Figure 3.2.4.1 Wind speed variations in Paris throughout the year, ranging from 0 to 18 m/s.

short intervals of moderate to strong winds during winter and autumn months but low wind speeds continue to prevail during spring and summer. The information helps developers create better building energy systems and natural ventilation networks and structural protection plans. The knowledge of wind speed patterns enables designers to create outdoor spaces and pedestrian areas that provide better comfort through landscape design solutions.

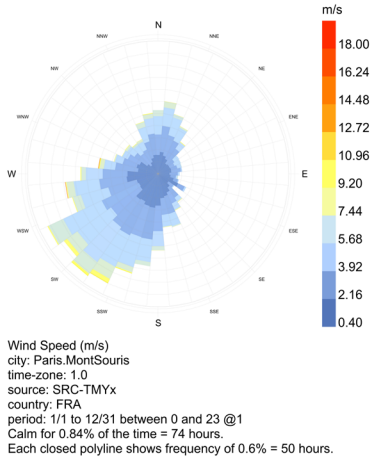


Figure 3.2.4.2 Wind rose diagram for Paris, showing wind directions, speeds, and frequencies.

The wind rose diagram shows a complete picture of wind directions and their corresponding speeds and occurrence rates in Paris. The E, ENE and ESE wind directions bring gentle breezes which occur rarely but work well for ventilation systems. The SW and SSW and WSW wind directions provide suitable conditions for cross-ventilation and renewable energy implementation because they have moderate wind speeds and regular occurrences. The W and WNW wind directions produce powerful gusts which require additional structural support and protective systems to maintain stability and ensure pedestrian comfort.

### 3.2.5. Temperature Anlysis

The temperature heatmap shows annual temperature fluctuations through a color gradient which transitions from blue for cold temperatures to red for hot temperatures.

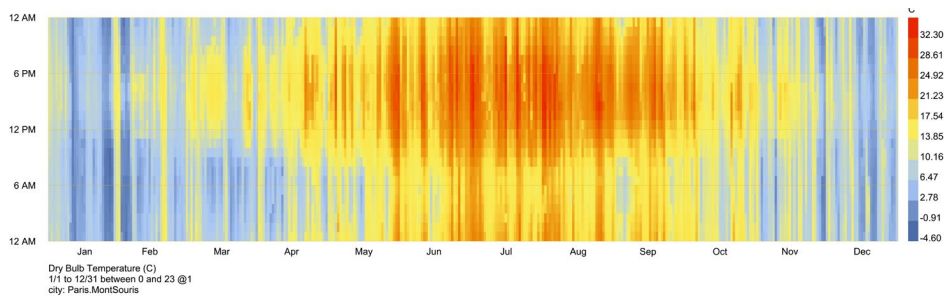


Figure 3.2.5. Temperature variation heatmap for Paris, illustrating seasonal differences.

The building design needs better insulation during winter months because of low temperatures (blue tones) and summer heat demands better shading systems because of high temperatures (red tones). The Montparnasse Tower needs two fundamental façade elements based on these findings which include improved thermal insulation for winter heat retention and adaptive shading systems for summer heat management. The dual requirements for façade design stem from these findings which demand material choices and module arrangements that achieve thermal comfort and daylight performance.

### 3.2.6. Shadow Analysis

The Tour Montparnasse building experiences substantial changes in its shadow patterns because of how sunlight angles and positions shift across different seasons. The study evaluated shadow effects on the building’s northwest and southeast orientations through three specific dates which included December 21 (winter solstice) and September 21 (autumn equinox) and June 21 (summer solstice).

#### December 21 (Winter Solstice)

The sun reaches its lowest point in the sky during this time which creates long shadows that spread throughout the urban area (Figure 3.2.7.1). The southeast side of the building gets direct sunlight during the morning hours before becoming completely shaded for the rest of the day while the northwest side remains in shadow until afternoon. The extensive shadow patterns during winter months demonstrate how daylight

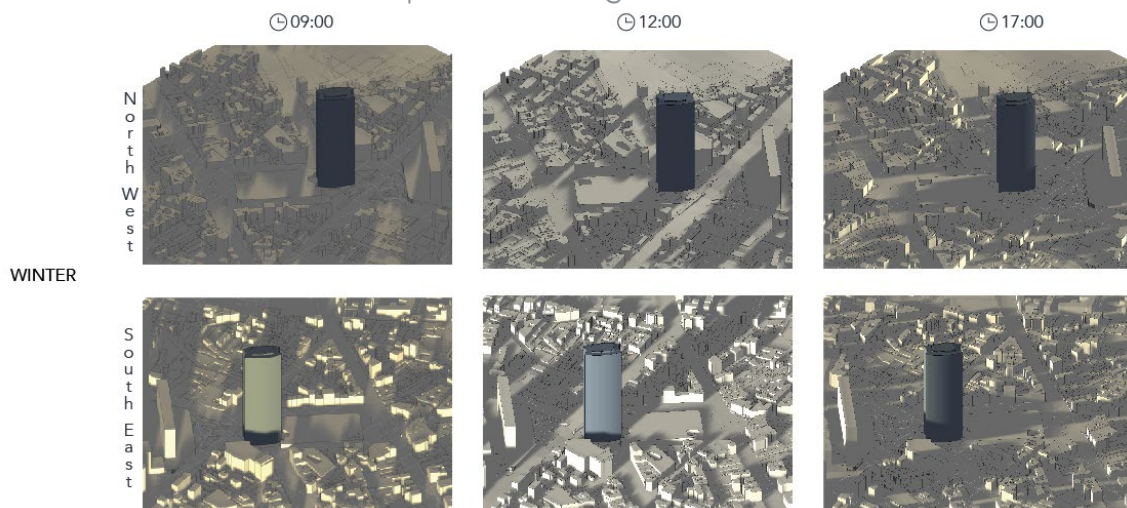


Figure 3.2.6.1 Shadow analysis diagrams for Tour Montparnasse during winter solstice (December 21).

access becomes limited which supports the requirement for design solutions that enhance low-angle solar light entry.

### September 21 (Autumn Equinox):

The solar altitude during the equinox (Figure 3.2.7.2) creates balanced sunlight distribution across the entire day. The building produces shorter shadows than winter months while its shadow area remains small during the peak sun time at noon. The southeast side of the building experiences partial sun exposure during the morning hours before the sun moves to the northwest side in the afternoon.

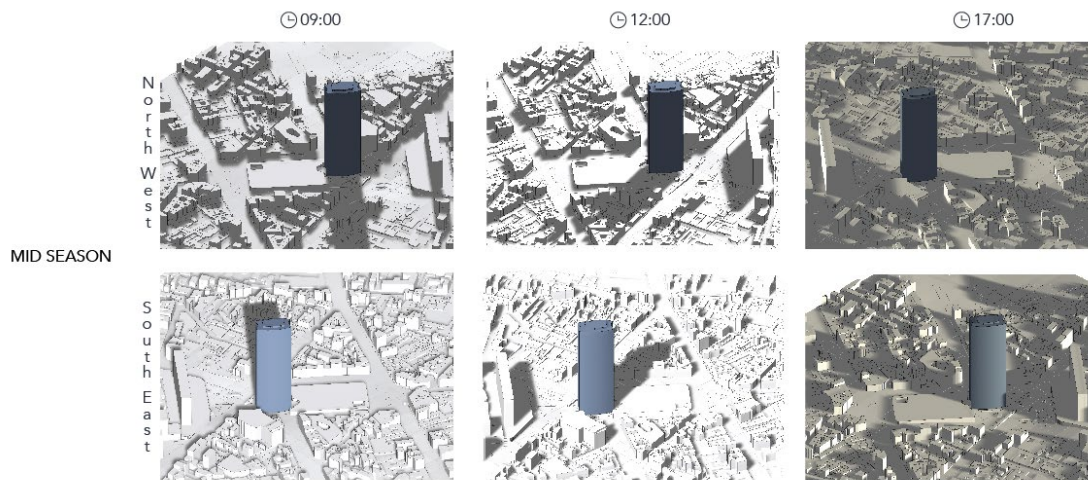
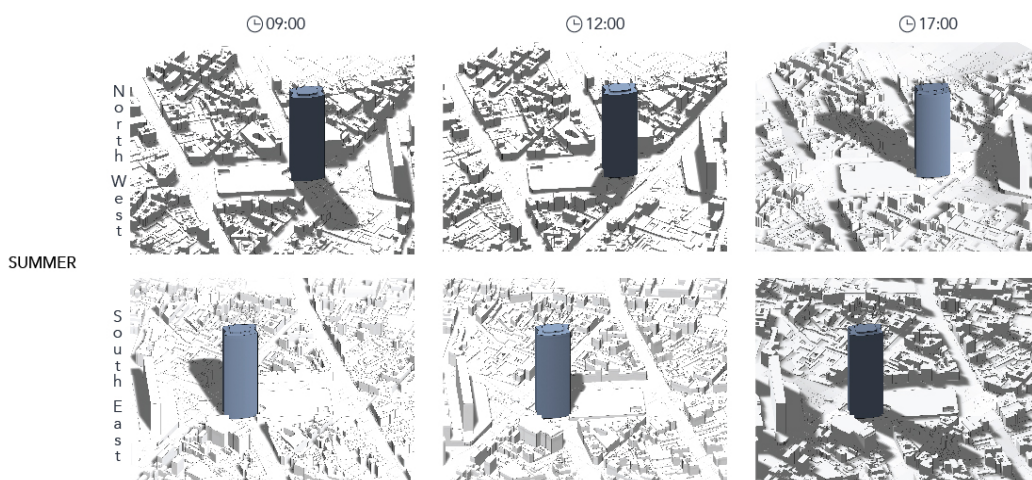


Figure 3.2.6.2 Comparative shadow analysis showing seasonal variations between summer and winter

The transitional period creates an optimal setting to assess façade transparency because it avoids both under- and over-exposure risks.

### June 21 (Summer Solstice):

Summer brings the sun to its peak position which creates extremely brief shadows. The southeast side of the building gets complete sunlight during the morning hours before the northwest side starts to receive sunlight in the afternoon.



3.2.6.3 Shadow analysis diagrams for Tour Montparnasse during summer solstice (June 21).

The tower and surrounding buildings experience complete solar exposure during mid-day because shadows become almost invisible (Figure 3.2.7.3). The summer sun exposure on the southeast façade requires immediate solar control measures which makes it the most important orientation for shading solutions.

The shadow analysis shows how sunlight access and protection levels transform across various seasons. The winter season needs solutions to capture sunlight at low angles yet summer requires powerful shading systems to protect against heat and glare. The dual requirements led to the investigation of inclined façade designs which block summer sun rays while allowing winter sunlight to enter.

The research demonstrates that building facades need to adapt to seasonal changes instead of using a single design solution for all times. The southeast façade needs deeper and more opaque modules for excessive sunlight protection but the northwest façade requires lighter transparent modules to achieve maximum daylight entry. The building reaches its highest level of energy efficiency and visual comfort and contextual integration through this particular design approach which boosts its architectural and environmental performance.

# ***CHAPTER IV***

Case Studies on Sustainable  
Façade Design

### 4.1. BBVA Bancomer Operations Center

The BBVA Bancomer Operations Center in Mexico City serves as a 135-meter-high 30-story tower which demonstrates how façade design achieves modularity through material innovation and sustainability. The tower features a glass curtain wall system that uses staggered vertical aluminum louvers which follow solar orientation patterns. The modular system functions to block solar heat while allowing daylight to enter the building which produces a changing exterior appearance based on sun position and viewer perspective while ensuring comfortable interior lighting. The vertical elements which repeat in a modular pattern create a consistent façade rhythm that supports architectural identity and environmental performance.

The façade strategy at this building incorporates sustainability as an essential design element. The combination of high-performance glass with aluminum sunshades enables the building to reduce cooling needs in hot Mexican City weather while preserving clear views and sufficient interior lighting. The building uses on-site water treatment facilities to process gray and black water which decreases the strain on local water infrastructure. The building achieves energy efficiency through solar water heating and cogeneration systems which also help decrease environmental emissions. The building achieves environmental excellence through its rooftop gardens and outdoor spaces and extensive tree planting which demonstrates how design can expand beyond physical boundaries to connect with the surrounding urban area.

The BBVA Bancomer Operations Center achieves sustainable high-rise office building excellence in Latin America through its combination of modular façade design and efficient materials and environmental systems. The project demonstrates how a technologically advanced solar-sensitive façade functions as both an environmental control

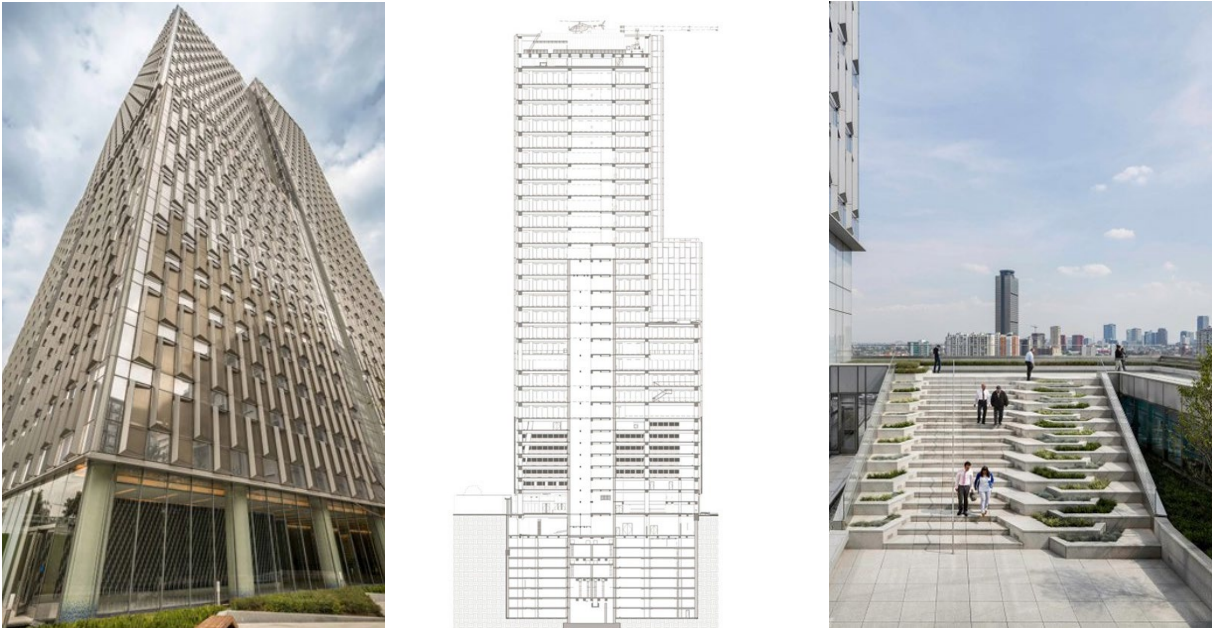


Figure 4.1: BBVA Bancomer Operations Center façade system showing modular glass curtain wall with vertical aluminum louvers calibrated for solar orientation, enhancing daylight performance and sustainability.

system and an architectural element which unites corporate branding with sustainable building performance.

### 4.2. Manhattan Loft Gardens

SOM designed Manhattan Loft Gardens as a 42-storey mixed-use tower in Stratford East London to serve as a model for high-rise living through its combination of residential units and hotel and community facilities as part of the large-scale Olympic regeneration plan. The building serves as a model for high-density residential development through its implementation of community-oriented spatial designs.

The building exterior consists of serrated glass elements and glass-fiber reinforced concrete (GRC) panels arranged in a triangulated design pattern. The serrated design produces a wavy appearance which produces shifting effects between transparent and solid appearances based on the observer's position. The building's structural design functions as a brise-soleil system which blocks 7% of solar radiation while allowing maximum daylight entry. The building's façade receives additional animation through Juliet balconies which create a rhythmic pattern and enhance the residential scale of the building.

The building structure uses a steel frame system with post-tensioned concrete elements to achieve its double-cantilevered design while building achieved a 42% better energy performance than required by regulations through its annual emissions which reached 17.25 kgCO<sub>2</sub>/m<sup>2</sup>. The three-level sky garden system with native plants and bird minimizing material usage and reducing environmental impact. The structural system directly connects performance optimization to environmental sustainability.

The feeders and insect habitats creates biodiversity while improving air quality through its landscaped design.

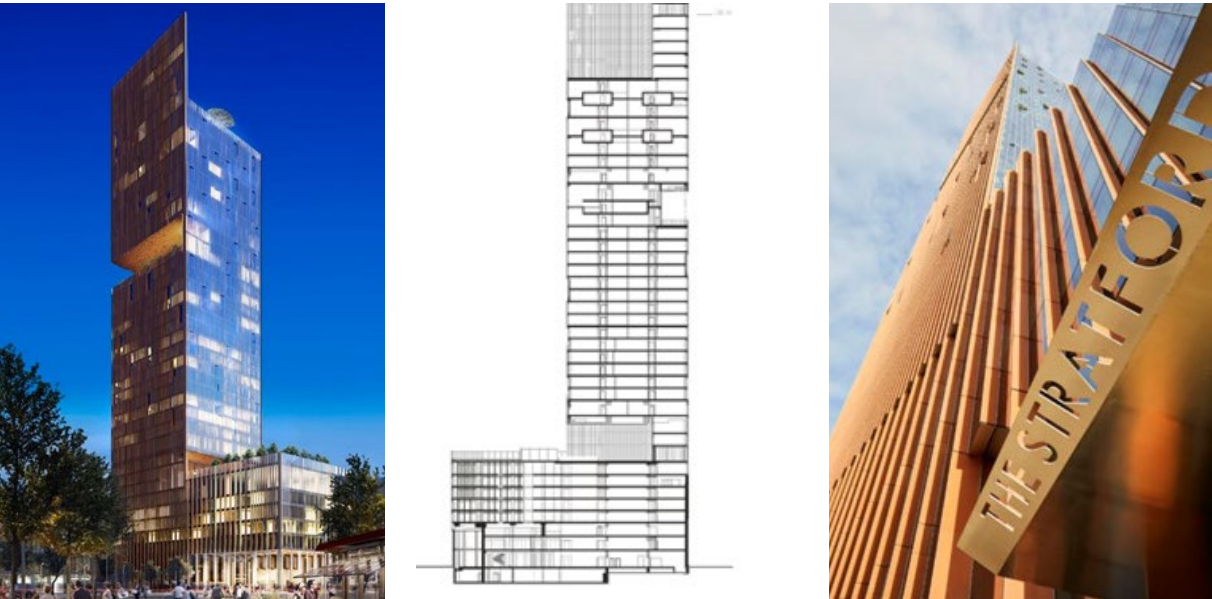


Figure 4.2: Manhattan Loft Gardens façade articulation with serrated glass and GRC cladding in a triangulated geometry, integrating Juliet balconies and sky gardens as sustainable design elements.

The building achieved BREEAM Outstanding certification through its integrated design approach which made it one of the most sustainable buildings in the UK. The building demonstrates a harmonious approach to high-rise construction through its use of modular façade components and sustainable building materials and ecological systems which unite energy efficiency with urban biodiversity and architectural design.

### 4.3. Shenzhen Zhongzhou Holdings Financial Center

The Shenzhen Zhongzhou Holdings Financial Center serves as a 223-meter mixed-use tower which unites office and hospitality operations through a single vertical structure after its 2015 completion. The building design represents Shenzhen’s vertical densification approach by uniting multiple urban functions into a small vertical space.

The building exterior features a modern rectangular design that uses large glass surfaces and metallic framing elements to create a crystalline appearance which represents corporate identity through its clean lines and precise edges. The building’s glazing system provides both clear views of the Futian district and transparent city views while maintaining panoramic views of the surrounding area. The tower’s gentle slope at the top creates a design element that makes the building appear more slender while enhancing its position among Shenzhen’s growing high-rise buildings.

The building’s façade features insulated glazing units which help control solar heat gain because of Shenzhen’s hot and humid climate. The building achieves deep daylight penetration through its high-performance glazing system which reduces artificial lighting needs while managing heat loads effectively. The building promotes sustainability by bringing together commercial and hospitality spaces under one roof, making more efficient use of land and reducing the need for outward urban growth. The building’s location near public transportation hubs enables low-carbon transportation



Figure 4.3: Shenzhen Zhongzhou Holdings Financial Center showcasing rectilinear glazed façade with insulated units, designed to balance transparency, thermal efficiency, and mixed-use urban integration

options and strengthens its position as a transit-oriented development center.

This project features a glass-covered skyscraper designed for subtropical climates, blending business functions with energy-saving features. It shows how tall buildings in fast-growing cities can achieve sustainability through innovative façades while also symbolizing economic power in a global metropolis.

#### 4.4. Modular Design: Beijing Greenland Center Skidmore

The Beijing Greenland Center serves as a 260-meter-high 55-story tower designed by SOM which demonstrates how innovative façade solutions can enhance structural strength and environmental performance. The building design uses origami principles to create prismatic trapezoidal glass panels which achieve both energy-efficient performance and visually appealing effects. The parametric modeling process allowed designers to create this modular façade system which enabled them to test different panel arrangements and protrusions. The specific placement of upward- and downward-facing modules on the façade maximized self-shading effects which resulted in turn reduced solar heat gain by 30% compared to standard flat glass systems.

The building design unites visual appeal with operational efficiency through its ability to block solar heat while preserving clear views and glass clarity. The trapezoidal design of the façade directs sunlight into deeper building spaces which enhances indoor environmental quality and decreases the need for artificial lighting. The Direct Digital Control (DDC) system operates as a climate management system which optimizes heating and cooling and ventilation operations to minimize energy usage.

The Greenland Center implements sustainability through its mixed-use design and human-friendly building layout. The building contains office and serviced apartment



Figure 4.4: Beijing Greenland Center parametric façade modules with prismatic trapezoidal geometry, optimized through digital modeling to enhance self-shading, energy efficiency, and architectural dynamism.

spaces in one vertical structure which becomes part of a master-planned district that focuses on pedestrian-friendly design and green areas and public transportation access. The project demonstrates its contribution to sustainable neighborhood development through its urban integration approach which supports low-carbon transportation systems.

The Beijing Greenland Center showcases how parametric façade technologies working with advanced materials and ecological approaches create a high-rise building that combines architectural creativity with material optimization and environmental stewardship.

# ***CHAPTER V***

## Daylight Analysis

## 5.1 Introduction

The façade design process of this thesis includes daylight optimization as its fundamental element. The solution requires two main objectives to achieve maximum interior light penetration while preventing excessive solar radiation that creates glare and heat buildup. The building requires special attention at Tour Montparnasse because its current façade fails to maintain adequate daylight autonomy while experiencing severe solar radiation problems. The solution needed a façade system which would unite these conflicting requirements while adapting to Paris’s environmental and urban conditions.

The proposed façade system used parametric modeling to unite architectural design elements with environmental performance requirements. The model allowed to perform repeated tests of various design alternatives which delivered both performance data and design-related qualitative findings about façade structure.

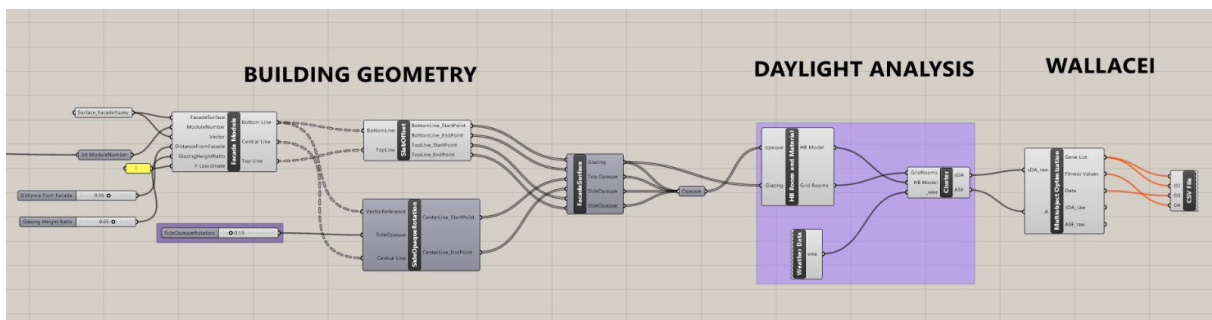


Figure 5.1: Parametric façade workflow integrating building geometry, daylight analysis, and optimization with Wallacei

The Grasshopper environment hosted the complete workflow through a unified script (Figure 5.1) that managed all operations. The parametric façade geometry definition linked directly to Honeybee daylight simulations and Wallacei multi-objective optimization through a single computational model. The integrated system maintained a continuous feedback system which allowed geometry to work together with simulation and optimization as connected processes. The system processed numerous façade design options at high speed which allowed for extensive exploration while preserving complete control of all parametric elements.

The LEED daylight credits served as performance benchmarks to establish two essential assessment criteria.

The sDA300/50% metric evaluates floor area coverage that reaches 300 lux light levels during 50% of annual occupied time.

The ASE1000/250 metric evaluates the amount of floor space which experiences direct sunlight above 1000 lux for more than 250 hours during the year.

The optimization process in this research focused on achieving sDA values exceeding 55% and ASE values under 10% to meet worldwide sustainable daylighting standards.

## 5.2 Daylight Metrics and Performance Indicators

The optimization process requires knowledge of daylighting principles and performance assessment methods which served as the basis for all analyses. The indicators served as a basis to evaluate the Montparnasse Tower at its initial state and guide the development of the optimized façade system.

The Daylight Autonomy (DA) metric shows how often a space reaches 300 lux levels of natural light during occupied hours. The level of artificial lighting requirements decreases when DA values reach their highest points but spaces need additional lighting when DA values remain low.

The Useful Daylight Illuminance (UDI) system divides daylight conditions into three categories which include UDI Low (<100 lux) for insufficient lighting and UDI Useful (100–3,000 lux) for comfortable working conditions and UDI High (>3,000 lux) for excessive daylight that creates glare and heat issues.

Spatial Daylight Autonomy (sDA) metric expands upon DA by determining the percentage of floor space that reaches 300 lux illumination during fifty percent of working hours. The sustainability standard LEED v4 uses this metric to verify that all building areas receive suitable daylight exposure.

Annual Sunlight Exposure (ASE) metric works together with sDA to detect areas where sunlight exposure exceeds normal levels. The ASE metric calculates the percentage of floor area that receives direct sunlight above 1,000 lux for more than 250 occupied hours during a year. The ASE measurement generates unfavorable results because it reveals areas that produce dangerous glare and heat-related discomfort.

Glare Autonomy (GA) evaluates visual comfort through its assessment of acceptable glare periods yet it remains outside the LEED framework.

The assessment framework evaluated daylight advantages against both exposure risks and discomfort factors through these specific metrics.

## 5.3 Computational Workflow in Grasshopper

The thesis performed daylight analysis and optimization through Grasshopper by implementing an integrated workflow that combined Ladybug Tools (Ladybug, Honeybee) with Wallacei. The methodology provided the following capabilities:

1. The definition of building geometry,
2. Assignment of material properties,
3. Integration of climate-based weather data,
4. Generation of analysis grids, and model assembly,

## 5. Evaluation of performance metrics (DA, UDI, sDA, ASE, GA).

The parametric chain between these processes enabled fast and exact testing of different façade solutions. The parametric system provided both extensive solution exploration and detailed optimization of essential variables which led to the discovery of optimal façade solutions.

### 5.3.1 Input Parameters and Geometry Setup

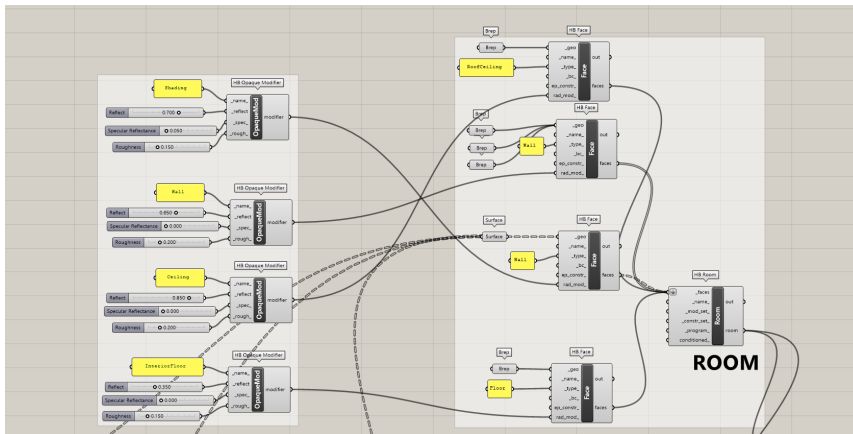


Figure 5.3.1. Grasshopper definition for geometry and material setup. This configuration established the baseline for evaluating alternative façade strategies in subsequent analyses.

The first step of the workflow involved defining the building geometry and assigning material properties to the opaque elements (Figure 5.3.1).

The HB Faces and Rooms system treated every wall and ceiling and floor and shading surface as individual components. The HB Room component unified all HB Face components to establish the daylight analysis test area.

The workflow started by establishing building dimensions and material characteristics for all opaque elements (Figure 5.3. different surfaces received their material properties through the assignment of reflectance values and roughness and specular reflectance characteristics. The walls received a reflectance value of 0.65 but ceilings received 0.85 to achieve realistic interior light distribution.

The urban environment received modeling treatment to represent external barriers which affect daylight entry.

### 5.3.2 Glazing and Shading Definition

The second step defined the transparent and shading elements of the façade within Grasshopper (Figure 5.3.2).

The glazing elements received their properties through the assignment of transmittance (0.52) and reflectance (0.15) values and thickness (0.24 m) and solar heat gain coefficient specifications. The parameters used for simulation maintained precise light transmission accuracy.

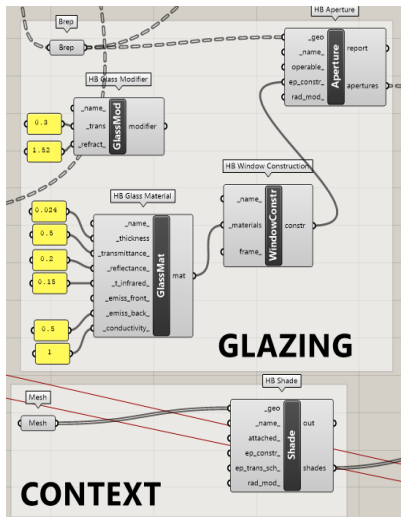


Figure 5.3.2. Grasshopper workflow for glazing and external shading parameterization.

The external shading devices received parametric definitions which enabled to test various façade configurations under the same environmental conditions.

### 5.3.3 Climate and Weather Data

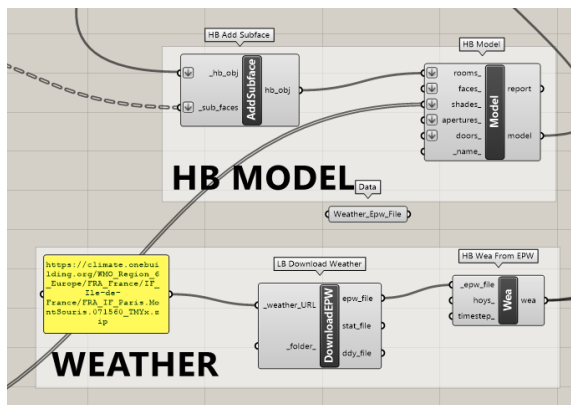


Figure 5.3.3. Integration of EPW climate and weather data in Grasshopper

The weather data entered the system through Paris region EPW files which contained climate-based simulation inputs including solar radiation and sun angles and sky conditions (Figure 5.3.3). The integration of this data allowed the simulations to accurately represent the actual environmental conditions found at the Montparnasse site.

### 5.3.4 Simulation Grids and Model Assembly

The test floors received analysis grids for daylight penetration assessment through different façade designs at positions 6th and 35th. The GRIDS setup determined sensor grid placement and resolution through its definition of grid dimensions and wall offset values and point quantity parameters.

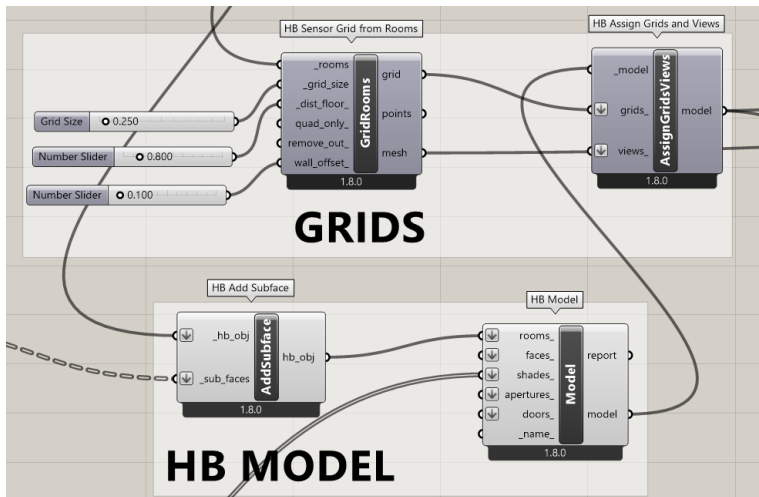


Figure 5.3.4: Setup of daylight simulation in Grasshopper, showing (top) the definition of analysis grids and (bottom) the assembly of the HB Model integrating geometry, glazing, shading, and weather data.

The HB MODEL component combined all building geometry with glazing elements and shading systems and weather data into a single simulation model. The combined model served as input for daylight analysis to enable uniform evaluation of different façade designs under identical simulation parameters.

### 5.3.5 Visualization and Results

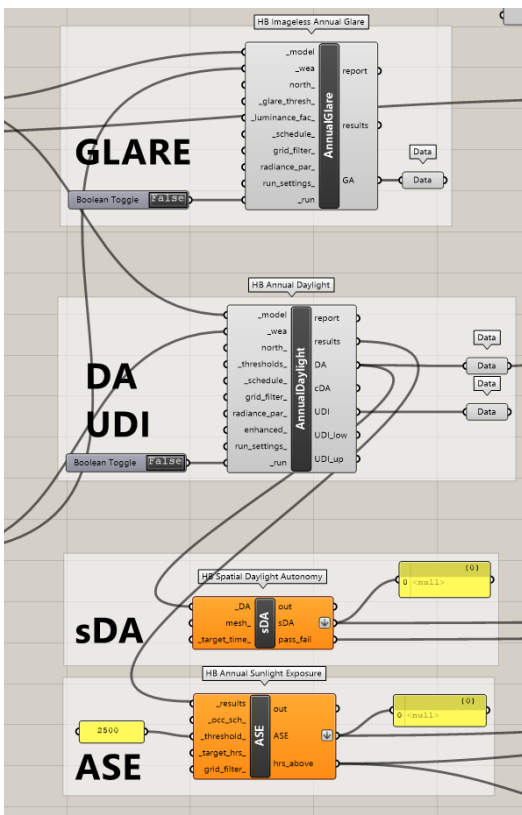


Figure 5.3.5. Visualization of daylight performance metrics (sDA and ASE) in Grasshopper

The results appeared as visual diagrams and heatmaps through Grasshopper which allowed direct evaluation of different façade approaches (Figure 5.3.5).

The computational system enabled the project team to establish a direct relationship between façade shapes and daylight performance metrics (sDA and ASE). The system enabled fast evaluation of various shoebox case studies followed by genetic algorithm optimization of the best strategies within Wallacei.

### 5.4 Shoebox Tests and Façade Experiments

The optimization process started with basic experiments which progressed into more intricate system configurations. The initial testing phase used a shoebox model to evaluate a range of different planar shading methods which included horizontal and vertical systems and their combination.

These preliminary studies revealed the limitations of conventional approaches, showing that no single planar device could provide both high daylight autonomy and acceptable control of solar exposure. As a result, the investigation shifted toward more adaptive geometries, culminating in the introduction of angled façade modules. Finally, inspiration was drawn from the Schüco Parametric Façade, which provided a conceptual precedent for modular, multi-surface design, though adapted here with significant modifications.

#### 5.4.1 Base Analysis – Original Façade

The baseline façade of Tour Montparnasse displayed poor daylight autonomy and annual sunlight exposure performance because it used dark glazing without external shading, according to Figure 5.4.1.

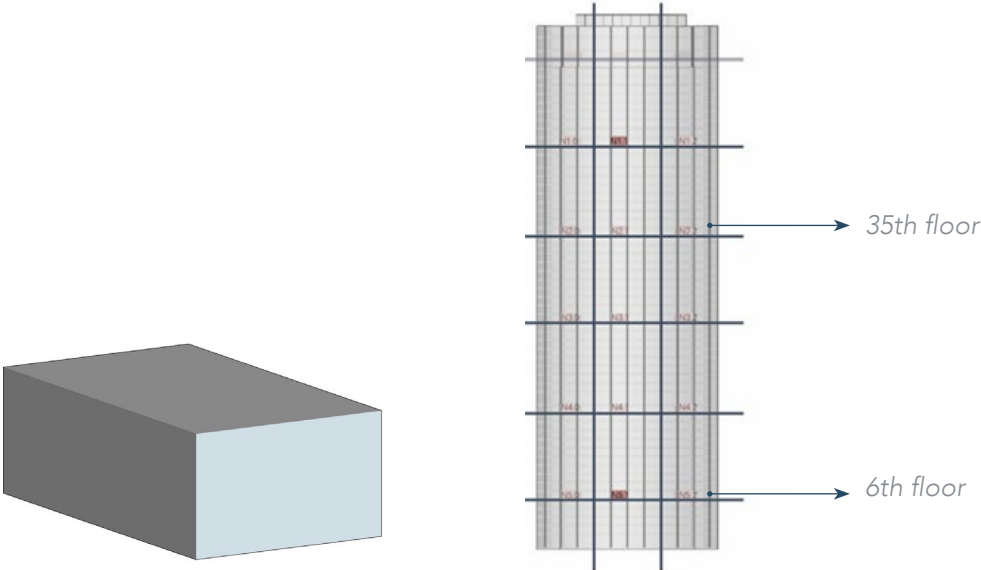


Figure 5.4.1: Daylight performance of the original Montparnasse façade (baseline case), showing sDA and ASE results for Southeast and Northwest façades at the 6th and 35th floors

Orientation	Floor	sDA	ASE	LEED Compliance
Southeast	6th	43%	42%	High ASE
Southeast	35th	49%	48%	High ASE
Northwest	6th	40%	14%	Low sDA
Northwest	35th	38%	14%	Low sDA

The analysis demonstrated that the current building envelope performed poorly because the Southeast orientation received insufficient daylight while experiencing excessive solar radiation throughout the year. The Northwest façade maintained acceptable ASE values but failed to reach the necessary sDA requirements.

The Southeast side of the building struggled to meet LEED daylight targets because of its high ASE levels, while the Northwest side stayed within the limits, proving to be the better orientation for sustainable daylighting.

### 5.4.2 Vertical Fins

The system of vertical fins underwent testing at multiple positions which included different angles and depths (10°, 30°, 45°, 60°, 90°).

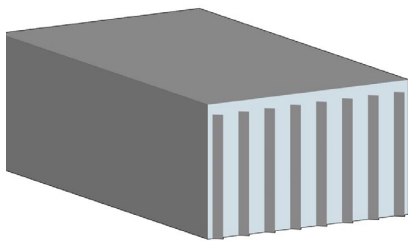


Figure 5.4.2: Shoebox test model in Grasshopper showing variations of vertical fins with different angles and depths. (Grasshopper model illustrating the application of vertical fin systems tested at 10°, 30°, 45°, 60°, and 90°.)

The simulation results for shoebox configurations in Figure 5.4.2 indicated that sDA values stayed under 55% (ranging from 40–52%) and ASE values stayed at 30%. The vertical fins managed to block some eastern and western low-angle sunlight but they failed to boost daylight autonomy effectively. The strategy proved insufficient because of these results.

### 5.4.3 Overhangs

The study examined horizontal overhangs with different depths at 40 cm, 50 cm, 75 cm, 1 m and 1.5 m.

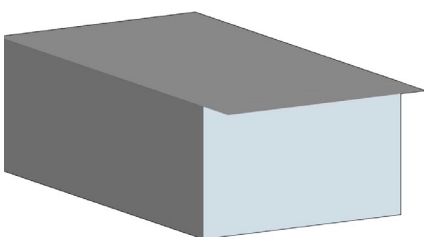


Figure 5.4.3 Shoebox test model in Grasshopper illustrating horizontal overhang strategies.

The simulation data from Figure 5.4.3 demonstrated that shoebox models achieved their target sDA values at first but these values decreased under 55% when the overhang depth increased. The ASE values stayed between 40–50% throughout the analysis. The summer sun protection from overhangs came at the expense of reduced daylight access to deeper interior areas. The strategy failed to work as an independent solution because of its unbalanced performance.

#### 5.4.4 Overhangs + Vertical Fins

To enhance performance, overhangs were combined with vertical fins. The simulation outcomes for the configurations in Figure 5.4.4 indicated that this integration worsened results rather than improving them.

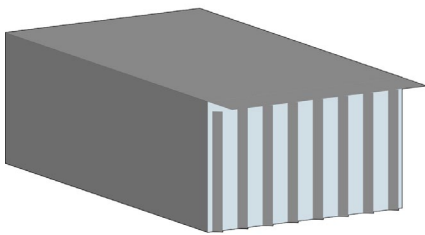


Figure 5.4.4. Shoebox test model in Grasshopper combining vertical fins and horizontal overhangs. (Hybrid strategy integrating both shading devices to evaluate combined performance.)

sDA values dropped to around 40–50%, while ASE remained around 30%. The reason ASE did not decrease is that the combination primarily blocked high-angle solar radiation but failed to adequately intercept low-angle sunlight from the east and west. As neither performance criterion was met, this hybrid strategy was excluded from further consideration.

#### 5.4.5 Symmetric and Asymmetric Vertical + Horizontal Shading Combinations

Another variation involved combining vertical and horizontal elements in both symmetric and asymmetric layouts.

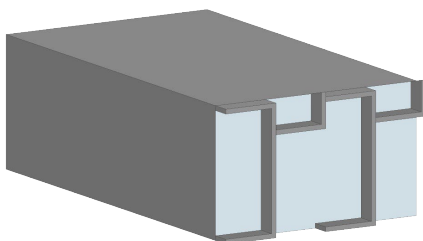


Figure 5.4.5: Shoebox test model in Grasshopper showing symmetric and asymmetric combinations of vertical and horizontal shading devices.

The shoebox models in Figure 5.4.5 produced simulation results showing sDA values above 55% which indicates better autonomy performance. The ASE values remained higher than 35% in every tested configuration. The systems failed to block solar rays at any angle because they maintained continuous exposure to sunlight. The daylight au-

onomy enhancement did not compensate for the inability to manage low-angle glare which made this approach useless.

#### 5.4.6 Brise-Soleil Systems

Horizontal brise-soleil systems, inspired by the Zhongzhou Holdings Financial Center, were tested in multiple depths and angles.

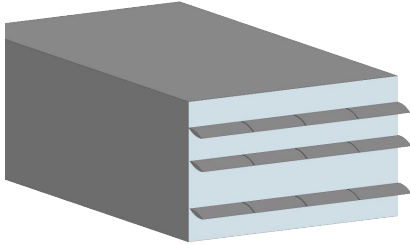


Figure 5.4.6 Shoebox test model of horizontal brise-soleil case study with varying depths and angles.

Simulation results for the shoebox models in Figure 5.4.6 showed that these strategies achieved relatively higher sDA values on the Southeast façade compared to previous systems. However, ASE rarely dropped below 30%, and performance on the Northwest façade was significantly weaker. The failure of this strategy can be explained by three factors:

1. The main function of brise-soleils protects buildings from overhead sun exposure yet they fail to protect against sunlight entering from lower angles.
2. The deep brise-soleil devices created excessive shading which blocked sunlight from entering both the lower floors and interior areas.
3. The implementation of extensive brise-soleil systems leads to higher maintenance needs and more complicated construction processes.

The strategy failed to meet requirements because of these critical weaknesses.

#### 5.4.7 SOM Manhattan Garden Reference

The second experiment followed the design principles of SOM Manhattan Garden.

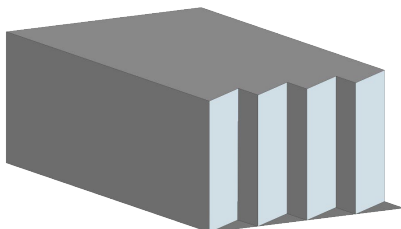
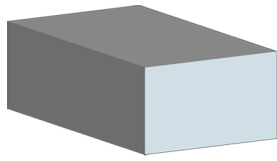


Figure 5.4.7: Shoebox test model in Grasshopper based on the SOM Manhattan Garden reference façade design.

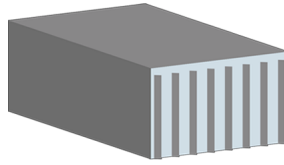
The shoebox test results showed extremely high sDA values which proved the building had excellent daylighting potential. The ASE values experienced a significant increase which sometimes exceeded 70% in certain cases. The excellent autonomy performance of this façade became unusable because of its excessive overexposure.

## Daylight Performance of Shoebox Tests



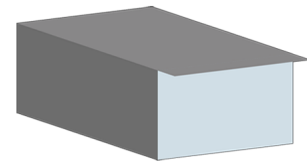
**Original Facade**

	sDA	ASE
6th floor	43 %	42%
35th floor	49 %	48 %



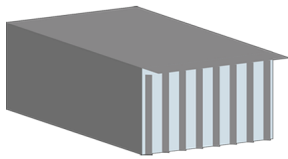
**Vertical Fins**

	sDA	ASE
6th floor	51 %	35 %



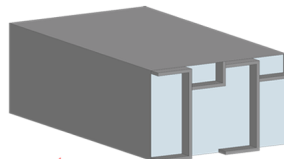
**Overhangs**

1 m	sDA	ASE
6th floor	56 %	38 %



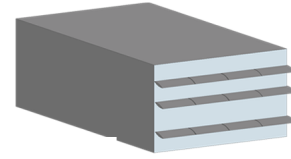
**Overhangs + Vertical Fins**

60 Angle	sDA	ASE
6th floor	50 %	33 %



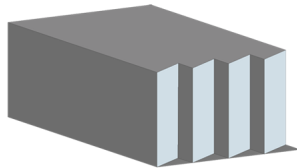
**Asymmetric Vertical+ Horizontal Shading**

	sDA	ASE
6th floor	68 %	36%



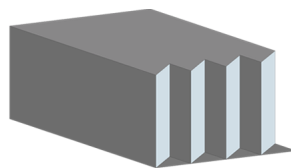
**Horizontal**

60 cm	sDA	ASE
6th floor	46 %	17%
35th floor	72 %	29%



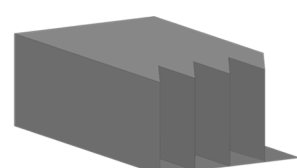
**SOM MG 30 Degree**

1.5 m	sDA	ASE
6th floor	85 %	75 %



**SOM MG 45 Degree**

1 m	sDA	ASE
6th floor	57 %	34 %

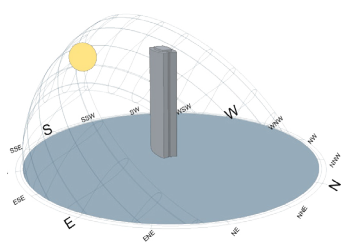


**SOM MG 60 Degree**

1.5 m	sDA	ASE
6th floor	67 %	38%

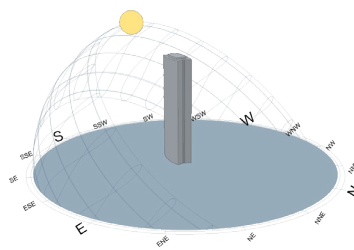
Figure 5.4.7: Shoebox test model in Grasshopper based on the SOM Manhattan Garden reference façade design.

### 5.4.8 Angled Façade Modules



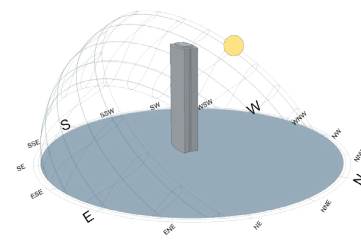
**SOMMER SOLSTICE**

21st June, 10 AM



**SOMMER SOLSTICE**

21th June, 1 PM



**SOMMER SOLSTICE**

21th June, 5 PM

Figure 5.4.8.1: Solar path diagrams for the Montparnasse site on June 21 (Summer Solstice) at 10:00 AM, 1:00 PM, and 5:00 PM.

The final approach involved using angled façade modules which resulted from analyzing solar paths at the Montparnasse site. The solar diagrams (Figure 5.4.8.1) display the sun's position and its angle of incidence during June 21 (Summer Solstice) at three different times of day: 10:00 AM, 1:00 PM and 5:00 PM. The visualizations demonstrate how sunlight hits the façade at different angles during the day with steep angles during midday and gentler angles during morning and afternoon hours.

The observed patterns indicated that a sloping façade surface could redirect sunlight toward the ceiling surface which would create uniform interior lighting and reduce glare effects.

Based on this hypothesis, the shoebox tests were extended to include angled geometries. The simulation tested four outward-inclined façade modules at 20°, 30°, 40° and 45° to determine how different angles would affect performance. The simulation results demonstrated that this design method showed promise (Figures 5.3.8.2–5.3.8.3):

The northwest façade on the 6th floor with a 20° angle achieved sDA 91% and ASE 6% which met LEED standards.

The southeast façade on the 6th floor with a 30° angle achieved sDA 81% and ASE 29% which proved to be the most effective combination among all tested approaches.

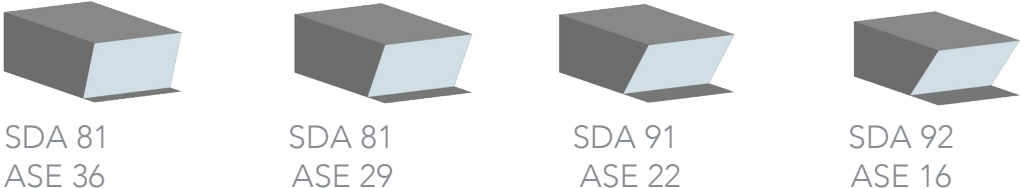


Figure 5.4.8.2: Angled façade modules (20°, 30°, 40°, and 45°) and daylight simulation results for Southeast façade, 6th floor.

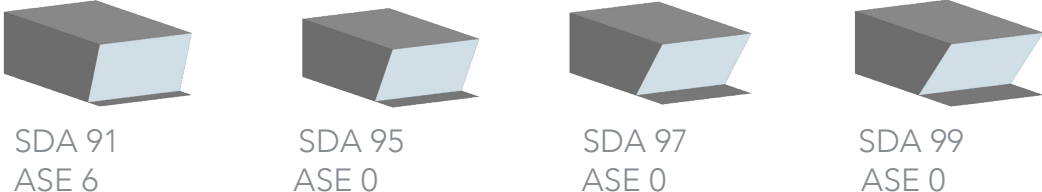
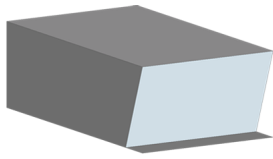


Figure 5.4.8.3: Angled façade modules (20°, 30°, 40°, and 45°) and daylight simulation results for Northwest façade, 6th floor.

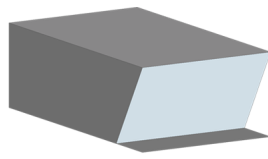
The results showed that using angled façade modules produced both enhanced daylight autonomy and controlled solar exposure. The angled system received selection as the fundamental design for Wallacei optimization work.

## Daylight Performance of Shoebox Tests for Angled Facade-South



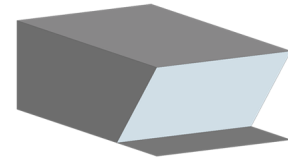
### 20 Degree

	sDA	ASE
6th floor	81 %	36 %
35th floor	99 %	45 %



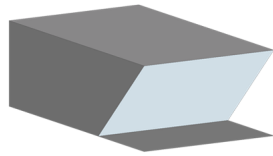
### 30 Degree

	sDA	ASE
6th floor	85 %	29 %
35th floor	100 %	40 %



### 40 Degree

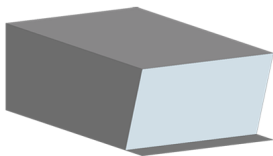
	sDA	ASE
6th floor	91 %	22 %
35th floor	99 %	34 %



### 45 Degree

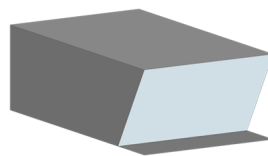
	sDA	ASE
6th floor	85 %	29 %
35th floor	100 %	40 %

## Daylight Performance of Shoebox Tests for Angled Facade-North



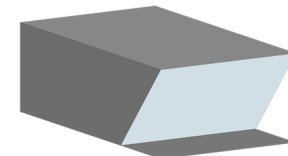
### 20 Degree

	sDA	ASE
6th floor	91 %	6 %
35th floor	95 %	6 %



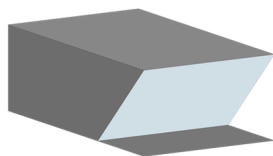
### 30 Degree

	sDA	ASE
6th floor	95 %	0 %
35th floor	98 %	0 %



### 40 Degree

	sDA	ASE
6th floor	97.7 %	0 %
35th floor	98.8 %	0 %



### 45 Degree

	sDA	ASE
6th floor	99 %	0 %
35th floor	99 %	0 %

Figure 5.4.8.4: Comprehensive shoebox test results for the Southeast and Northwest façades across multiple shading strategies, comparing the limitations of planar and hybrid systems with the superior performance of angled modules.

## 5.5 Summary of Daylight Analysis

The daylight analysis conducted in this chapter revealed the limitations of conventional planar shading systems and emphasized the necessity of adopting more adaptive façade geometries. Vertical fins, horizontal overhangs, and their combinations demonstrated partial improvements but consistently failed to establish the required balance between Spatial Daylight Autonomy (sDA) and Annual Sunlight Exposure (ASE). Reference-based precedents, such as the Zhongzhou Holdings Financial Center and the SOM Manhattan Garden, provided useful insights; however, they also revealed critical

shortcomings, particularly their inability to mitigate excessive solar exposure or effectively control glare.

Within this context, a series of systematic shoebox experiments were carried out to test a wide range of façade strategies. The analysis focused on the Southeast orientation and 6th floor because these areas needed the most attention due to their low sDA values and ASE levels which exceeded 30% and their exposure to the surrounding urban environment. The analysis started with the most difficult conditions first because these represented the worst case for LEED daylighting requirements (see Figure 5.5).

The 6th floor Southeast façade received the only simulation for vertical fins and horizontal overhangs and hybrid systems because their poor performance in sDA and ASE measurements made further testing on the 35th floor and Northwest façade unnecessary. The angled façade modules showed successful results at the Southeast orientation by delivering better daylight access while minimizing excessive sunlight exposure. The positive results from the Southeast façade tests prompted additional testing at the 35th floor and Northwest orientation.

The simulation results demonstrated that angled shapes performed better than flat and combined design approaches. The Northwest orientation produced sDA values exceeding 95% together with ASE values under 10% which met LEED requirements although the Southeast orientation reached its maximum daylight exposure threshold. The analysis in Figure 5.5 proved that the Northwest orientation provides the best sustainable daylighting performance so it became the reference point for further development. The validation process established angled modules as the most effective solution which became the baseline for further development through Wallacei optimization in the following research stages.

## **5.6 Transition to Parametric Module Development**

The evaluation of shoebox experiments showed that angled façade modules provided the best combination of daylight access and solar protection. This configuration was chosen as the starting point for additional development work. The Grasshopper software allowed researchers to create parametric models of angled modules which enabled precise control over geometric parameters including inclination angle and depth and transparency levels while maintaining direct daylight simulation connections.

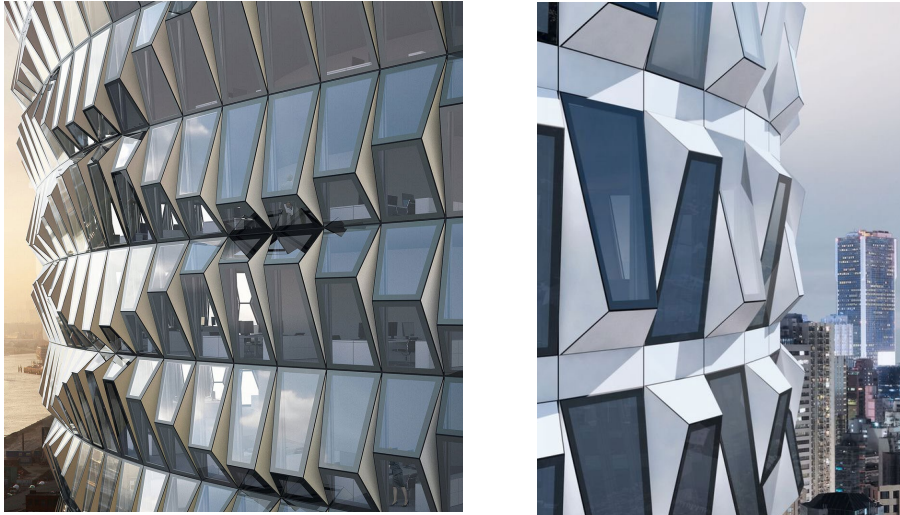


Figure 5.6.1: Schüco façade reference adapted into the parametric framework, demonstrating the differentiation of opaque shading elements at the top and transparent glazing at the bottom to balance solar control with daylight penetration.

The Schüco façade module served as the reference system which received functional surface division for the design:

The upper section of the façade operated as a solid shading element while the lower section maintained transparency to allow daylight entry and maintain visual access. The functional separation between these areas led to the development of essential variables for the parametric design system. The optimization process required the control of two essential parameters which were distance from façade and window line height ratio.

The façade system transformed into a structure that could adapt through parametric design which became the base for the multi-objective optimization system in Chapter 6 using Wallacei.

## 5.7 Grasshopper Parametric Implementation

The angled façade system received its parametric implementation through Grasshopper which enabled the conversion of conceptual ideas into a flexible computational framework. The façade geometry in this environment used modular design principles to create a system which allowed users to modify parameters such as building envelope distance and window height ratio and angle of inclination. The system linked performance simulations to these parameters through direct connections which enabled instant environmental evaluation of every geometric change. The Grasshopper definition contained separate clusters which combined surface modeling functions with data management tools and environmental analysis plugins such as Ladybug and Honeybee.

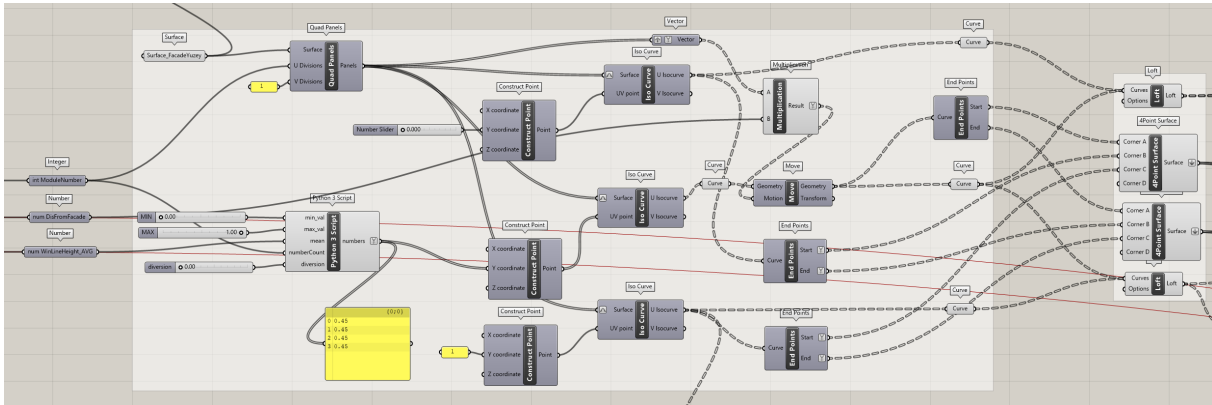


Figure 5.7.1: Integration of data management and geometric operations in Grasshopper, showing the systematic parametric generation of façade modules.

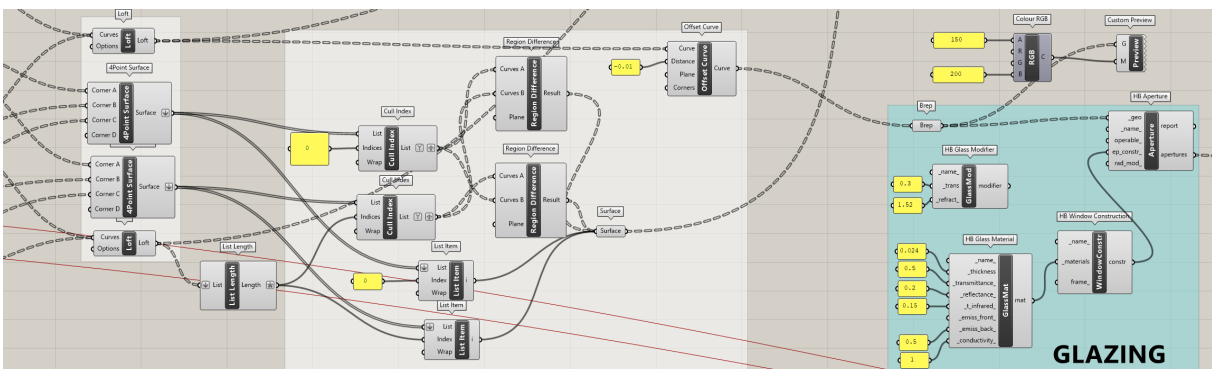


Figure 5.7.2: Parametric workflow linking geometry with environmental analysis (Honeybee daylight simulations), demonstrating the direct connection between form and daylight metrics (sDA, ASE) and establishing iterative performance feedback.

The clusters in Figure 5.7.1 combined data management capabilities with geometric operations to produce systematic façade configurations. The workflow expanded to connect geometric parameters with environmental simulations through Honeybee which created continuous performance feedback loops between form and daylight analysis (Figure 5.7.2).

The Schüco façade modules served as reference systems to guarantee both architectural feasibility and construction readiness. Grasshopper operated as both a parametric design platform and a simulation-based decision tool which united design creativity with environmental performance optimization. The parametric system established the base for the evolutionary optimization system described in Chapter 6 through Wallacei. presented in Chapter 6 using Wallacei.

# ***CHAPTER VI***

Multiobject Optimization - Wallacei

## 6.1 Optimization Workflow

The Wallacei optimization system in this research study operated through a four-stage process which is shown in Figure 6.4.

The first step of environmental analysis through Ladybug software evaluated solar exposure by measuring direct sun hours and performing sun path and shadow analysis. The results from these analyses formed the base for evaluating different façade designs.

The second step of the process used Honeybee to perform daylight simulations which applied shoebox test models to various façade design approaches. The simulation results produced spatial Daylight Autonomy (sDA) and Annual Sunlight Exposure (ASE) values which served as the main evaluation criteria for optimization.

The third stage combined daylight simulation outputs with Wallacei's evolutionary optimization system. The optimization process used Wallacei to vary façade projection distances and window height ratios for creating numerous design populations. The evolutionary process of selection and crossover and mutation under Wallacei control used Honeybee simulation results to evaluate each design alternative. The system used performance-based daylight metrics to optimize façade geometries through evolutionary search.

The fourth and final step of the process included design optimization. The Wallacei output results were exported to Excel for LEED daylight threshold verification after the optimization process. The evaluation process at this point focused on practical design aspects which included visual comfort and maintenance requirements and construction feasibility. The optimized results produced three additional façade types which included Regular and Random and Wave designs to evaluate different design expressions while maintaining performance standards.

The systematic design workflow enabled researchers to test hundreds of different façade designs which would have required excessive time when using traditional manual testing methods.

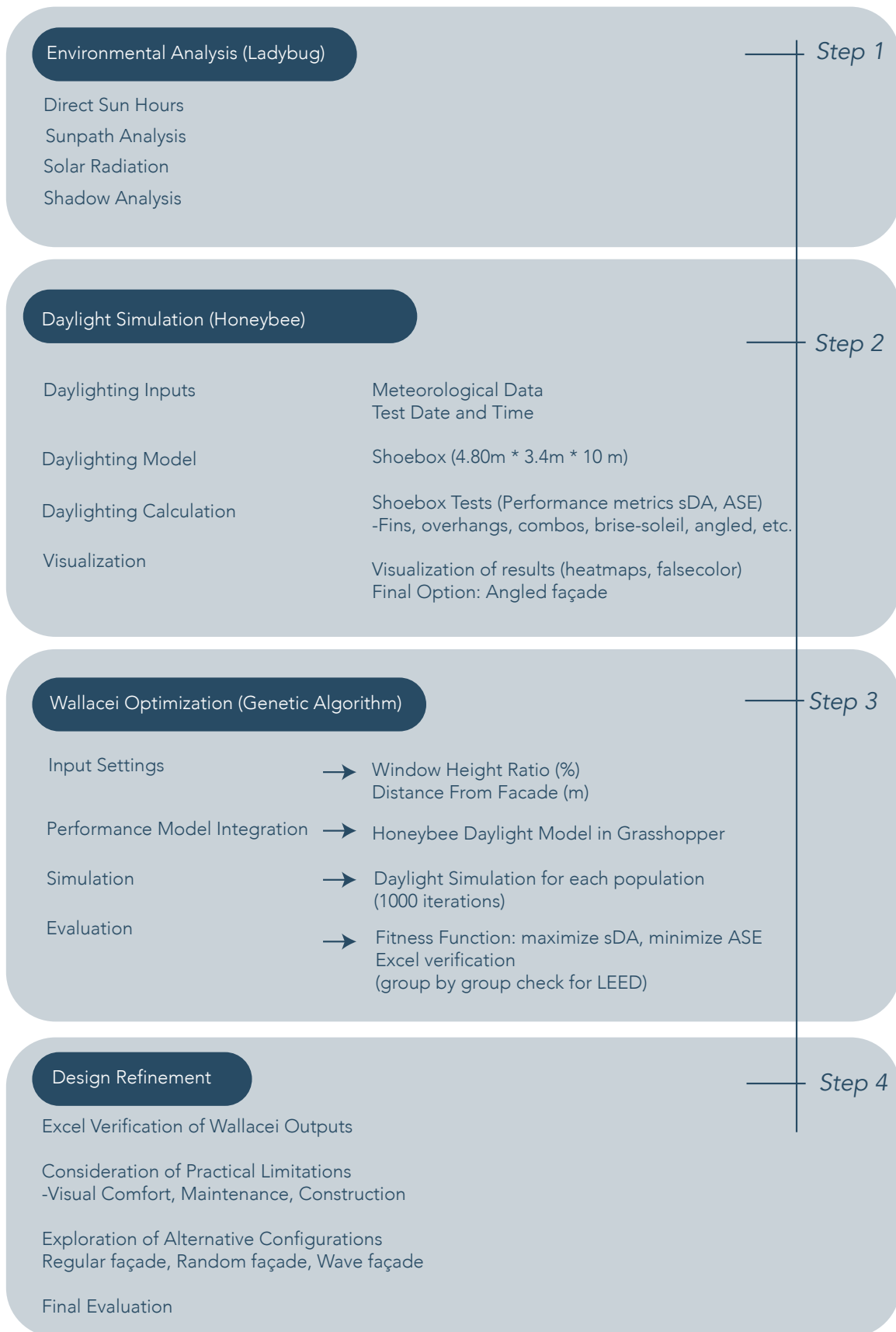


Figure 6.1: Integrated workflow for façade optimization, combining environmental analysis, daylight simulations, evolutionary optimization, and final design refinement

## 6.2 Why Wallacei Was Selected

Several optimization techniques were evaluated at the beginning by examining both deterministic methods and machine learning approaches. The researchers chose Wallacei as the optimization tool because of three essential factors. The system enables designers to control design variables directly which lets them work with specific parameters they want to study. The system provides clear feedback which enables users to understand how design parameters affect performance results. The decision-making operations of machine learning models remain invisible to users because they operate as uninterpretable systems.

The native integration of Wallacei with Grasshopper provides users with effortless access to Honeybee and other environmental analysis tools. The selection of Wallacei as the optimization tool occurred because it supported Grasshopper workflows and handled multi-objective trade-offs which produced Pareto front results. The daylight-driven façade optimization process requires designers to choose between maximizing daylight autonomy (sDA) and controlling annual sunlight exposure (ASE) because these performance metrics compete against each other.

The main difference between Wallacei and machine learning emerges a restricted set of simulation results to create a continuous function which predicts values between tested cases. The method delivers fast computation but produces imprecise results. The simulation-based approach of Wallacei produces exact results from their output generation methods (Figure 6.3). The training process of machine learning algorithms uses for each design configuration because it runs direct evaluations of every design. The exact results from Wallacei become essential in daylight analysis because small geometric changes between window height and façade depth produce substantial performance effects.

The evolutionary algorithm built into Wallacei allows designers to test numerous design options which lead to Pareto-optimal solutions that fulfill multiple performance requirements. The ability to optimize multiple criteria while maintaining result interpretability made Wallacei the optimal choice for this research.

The research adopted Wallacei as its optimization tool because it offered clear methodology and result understanding and complete integration with parametric design systems.

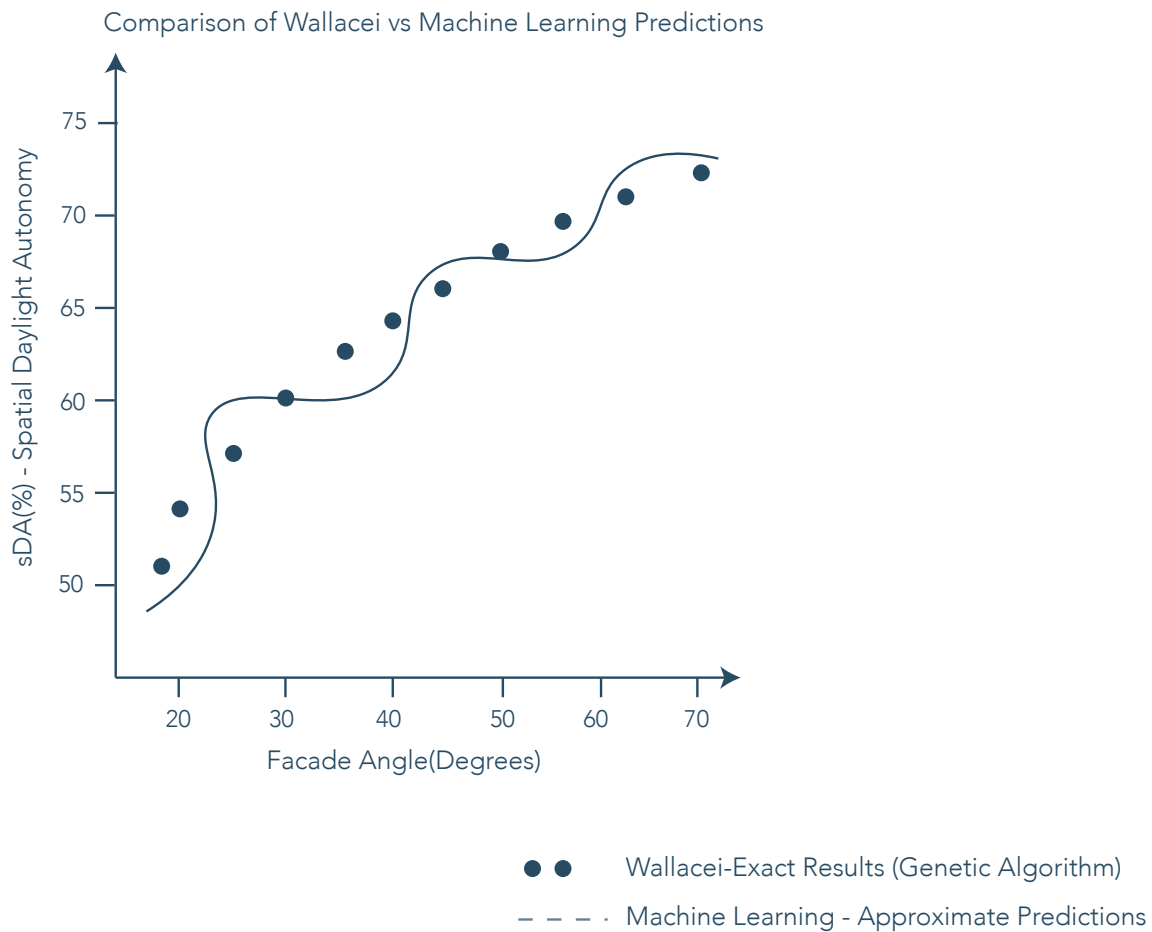


Figure 6.2: Comparison diagram of deterministic optimization, machine learning, and evolutionary optimization approaches.

### 6.3 Introduction to Wallacei

Wallacei functions as a multi-objective evolutionary optimization tool which operates within Grasshopper as a plugin. The system uses Genetic Algorithms (GAs) to replicate natural selection processes through selection and crossover and mutation operations which generate design alternatives between successive generations. The algorithm generates multiple high-performing solutions through its Pareto front analysis which demonstrates the trade-offs between conflicting objectives (Figure 6.3.1). The system provides essential functionality for architectural design because no solution exists which optimizes all evaluation criteria at once.

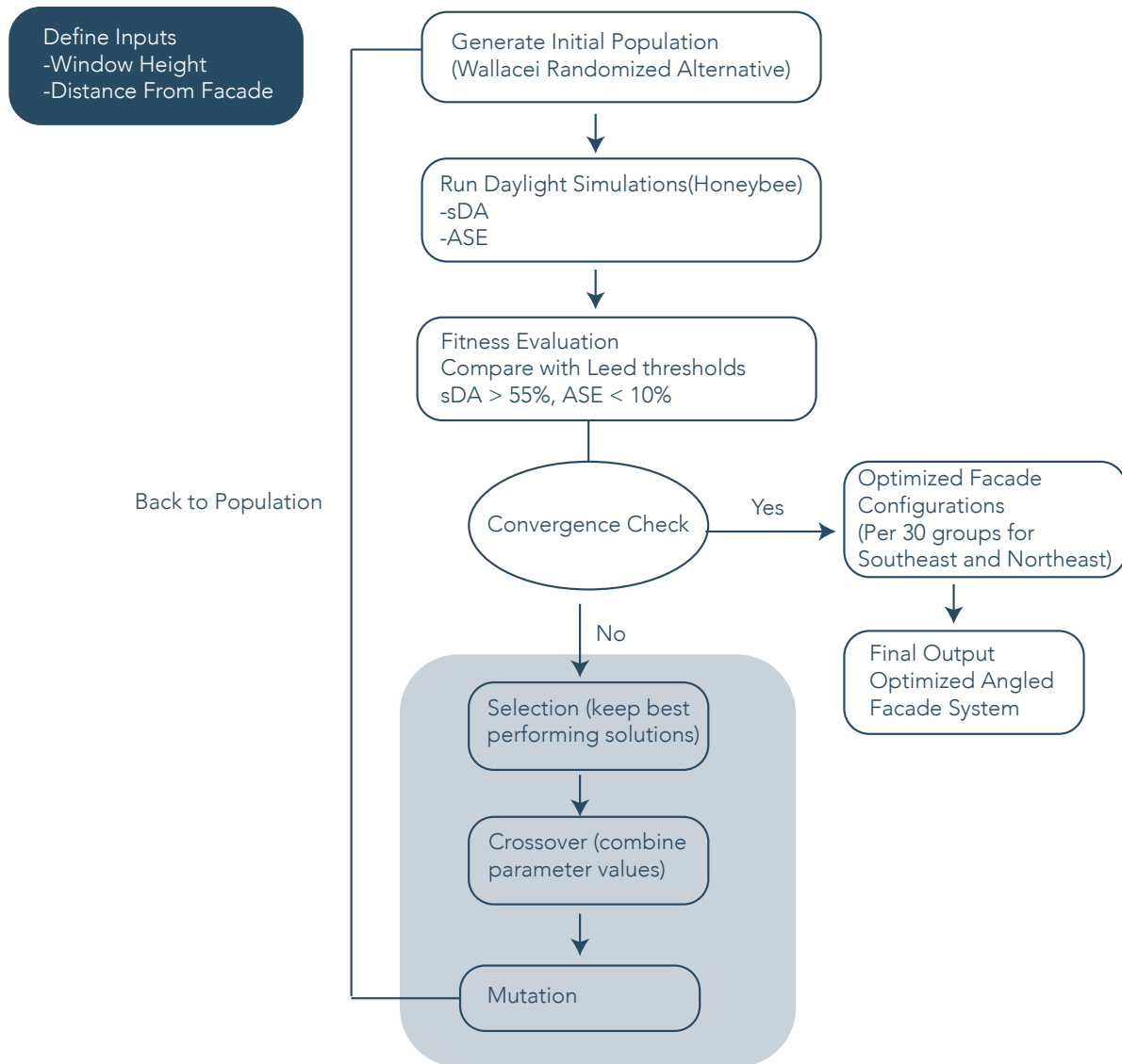


Figure 6.3.1: Conceptual diagram of the genetic algorithm workflow in Wallacei, illustrating population generation, daylight simulation, evaluation against LEED thresholds, selection, crossover, mutation, and convergence.

The design problem framework of Wallacei contains three main elements which match the requirements of this thesis: inputs and objectives and outputs. The design variables used as inputs included window height ratio and façade element distance from vertical planes. The two design parameters controlled the angle of façade modules which determined the relationship between daylight access and solar protection.

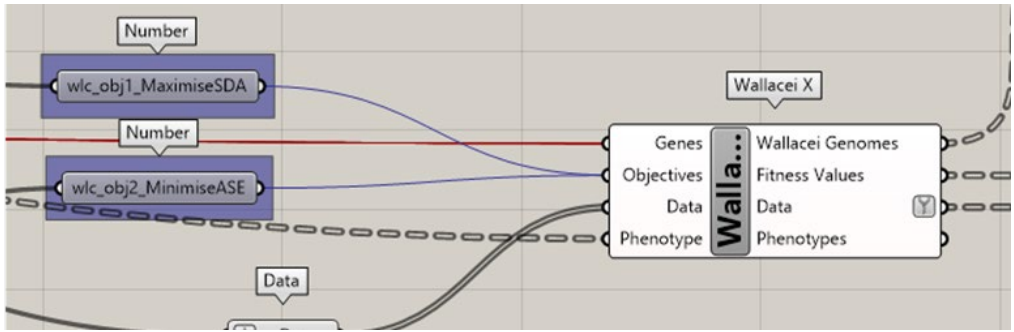


Figure 6.3.2: Wallacei setup in Grasshopper, showing the definition of objectives (maximize sDA, minimize ASE) and data connections for evolutionary optimization.

The objectives (Figure 6.3.2) followed LEED standards by maximizing Spatial Daylight Autonomy (sDA) and minimizing Annual Sunlight Exposure (ASE). The system produced a sequence of façade designs which improved their performance through multiple rounds of evolutionary processing.

The operation of Wallacei becomes clearer through its fundamental terminology and operational concepts which need explanation.

The parametric façade modules which Grasshopper developers created became directly connected to Honeybee for daylight simulation operations.

**Control Panel**

**Population**

Generation Size	50
Generation Count	20
Population Size: 1000	

**Algorithm Parameters**

Crossover Probability	0.9
Mutation Probability <input checked="" type="checkbox"/> 1/n	
Crossover Distribution Index	20
Mutation Distribution Index	20
Random Seed	1

**Simulation Parameters**

No. of Genes (Sliders)	2
No. of Values (Slider Values)	38
No. of Fitness Objectives	2
Size of Search Space	3.6e2

**RunTime** ● Number of nulls:

Current Solution / Generation	
Number of Pareto Front Solutions	
Eval. Time Per Solution	
Estimated Time Remaining	
Simulation Runtime	17:11

Figure 6.3.3: Wallacei control panel in Grasshopper, displaying the setup of evolutionary optimization parameters.

*Population:* The population of solutions in each generation consists of distinct solution combinations that represent different input variable values (Figure 6.3.3).

*The evolutionary* process advances through multiple generations which form the basis of its operation. The evaluation process of each generation selects top-performing solutions which become parents for creating the following generation.

*Fitness* represents the extent to which an individual meets performance requirements through its ability to achieve higher sDA and lower ASE values. The evaluation process for multi-objective problems requires assessment of multiple fitness criteria at the same time.

*The selection* process chooses high-performing individuals to transfer their genetic attributes to the following generation.

*The crossover* operation between chosen individuals leads to the creation of new offspring through genetic code exchange which combines elements from both parents.

*The process of mutation* introduces random changes to prevent the algorithm from getting stuck at suboptimal solutions.

*The Pareto Front* contains all non-dominant solutions which show the optimal trade-offs between conflicting objectives. The improvement of daylight autonomy through sDA requires sacrificing some solar exposure but excessive ASE reduction restricts daylight availability.

Wallacei used its mechanisms to analyze hundreds of façade configurations in this research through Figures 6.1.1–6.1.2. The evolutionary loop received performance data from daylight simulations conducted in Honeybee for each configuration assessment. The optimization process through multiple generations produced suitable solutions for parametric development by finding equilibrium between daylight access and solar exposure control.

## **6.4 Transition from Shoebox to Optimized Modules**

The hybrid opaque-transparent angled module served as the starting point for optimization work before it received integration into Wallacei evolutionary runs. The Schüco Parametric Façade served as a reference point because it showed how modular systems unite architectural and technical performance capabilities. The Montparnasse Tower received its essential modification through the upper section of each module which became an opaque shading element while the lower section maintained transparency for daylight entry and outdoor view preservation.

The optimization process started with this specific design configuration. The hybrid opaque-transparent angled module served as the fundamental design element for all subsequent Wallacei analysis runs.

### 6.4.1 Integration with Daylight Simulation

The workflow allowed designers to link window height ratios and façade offset distances to performance metrics which included Spatial Daylight Autonomy (sDA) and Annual Sunlight Exposure (ASE) for fast evaluation of different design options. The workflow established a continuous design-performance feedback loop which connected building envelope geometry to environmental assessment (Figure 6.2.1.1).

The simulation workflow produced daylight performance results (sDA and ASE) for each design configuration which Wallacei used as optimization targets (Figure 6.2.1.1). The integration between simulation and optimization used actual daylight metrics which emerged from simulation results instead of theoretical fitness functions.

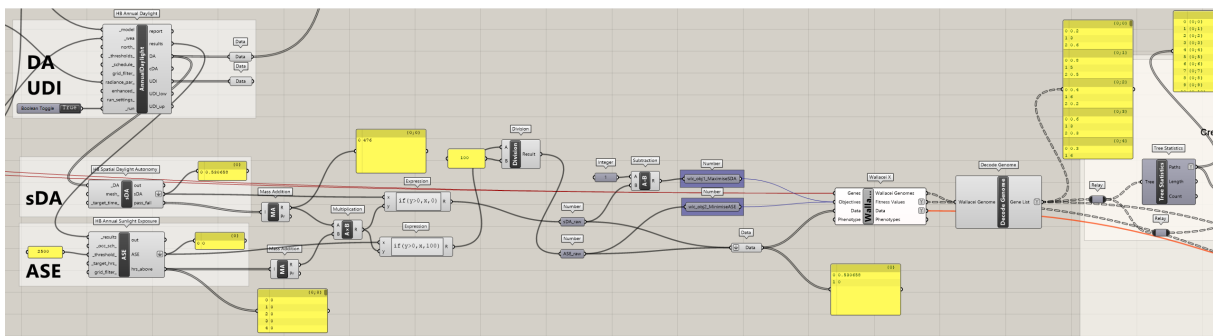


Figure 6.4.1.1: Simulation workflow showing calculation of daylight performance metrics (sDA and ASE) and their integration into Wallacei optimization.ing geometric parameters to performance metrics (sDA and ASE).

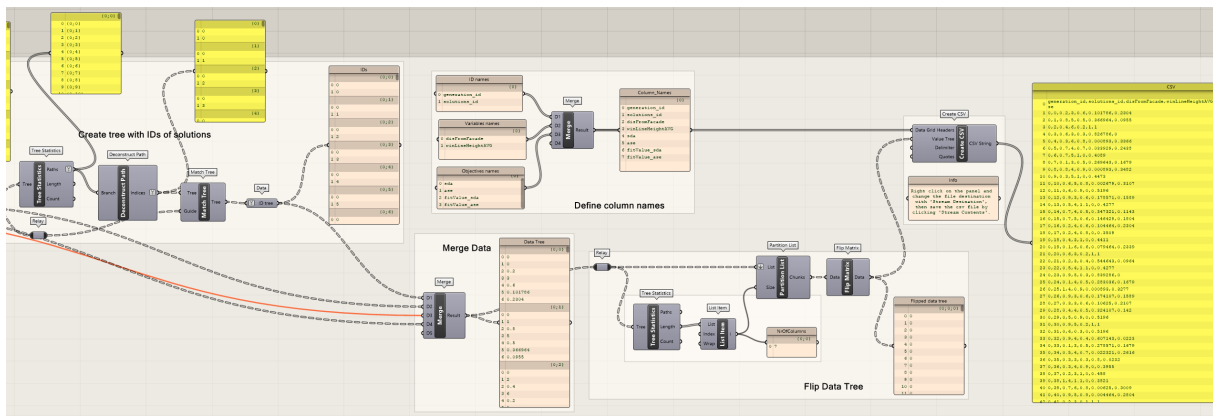


Figure 6.4.1.2: Export of optimization results into structured CSV datasets, enabling traceability and validation of daylight performance.

The genetic algorithm results received additional evaluation through structured CSV dataset export (Figure 6.2.1.2). The process allowed researchers to verify each solution through a systematic analysis of generation ID and solution ID and façade offset and window height ratio and their corresponding daylight performance results. The structured datasets enable the performance of extensive data analysis while validating specific solutions through thorough verification.

The combination of parametric geometry with Honeybee daylight simulation and

Wallacei evolutionary optimization through Figures 6.2.1.1–6.2.1.2 created an ongoing feedback mechanism which connected design exploration to quantifiable environmental results.

### 6.5 Subdivision Strategy for High-Rise Optimization

The Montparnasse Tower’s massive size together with its curved façade made it impossible to optimize the building envelope as one unified system through computation. The façade received vertical and horizontal subdivision treatment according to the approach shown in Figure 6.5. The tower received vertical segmentation into five sections which spanned ten floors to handle changing daylight exposure at different heights. The horizontal division of the façade required three separate sections because of its curved design. The façade receives solar radiation from both the Southeast and Northwest directions at the same time so a three-part division proved to be the most successful method for capturing these combined effects.

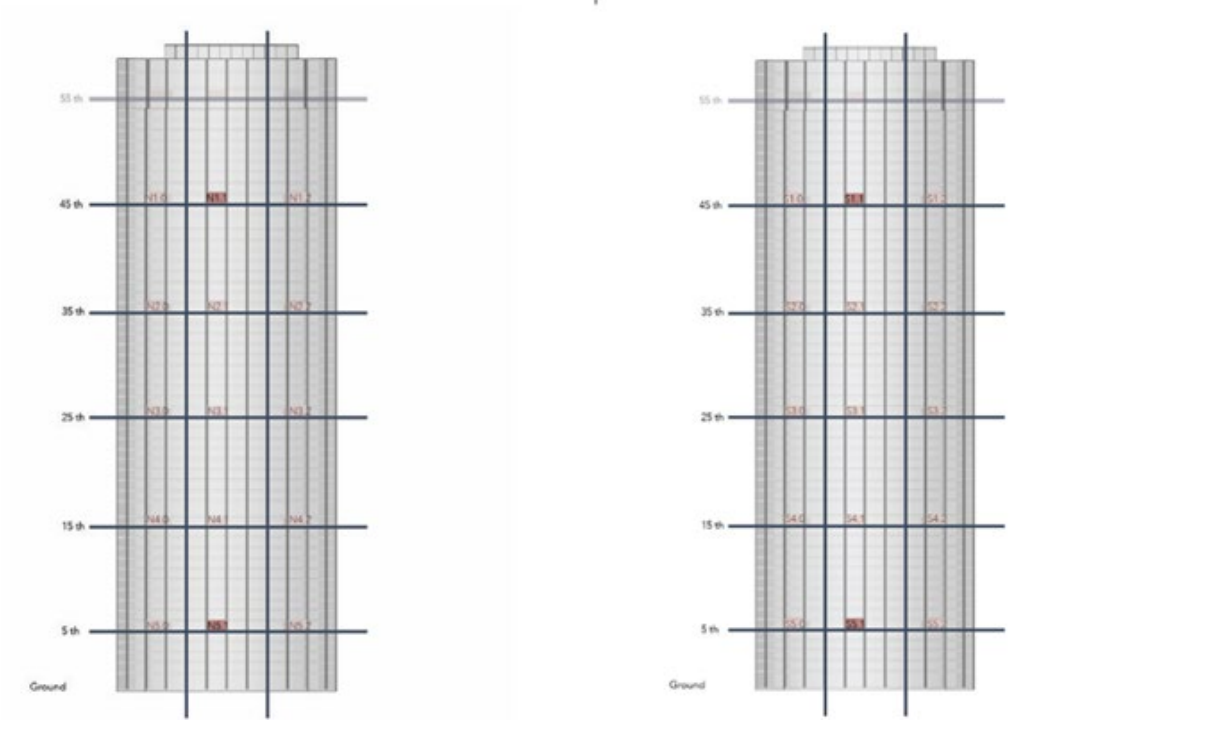


Figure 6.5: Subdivision strategy of the Montparnasse Tower façade, divided into 15 groups (5 vertical × 3 horizontal) to capture variations in solar exposure, with systematic group naming (e.g., S0-0,S1-2 for Southeast, N0-0, N1-2 for Northwest).

The optimization process divided the building into fifteen separate groups which operated independently from each other. The optimization system processed orientation-based solar conditions through this method while maintaining workable computational requirements. The simulations showed that the two highest groups generated matching results (Figure 6.5) because daylight performance remained steady at the tower’s uppermost sections. The optimization process eliminated unnecessary computation because the top two groups produced identical results.

To verify the reliability of the optimization process, all results were exported from Wallacei in CSV format and systematically checked in Excel (Figure 6.6.2). Each of the fifteen façade groups was analyzed individually, with results sorted by sDA and ASE performance. This additional step confirmed which groups satisfied LEED criteria and highlighted cases where geometric feasibility or user comfort considerations required further adjustment.

The optimization process required a systematic naming system to maintain clarity throughout the analysis. The Southeast-facing exterior received its first row of labels starting from S0-0 to S1-2 followed by S1-0 to S1-2 for the second row and continuing this pattern down to the bottom levels. The Northwest-facing exterior received its group labels starting from N0-0 to N0-2 followed by N1-0 to N1-2 and continuing this pattern for all levels. The established nomenclature system enabled the identification and comparison of results between groups while making data management and visualization simpler throughout the analysis, which later helped with Wallacei optimization runs.

### 6.6 Evolutionary Outcomes

The optimization process demonstrated a distinct pattern of solution convergence. The initial population solutions showed wide-ranging values but most of them did not meet LEED daylight requirements. The optimization process led to a substantial growth of solutions that met both  $sDA \geq 55\%$  and  $ASE \leq 10\%$  criteria and the final Pareto front contained solutions with high performance values (Figure 6.6.1).

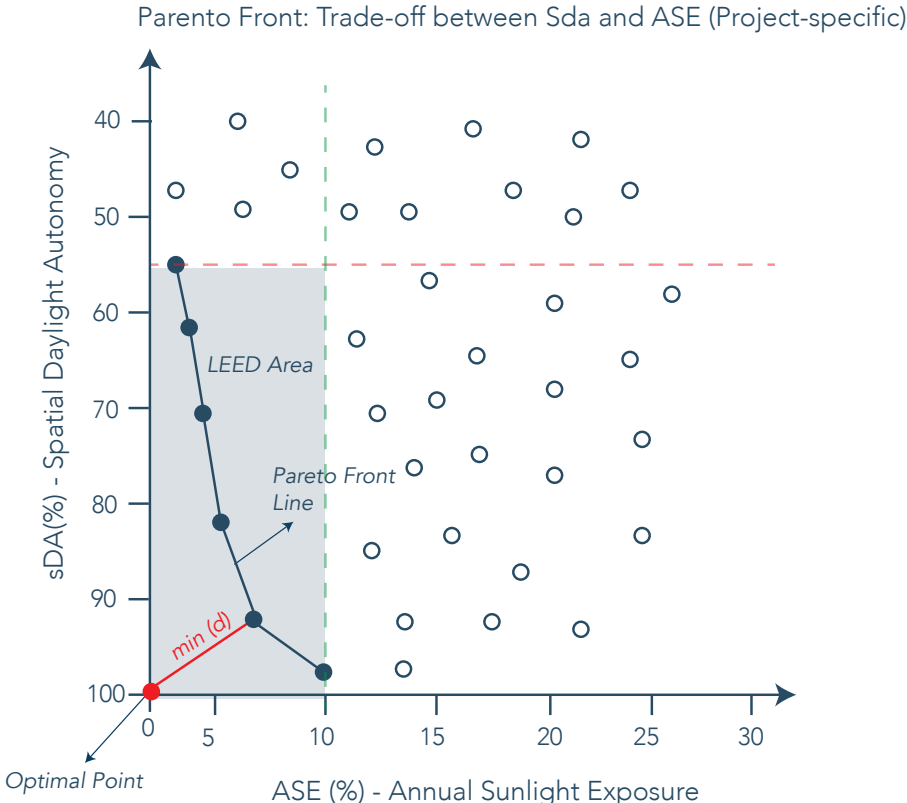


Figure 6.6.1: Pareto front diagram showing trade-offs between sDA and ASE across optimized solutions.

The results demonstrated that better daylight autonomy requires sacrificing some level of overexposure in building design. The results indicated that higher sDA values produced greater ASE values but ASE values below a certain threshold resulted in decreased daylight penetration. Wallacei provided a clear view of the performance tradeoffs between daylight autonomy and overexposure, enabling the finding of optimal solutions without compromising either metric.

The process reliability was confirmed through exporting results from Wallacei to CSV format which was then reviewed in Excel for systematic analysis. The fifteen façade groups received individual evaluation through sDA and ASE performance classification. This additional step confirmed which groups complied with LEED criteria while also identifying cases where geometric feasibility or occupant comfort considerations required further refinement (Figure 6.6.2).

Sheet	Valid Solutions (sDA > 0.55, ASE < 0.15)	Distance from Facade min (m)	Distance from Facade max (m)	Glazing Height Ratio min (%)	Glazing Height Ratio max (%)
S1-0	146	0.7	1	45%	50%
S1-1	186	0.7	1	45%	50%
S1-2	126	0.4	1	45%	50%
S2-0	163	0.7	1	45%	50%
S2-1	179	0.7	1	45%	50%
S2-2	144	0.7	1	50%	55%
S3-0	62	0.9	1	50%	50%
S3-1	83	0.8	1	50%	50%
S3-2	118	0.7	1	50%	50%
S4-0	0	0	0	0%	0%
S4-1	32	0.8	1	50%	50%
S4-2	113	0.7	1	50%	55%
S5-0	0	0	0	0%	0%
S5-1	3	0.95	0.95	60%	50%
S5-2	0	0	0	0%	0%

Figure 6.6.2: Example of Excel verification of Wallacei outputs, validating daylight performance results for façade groups.

The south façade, identified as the most critical in terms of daylight performance, was examined in greater detail. For each shoebox model, 1,000 outputs were assessed under three different conditions. The first condition required sDA values above 55% and ASE values below 10% to meet LEED daylight standards. The models S4-0 and S5-0 and S5-2 failed to generate valid results under this specific condition. The design constraints included a minimum distance of 0.70 m from the façade and a maximum glazing height ratio between 50–55% which would be established in future stages.

The second condition introduced a blind system for LEED compliance evaluation through modified criteria which required sDA > 55% and ASE < 15%. The shoebox models S5-0 and all other models produced valid results under this scenario. In certain cases, the distance from the façade decreased to 0.25 m, while shoeboxes on the upper floors maintained values around 0.70 m. The glazing height ratio also extended to the 55–60% range.

The third condition, defined as sDA > 55% and ASE < 20%, produced valid outcomes across all shoebox models. In this case, both the distance from the façade and the glazing height ratio exhibited broader ranges of values.

The research results support the development of design restrictions for future chapters which must use  $sDA > 55\%$  and  $ASE < 20\%$  while enabling blind system applications. The decision supports both design strategies and LEED daylight performance requirements for the entire project which establishes a solid base for the upcoming retrofit solutions.

The optimization process revealed that reaching the highest level of daylight autonomy creates an opposing requirement to stop excessive sunlight penetration. The solutions which achieved maximum  $sDA$  values also showed higher  $ASE$  measurements while solutions with minimal  $ASE$  values resulted in reduced daylight access. The system used by Wallacei demonstrated its power by showing how to find solutions that balanced daylight autonomy with  $ASE$  requirements, rather than choosing one objective over the other.

The optimization results from Wallacei were exported to CSV format for Excel verification through Excel analysis (Figure 6.6.2). The analysis of each of the fifteen façade groups occurred separately through Excel where results were arranged based on  $sDA$  and  $ASE$  performance. The additional verification process showed which groups met LEED requirements while identifying specific cases that needed modifications for geometric feasibility and user comfort.

## **6.7 Implementation of the Optimization**

The shoebox analysis results showed that the angled façade strategy offered the best potential so Wallacei was used to optimize this design. The optimization process started with 1000 different façade populations which represented distinct variations of the established parameters. The genetic algorithm in Wallacei selected superior solutions to advance through generations while discarding inferior options. The optimization process used multiple cycles to enhance performance and discover the strongest design solutions.

### **6.7.1 Defined Variables**

The optimization process relied mainly on two key parameters which are shown in Figure 6.7.1.

1. The glazing surface projection distance from the façade plane measured in meters.
2. The window height ratio shows the relationship between transparent section height and total floor-to-ceiling height.

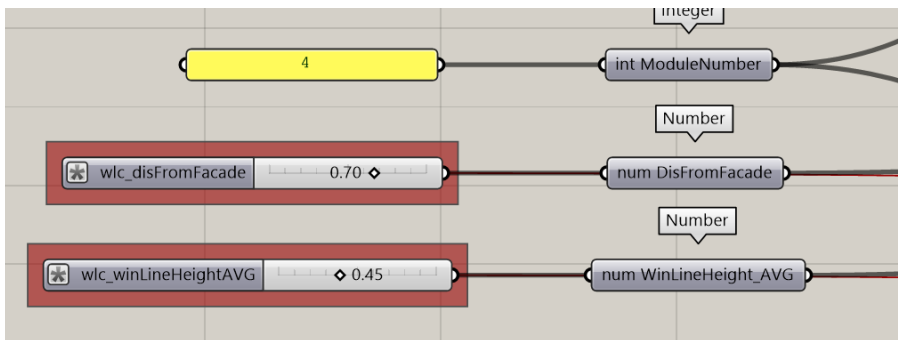
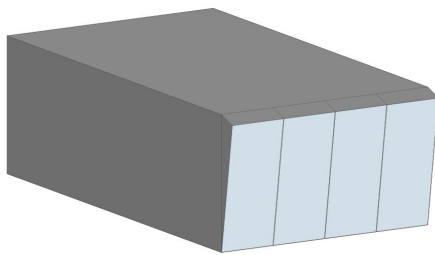
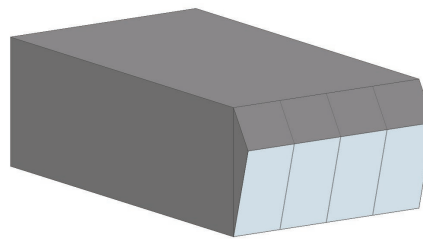


Figure 6.7.1.1: Parametric setup in Grasshopper defining the two optimization variables: façade projection distance and window height ratio.



-Distance from façade : 30 cm  
-Window height ratio : 95%



- Distance from façade : 65cm  
- Window height ratio : 55%

Figure 6.7.1.2: Illustrations façade modules generated by varying projection distance (30 cm–65 cm) and window height ratio (55%–95%), illustrating angular differences in geometry.

The variables shown in Figure 6.7.2 controlled the angle of façade modules which determined the optimal balance between daylight entry and solar protection. The optimization process evaluated multiple angular configurations through systematic distance and height combinations to determine their performance against daylighting requirements.

The module count per façade strip was fixed at four across all stages of the optimization process. The choice of four modules resulted from both design and construction requirements. The four-module façade system followed French façade engineering rules for panel sizes and mullion spacing and structural subframe integration while maintaining a balanced proportional design. The optimized design followed standard curtain wall technology requirements because it used existing systems without needing special modifications.

## 6.8 Results and Final Façade

The optimization results established specific parameters which defined the complete façade system.

The Southeast façade received the highest priority because it required a window

height-to-width ratio of 50% and offset distance between 0.95 m and 1.0 m to achieve the optimal solution. The specified window height ratio of 50% delivered the best numerical results yet it positioned windows at a level which affected eye-level visibility. The glazing height remained at 60% to protect both visual comfort and maintain occupant views. The higher glazing ratio resulted in ASE values reaching 13% which exceeded the LEED requirements. The supplementary control strategy of blinds solved this issue by maintaining both technical performance and user experience of the façade.

The daylight availability at the entrance level reached 53% because of the shading impact from surrounding buildings. The daylight levels reached sufficient levels for functional use although they did not meet the LEED requirements.

The study showed that daylight performance varied depending on the tower's orientation. On the Northwest side, fewer control measures were needed since more transparency could be allowed without issues of solar exposure. This highlighted that every façade needed its own design approach to keep performance balanced throughout the building.

The final design incorporated an angled modular system for the building envelope. The upper sections of each module received opaque treatment to function as permanent shading elements while the lower sections maintained transparency to let in daylight and maintain outdoor visibility. The optimized design geometry fulfilled performance requirements and simultaneously resolved the Montparnasse Tower's monolithic design issue through its sustainable and visually engaging façade design.

The optimized design solution proved that performance-based design methods can meet environmental standards and user needs and architectural goals to create a template for future high-rise building retrofits.

## **6.9 Discussion**

The research results show that performance-based parametric methods succeed in uniting environmental performance with architectural identity. The study revealed that applying  $ASE \leq 10\%$  as a strict performance criterion resulted in solutions that met technical requirements but produced inflexible designs with restricted design options.

The research established specific design constraints which proved essential for practical implementation. The study established that façade distance and window height ratio served as essential design factors because they directly influenced both visual comfort and construction feasibility and maintenance requirements. The study classified all configurations that exceeded these established ranges as non-usable even though they received positive daylight scores.

The research examined three different ASE threshold values which included  $\leq 15\%$  and  $\leq 20\%$  to extend design possibilities. The tested scenarios enabled designers to

create more diverse façade designs which expanded architectural options without compromising performance standards. The research presents a complete evaluation of these scenarios through Chapter 7 which examines Regular, Random and Wave typologies.

The research showed that the  $ASE \leq 10\%$  rule provides comfort assurance but it fails to account for the actual challenges of high-rise urban building retrofits which require balancing performance with construction feasibility and design aesthetics. The research tested different performance thresholds to establish a balanced method which unites performance requirements with design freedom.

The study demonstrates through its results that data-driven optimization techniques can create new possibilities for designing high-rise buildings. The optimized façade of the Montparnasse Tower achieved international sustainability standards while creating a new identity for the tower which transformed its modernist rigid appearance into a context-sensitive environmentally friendly landmark.

## Summary

The chapter explained how to enhance daylight performance at the Montparnasse Tower through Grasshopper-based parametric façade system development. The analysis started with daylight metrics which included sDA and ASE and DA and UDI and GA to establish a basis for evaluating both visual comfort and energy efficiency.

The planar shading systems consisting of vertical fins and overhangs and cross-shading and brise-soleil variations provided some benefits but they never achieved an optimal balance between sDA and ASE measurements. The angled façade modules proved effective because the Northwest façade met LEED requirements with sDA 95% and ASE 6% while the Southeast façade reached its highest performance level at sDA 55% and ASE 13%. The design process should proceed with angled modules because of these positive results.

The Wallacei system evaluated numerous parameter settings from hundreds of combinations across fifteen different façade groups. The analysis showed that achieving maximum daylight autonomy requires sacrificing some level of exposure to sunlight. The research produced orientation-based solutions which showed the Southeast façade needed breaklines at 65-70% of room height with 0.95-1.0 m façade offsets for optimal performance but the Northwest façade required higher transparency ratios with smaller offsets. The optimized façades reached sDA levels between 62% and 65% and ASE levels between 7% and 9% which surpassed the baseline façade results of sDA 47% and ASE 43%.

The final design implemented a four-module angled system which used opaque sections at the top and transparent sections at the bottom. The solution met LEED daylight requirements and handled practical needs by providing visual comfort and enabling maintenance access and construction feasibility.

The research demonstrates that parametric and evolutionary optimization methods help designers achieve better environmental results through innovative architectural designs. The seventh chapter demonstrates how flexible ASE ranges enable designers to generate new design options which extend past basic comfort requirements. The study demonstrates that data-driven design approaches transform high-rise building renovations into sustainable urban landmarks which respect their environmental context.

The research demonstrated that quantitative simulation needs to merge with qualitative assessment because technical optimization fails to produce optimal results when human comfort and construction feasibility and urban context receive no attention.

# ***CHAPTER VII***

## Facade Optioneering

## 7.1 Introduction

This chapter presents a parametric evaluation of façade modules developed through shoe-box-based simulations. The study seeks to investigate the performance of several module types: regular, random, and wave configurations under distinct façade conditions. The findings demonstrate their potential to enhance overall façade design. The analysis relies on Wallacei optimization outcomes that were then enhanced by specific design constraints to ensure technical feasibility and architectural design.

The chapter is structured straightforwardly to examine performance disparities among the façades, sample shoeboxes were initially chosen. The Wallacei outputs for these shoeboxes were then restricted according to determined design limitations. From the filtered results, three typologies regular, random, and wave were applied to each shoebox, creating modules at the shoebox scale. Then these modules were combined at the façade scale to test how the same strategies perform when applied to larger sections of the high-rise building envelope. This two-step approach allowed for evaluating both detailed module behavior and its collective architectural effects at the same time. (Figure 7.1.1.)

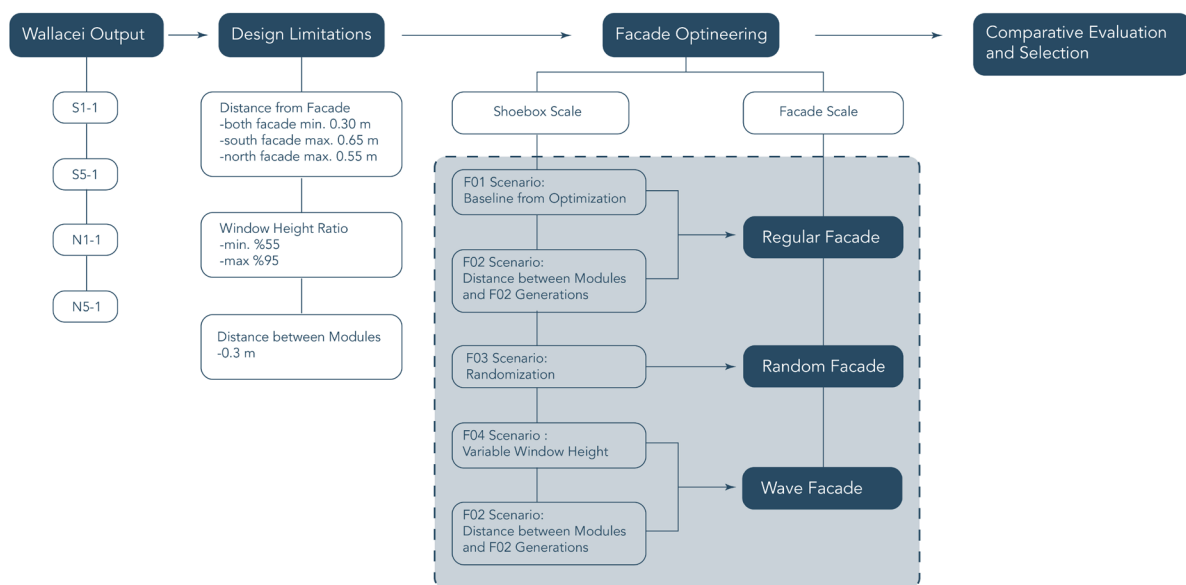


Figure 7.1.1. Facade Optimization Workflow

To understand the performance variations within the building envelope, shoebox models were made for the southeast and northwest façades. A total of 15 models were developed for each façade, and 4 representative cases were chosen: S1-1, S5-1, N1-1, and N5-1. (Figure 7.1.2. & Figure 7.1.3.) These cases demonstrate significant performance differences in highlighting between lower and upper zones, as well as across orientations. Since both façades are about 70m long and have a curved profile due to the almond-shaped building, shoeboxes were picked from the middle zones as well as the top and bottom extremes. This selection allowed for a comparison that looks at boundary conditions and transitional performance characteristics within the façade system.

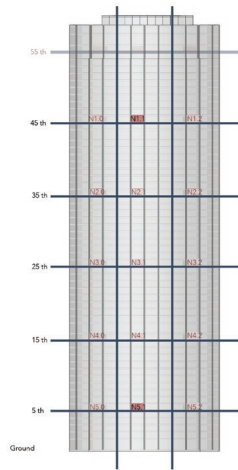


Figure 7.1.2. North-west selected facade shoebox

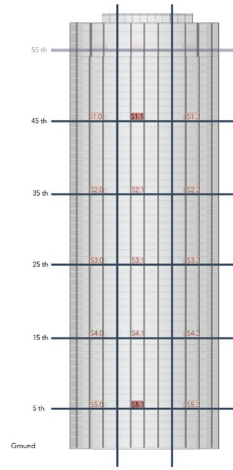


Figure 7.1.3 South-east selected facade shoebox

Constraints were imposed on two parameters derived from the Wallacei outputs, the distance from façade and the window height ratio, along with an additional factor, the spacing between modules. Limitations defined the acceptable design parameters used to evaluate various typologies on the chosen shoebox models. These limitations were intended to ensure visual comfort, ease of maintenance, construction feasibility, and architectural aesthetics. This method allowed for an assessment that harmonized architectural design with daylight performance.

This chapter examines how shoebox-scale analyses conducted at the façade level can be adapted into overall façade strategies for the high-rise building. First, daylight performance of individual rooms was assessed, and then these findings were applied to the selected area's entire façade. The results demonstrate both sustainability and architectural viability.

## 7.2 Design Limitations

The evaluation of Wallacei outputs revealed that while the best-performing generations achieved high environmental efficiency, they still required alignment with design practicality. The decision to introduce design limitations after the Wallacei analysis was deliberate: the initial aim was to observe façade behavior under extreme conditions and identify parameter ranges that best satisfied LEED daylighting criteria. This made it possible to clearly determine which values provided the highest compliance. In addition, this stage helped distinguish between solutions that were theoretically optimal and those that could realistically inform façade strategies.

However, meeting LEED standards alone was not sufficient. Visual comfort, construction feasibility, and maintenance accessibility also had to be considered. For this reason, the design space was narrowed after the analysis, adapting computational results to practical application. This approach balanced optimization outcomes with architectural constraints, ensuring that the proposed façade strategies were both environmentally performant and technically feasible.

## 7.2.1 Glazing Height Ratio and Distance from Façade

Two parameters from the Wallacei dataset were identified as critical: window height ratio and distance from façade.

Window height ratio was limited to values between 55% and 95%. Ratios below 55% did not provide sufficient visual access to the outside, while ratios above 95% were excluded to preserve the architectural continuity of the façade's opaque elements.. Figure 7.2.1. illustrates how the applied limitation translates into glazing geometry and shows that the ratio values can be understood both in terms of their measurable dimensions and their spatial impact on the user experience.

Distance from façade was limited to between 0.30 m and 0.65 m. Offsets greater than 0.65 m would have required additional structural systems, introducing further load and cost implications, while smaller values were retained to balance daylight performance with feasibility. Together, these constraints established the primary design space within which façade module configurations could be meaningfully evaluated.

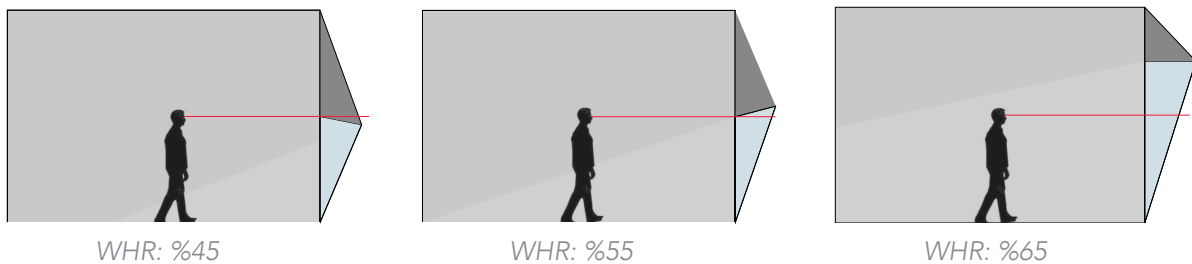


Figure 7.2.1. Impact of Window Height Ratio (WHR) on Geometry and User Experience

### 7.2.1.1. Case S1-1 (South-East, 45th Floor)

The southeast façade in the S1-1 scenario, situated on the 45th floor, experienced significant direct solar exposure, resulting in elevated ASE values. The 18th generation, 37th solution, featuring a façade offset of 0.85 meters and a window height ratio of 50%, was the optimal configuration according to the Wallacei results. This configuration achieved 65% sDA and 9% ASE (Figure 7.2.1.1.1.). This result satisfied the LEED daylight requirements but failed to achieve adequate visual comfort.

generation_id	solutions_id	disFromFacadeCorrected	winLineHeightAVGCorrected	sda	ase	sda-ase	Filter sDA>0.55; ASE<0.1	Filter sDA>0.55; ASE<0.15	Filter sDA>0.55; ASE<0.2
18	37	0.85	0.651087	0.0902	0.560887		1	1	1
15	32	0.95	0.644565	0.087	0.557565		1	1	1
5	16	1	0.640217	0.0837	0.556517		1	1	1
4	18	0.95	0.642391	0.087	0.555391		1	1	1
4	15	0.95	0.45	0.567391	0.0446	0.522791	1	1	1
19	10	0.95	0.45	0.567391	0.0446	0.522791	1	1	1
12	26	1	0.45	0.567391	0.0446	0.522791	1	1	1
2	16	0.9	0.45	0.577174	0.0565	0.520674	1	1	1
13	32	0.75	0.45	0.582609	0.0696	0.513009	1	1	1
19	43	0.85	0.45	0.576087	0.0663	0.509787	1	1	1

Figure 7.2.1.1.1. Example Wallacei result (S1-1) before design limitations

When visual comfort and construction limitations were applied, an alternative configuration emerged as more suitable: 3rd generation, 37th solution, with a façade offset of 0.65 m and a window height ratio of 55%. Under these conditions, 73% sDA and 14% ASE were achieved (Figure 7.2.1.1.2.) This modification improved daylight per-

formance and provided a solution that was compatible with construction feasibility by decreasing module's distance from facade and raising window height. However, the ASE value exceeded the LEED threshold of 10%. For this reason, the integration of solar control elements such as blinds was considered necessary to ensure compliance with visual comfort requirements.

generation_id	solutions_id	disFromFacadeCorrected	winLineHeightAVGCorrected	sda	ase	sda-ase	Filter sDA>0.55; ASE<0.1	Filter sDA>0.55; ASE<0.15	Filter sDA>0.55; ASE<0.2
3	37	0.65	0.55	0.73587	0.1402	0.59567	0	1	1
2	46	0.2	0.55	0.766304	0.188	0.578304	0	0	1
0	19	0.55	0.55	0.73587	0.1576	0.57827	0	0	1
2	45	0.15	0.55	0.767391	0.1902	0.577191	0	0	1
1	14	0.2	0.55	0.748913	0.188	0.560913	0	0	1
0	41	0.15	0.5	0.666304	0.1641	0.502204	0	0	1
0	11	0.25	0.45	0.591304	0.1196	0.471704	0	1	1
0	42	0.4	0.45	0.575	0.113	0.462	0	1	1

Figure 7.2.1.1.2. Example Wallacei result (S1-1) after design limitations

Figure 7.2.1.1.3 illustrates the Wallacei outputs subsequent to the application of design constraints, signifying that it depicts a refined subset of all configurations initially produced during the optimization process. Orange circles represent configurations that satisfy LEED daylighting criteria (sDA > 55%, ASE < 10%); blue squares denote viable options with ASE values between 10% and 20%; and black crosses indicate non-viable results that either surpassed ASE thresholds or violated geometric constraints.

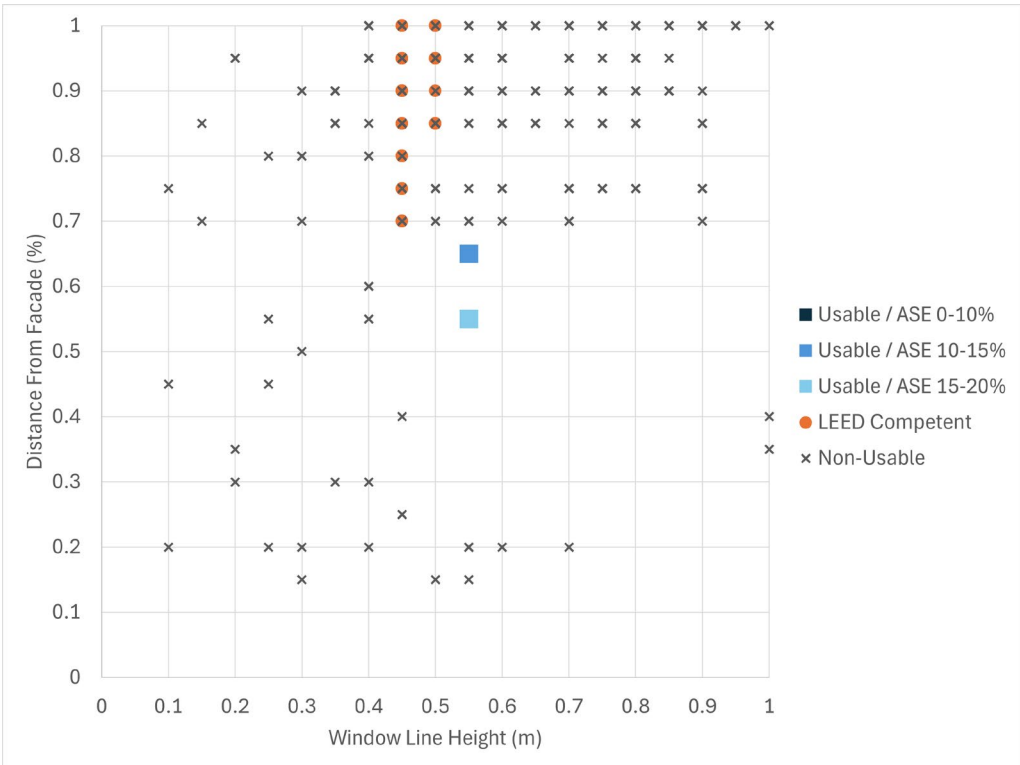


Figure 7.2.1.1.3. Filtered Wallacei results for S1-1 after design limitations

This assessment underscores that the intersection of daylight efficiency and practical limitations results in a limited array of feasible solutions. Solutions nearest to LEED compliance were prioritized, ensuring that both environmental and constructability criteria informed the final façade design.

### 7.2.1.2 Case S5-1 (South-East, 5th Floor)

In the S5-1 scenario, the south-east façade at the 5th floor produced specific challenges compared to the upper zones, such as being partially shaded by surrounding buildings. According to the Wallacei results, the 17th generation, 44th solution, which has a window height ratio of 60% and a distance from the facade of 0.95 meters, is the ideal configuration. This setup achieved 55% sDA and 9% ASE. (Figure 7.2.1.2.1) Although it represented the only configuration where ASE values remained below the 10% threshold, the outcome was still problematic. The façade offset of 0.95m exceeded the established limitation, and the sDA of 55% was just at the minimum acceptable boundary, leaving little tolerance for performance stability.

generation_id	solutions_id	disFromFacadeCorrected	winLineHeightAVGCorrected	sda	ase	sda-ase	Filter sDA>0.55; ASE<0.1	Filter sDA>0.55; ASE<0.15	Filter sDA>0.55; ASE<0.2
17	43	1	0.698913	0.8	0.698913	0.1826	0.516313	0	1
4	28	0.9	0.8	0.701087	0.1978	0.503287	0	0	1
11	49	1	0.8	0.684783	0.1826	0.502183	0	0	1
12	40	0.95	0.75	0.666304	0.1652	0.501104	0	0	1
10	43	0.9	0.8	0.690217	0.1978	0.492417	0	0	1
7	28	0.85	0.75	0.669565	0.1815	0.488065	0	0	1
5	29	0.95	0.75	0.653261	0.1652	0.488061	0	0	1
19	46	0.95	0.7	0.625	0.1402	0.4848	0	1	1
0	9	0.75	0.75	0.668478	0.1837	0.484778	0	0	1
8	30	1	0.7	0.619565	0.138	0.481565	0	1	1
10	34	1	0.75	0.641304	0.1598	0.481504	0	0	1

Figure 7.2.1.2.1. Example Wallacei result (S5-1) before design limitations

To reconcile these findings with the defined design constraints, the configuration was re-evaluated under more feasible parameters. Figure 7.2.1.2.2 indicates that the 3rd generation, 35th solution yielded a distance from facade of 0.65m and a window height ratio of 70%, had 62% sDA and 17.5% ASE. The ASE value above the LEED threshold, although this result was deemed acceptable when coupled with the implementation of sun control devices like blinds, aligns the ASE range within a permissible level of 15–20%.

generation_id	solutions_id	disFromFacadeCorrected	winLineHeightAVGCorrected	sda	ase	sda-ase	Filter sDA>0.55; ASE<0.1	Filter sDA>0.55; ASE<0.15	Filter sDA>0.55; ASE<0.2
3	35	0.65	0.7	0.628261	0.175	0.453261	0	0	1
4	43	0.65	0.7	0.628261	0.175	0.453261	0	0	1
0	22	0.5	0.7	0.630435	0.187	0.443435	0	0	1
1	20	0.5	0.7	0.630435	0.187	0.443435	0	0	1
1	19	0.65	0.7	0.617391	0.175	0.442391	0	0	1
2	25	0.65	0.7	0.617391	0.175	0.442391	0	0	1
2	26	0.6	0.7	0.618478	0.1826	0.435878	0	0	1
0	8	0.35	0.65	0.597826	0.1826	0.415226	0	0	1
1	47	0.35	0.65	0.597826	0.1826	0.415226	0	0	1
2	41	0.65	0.55	0.509783	0.0957	0.414083	0	0	0
0	19	0.55	0.55	0.508696	0.113	0.395696	0	0	0
1	5	0.55	0.55	0.508696	0.113	0.395696	0	0	0

Figure 7.2.1.2.2. Example Wallacei result (S5-1) after design limitations

After this modification, the S5-1 filtered results were combined and shown in Figure 7.2.1.2.3. A detailed summary of the optimization results is given in the figure, which displays the distribution of all tested configurations within the specified design constraints. Orange circles represent configurations that satisfy LEED daylighting criteria (sDA > 55%, ASE < 10%); blue squares denote viable options with ASE values between 10% and 20%; and black crosses indicate non-viable results that either surpassed ASE thresholds or violated geometric constraints. This comparative study highlights how the range of feasible solutions for the S5-1 shoebox model was greatly diminished by the combined application of daylight performance, construction feasibility, and visual comfort requirements.

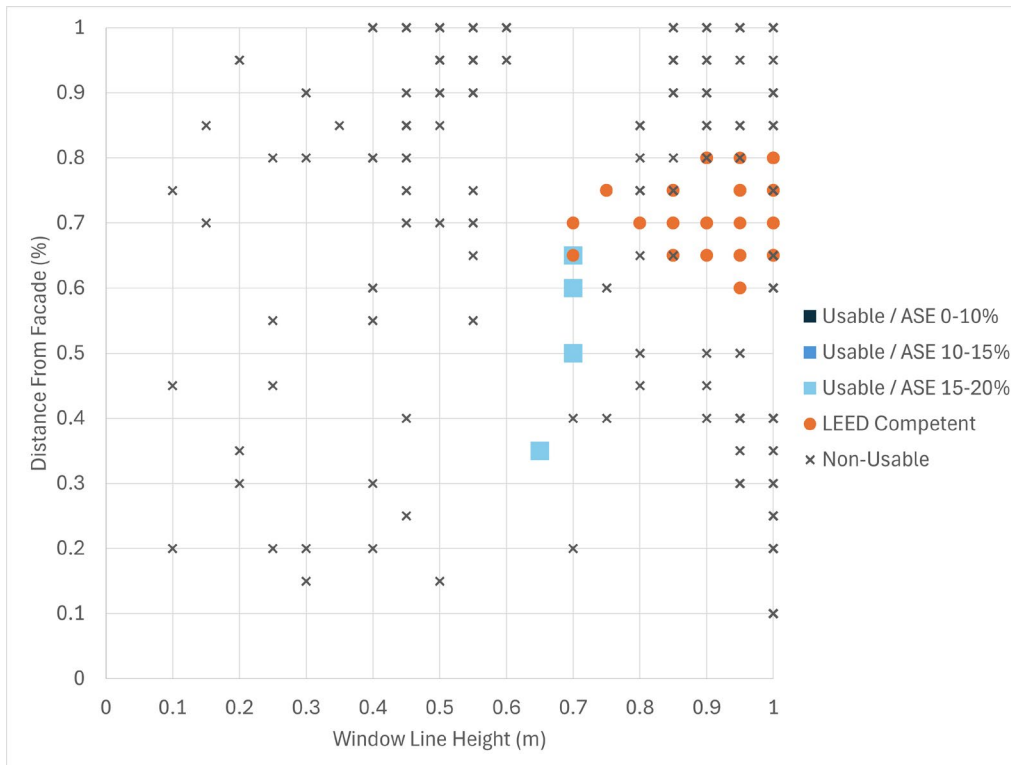


Figure 7.2.1.2.3 Filtered Wallacei results for S5-1 after design limitations

### 7.2.1.3 Case N1-1 (North-West, 45th Floor)

The north-west façade yielded extremely effective daylighting results in the N1-1 scenario. A variety of configurations in the Wallacei dataset demonstrated exceptional visual comfort potential by achieving higher sDA of over 85% while keeping ASE values below 10%. The 5th generation, 7th solution, which had a window height ratio of 100% and a distance from façade of 1 m, was one of the best-performing examples. With 99% sDA and 4% ASE, this configuration produced a nearly perfect balance between glare reduction and daylight availability. (Figure 7.2.1.3.1.) Nevertheless, the configuration exceeded the design limitations, since the maximum window height ratio was restricted to 95% and the façade offset had to remain at or below 0.50m.

generation_id	solutions_id	disFromFaçade	GlazingHeightRatio	sda	ase	sda-ase	Filter sDA>0.85; ASE<0.1
5	7	1	1	0.993478	0.0467	0.946778	1
12	24	0.95	1	0.994565	0.0478	0.946765	1
12	22	1	0.95	0.983696	0.0435	0.940196	1
7	13	0.9	1	0.995652	0.0576	0.938052	1
11	23	0.85	1	0.996739	0.0609	0.935839	1
1	4	1	0.9	0.966304	0.0315	0.934804	1
6	11	0.75	1	0.996739	0.062	0.934739	1
1	5	0.8	1	0.996739	0.063	0.933739	1
4	12	0.85	1	0.994565	0.0609	0.933665	1

Figure 7.2.1.3.1. Example Wallacei result (N1-1) before design limitations

After applying these constraints, a feasible alternative was identified, as reported in Figure 7.2.1.3.2. The 0th generation, 37th solution, with a façade offset of 0.50m and a window height ratio of 95%, achieved 99% sDA and 8% ASE. The results indicate that the difference in daylight performance between 1.0 m and 0.50 m distance from the façade is minimal, and with the applied design limitations, the LEED daylight requirements are still met.

generation_id	solutions_id	disFromFacade	GlazingHeightRatio	sda	ase	sda-ase	Filter sDA>0.85; ASE<0.1
0	37	0.5	0.95	0.991304	0.0804	0.910904	1
0	3	0.4	0.95	0.994565	0.0848	0.909765	1
1	14	0.45	0.9	0.978261	0.0739	0.904361	1
2	37	0.4	0.9	0.981522	0.0826	0.898922	1
2	33	0.25	0.95	0.996739	0.0989	0.897839	1
2	49	0.35	0.9	0.983696	0.0859	0.897796	1
1	20	0.25	0.95	0.995652	0.0989	0.896752	1
1	31	0.35	0.9	0.979348	0.0859	0.893448	1
1	34	0.5	0.8	0.9	0.0554	0.8446	1
1	33	0.4	0.8	0.906522	0.0707	0.835822	1
1	37	0.15	0.8	0.925	0.0913	0.8337	1

Figure 7.2.1.3.2. Example Wallacei result (N1-1) after design limitations

As with the other cases, the complete set of results for N1-1 was consolidated and visualized in Figure 7.2.1.3.3, illustrating the distribution of all tested configurations and clarifying how the design limitations guided the selection of usable solutions. Orange circles represent configurations that satisfy LEED daylighting criteria (sDA > 55%, ASE < 10%); blue squares denote viable options with ASE values between 10% and 20%; and black crosses indicate non-viable results that either surpassed ASE thresholds or violated geometric constraints.

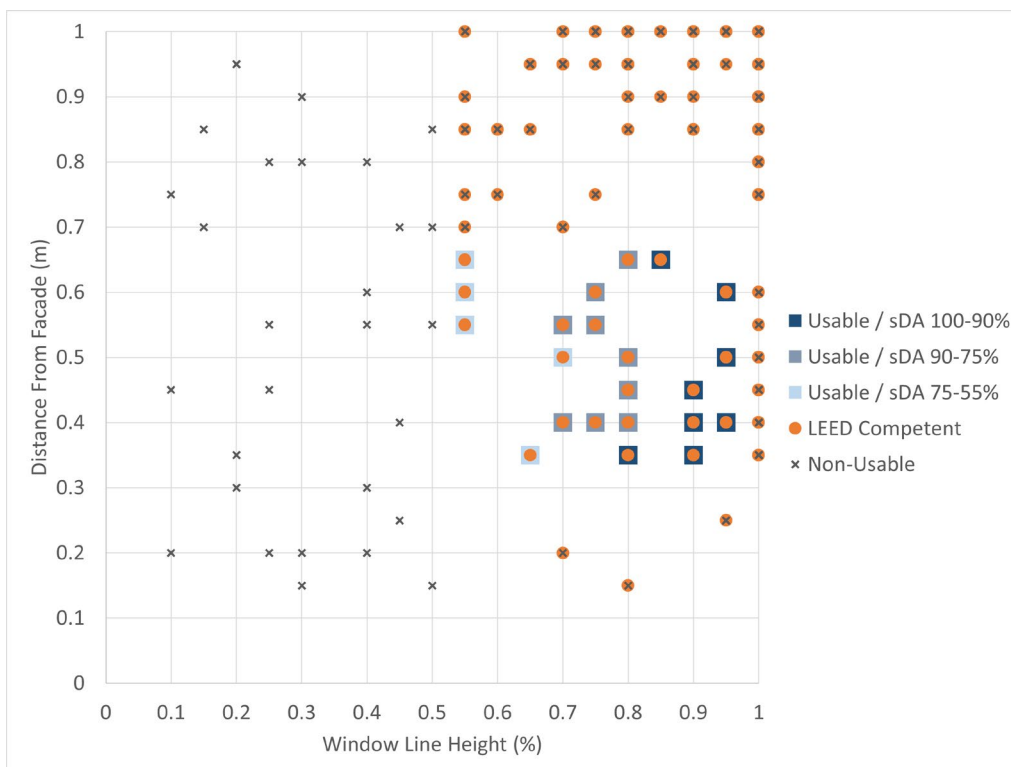


Figure 7.2.1.3.3 Filtered Wallacei results for N1-1 after design limitations

### 7.2.1.4 Case N5-1 (North-West, 5th Floor)

In the N5-1 scenario, the north-west façade produced a set of results that initially appeared highly favorable. Several configurations obtained sDA values above 85% along with ASE values below 10% when the Wallacei outputs were examined. These results, however, were often clustered very closely together, showing only minor variations in performance.

In Figure 7.2.1.4.1., the 13th generation, 10th solution reached a façade offset of 1.00m with a window height ratio of 100%, achieving 95% sDA and 4% ASE. Although this outcome was highly efficient in terms of daylight performance, it exceeded the established design limitations, since the window height ratio was capped at 95% and the façade offset was required to remain below 0.50m.

generation_id	solutions_id	disFromFacade	GlazingHeightRatio	sda	ase	sda-ase	Filter sDA>0.85; ASE<0.1
13	10	1	1	0.958696	0.0467	0.911996	1
8	9	0.75	1	0.970652	0.062	0.908652	1
10	21	0.8	1	0.961957	0.063	0.898957	1
3	5	0.95	1	0.945652	0.0478	0.897852	1
2	6	0.9	1	0.955435	0.0576	0.897835	1
12	22	0.75	1	0.959783	0.062	0.897783	1
15	36	0.8	1	0.958696	0.063	0.895696	1
6	8	0.8	1	0.956522	0.063	0.893522	1
17	38	0.5	1	0.975	0.0815	0.8935	1
4	16	0.8	1	0.955435	0.063	0.892435	1

Figure 7.2.1.4.1. Example Wallacei result (N5-1) before design limitations

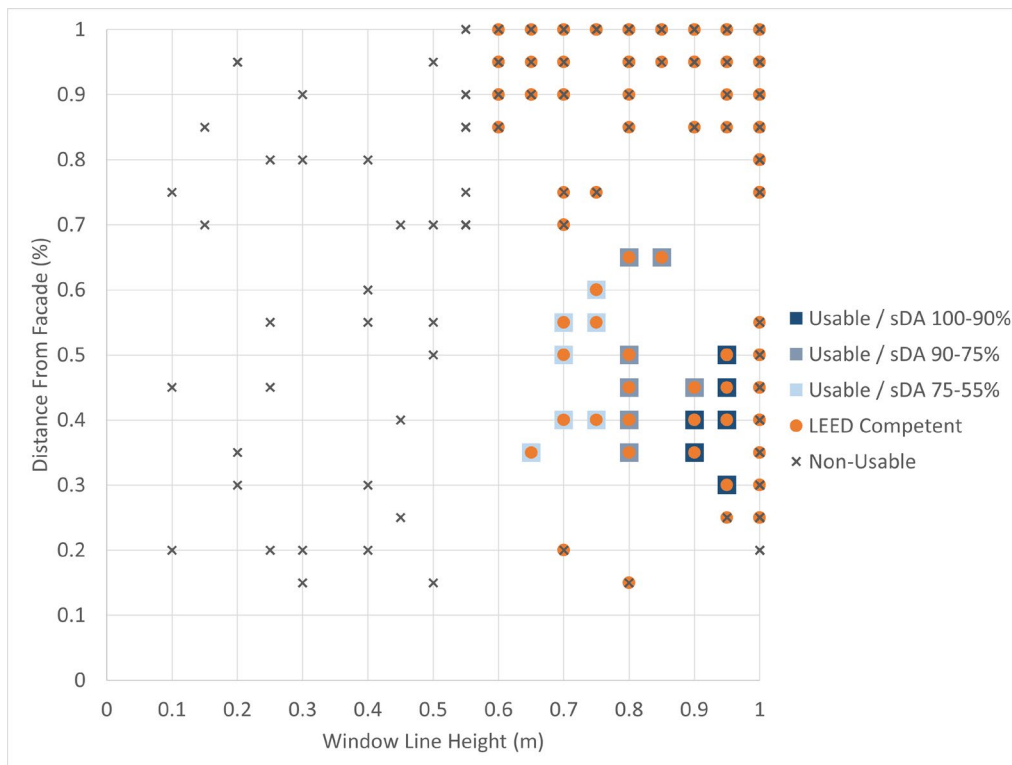
When these limitations were applied, a more representative solution emerged, as shown in Figure 7.2.1.4.2. The 4th generation, 11 solution, including a façade offset of 0.50 meters and a window height ratio of 95%, achieved 96% sDA and 8% ASE. This arrangement met the established limits while providing superior daylighting outcomes within the LEED compliance parameters.

generation_id	solutions_id	disFromFacade	GlazingHeightRatio	sda	ase	sda-ase	Filter sDA>0.85; ASE<0.1
4	11	0.5	0.95	0.96413	0.0804	0.88373	1
1	13	0.4	0.95	0.953261	0.0848	0.868461	1
2	44	0.3	0.95	0.951087	0.0946	0.856487	1
2	37	0.45	0.95	0.934783	0.0793	0.855483	1
1	21	0.25	0.95	0.954348	0.0989	0.855448	1
1	26	0.35	0.9	0.913043	0.0859	0.827143	1
1	15	0.4	0.9	0.908696	0.0826	0.826096	1
1	16	0.45	0.9	0.896739	0.0728	0.823939	1
1	29	0.35	0.8	0.809783	0.0717	0.738083	0
1	30	0.4	0.8	0.807609	0.0707	0.736909	0
1	36	0.5	0.8	0.786957	0.0554	0.731557	0

Figure 7.2.1.4.2. Example Wallacei result (N5-1) after design limitations

A comprehensive overview of the N5-1 case was obtained by consolidating the complete set of Wallacei outputs in Figure 7.2.1.4.3. illustrates the distribution of all configurations the application of design limitations, allowing a clear comparison between the unconstrained optimization results and the refined, feasible subset. This visualization demonstrates how narrowing the design space to viable parameters preserved high levels of daylight performance while ensuring architectural applicability. Orange circles represent configurations that satisfy LEED daylighting criteria (sDA > 55%, ASE < 10%); blue squares denote viable options with ASE values between 10% and 20%; and black crosses indicate non-viable results that either surpassed ASE thresholds or violated geometric constraints.

Overall, the comparative evaluation of S1-1, S5-1, N1-1, and N5-1 cases demonstrated that only a narrow subset of configurations met both daylight performance targets and design limitations, underscoring the need to balance environmental outcomes with architectural feasibility in the development of the façade strategy.



7.2.1.4.3 Filtered Wallacei results for N5-1 after design limitations

## 7.2.2 Spacing Between the Modules

To improve accessibility and practicality, the module spacing was optimized in addition to the two parameters derived from the Wallacei dataset. The modules were initially when 90 degree modules taken from the Schüco Parametric System Technical Documentation spacing between the modules set up with a distance of 3 cm.

Further evaluations demonstrated that this initial spacing was inadequate for both maintenance and installation. A distance of 3 cm did not allow for sufficient access between the modules, making façade cleaning and upkeep practically unfeasible. To address this limitation, the opaque side surfaces of the modules were reconfigured with angled geometries, and alternative spacing scenarios of 20 cm, 30 cm and 40 cm were examined.

In order to overcome this limitation, the modules' opaque lateral surfaces were redesigned with angled geometries, and various spacing arrangements of 20 cm, 30 cm, and 40 cm were examined. Each spacing setting proportionately diminishes the window width from both sides due to the fixed module width of 1.45 m. With a spacing of 40 cm, the glazing width decreases to 1.05 m; with 30 cm spacing, it measures 1.15 m; and at 20 cm spacing, it increases to 1.25 m. The maximum transparent area is achieved with a 20 cm gap; however, this does not allow sufficient space for maintenance. Conversely, daylight capacity decreases significantly at a distance of 40 cm. The 30 cm spacing was identified as the optimal choice, as it ensures accessibility while maintaining performance deterioration within acceptable limits.(Figure 7.2.2.)

These findings demonstrate that the distance between modules is not merely a

secondary technical detail but a critical design parameter that directly affects both environmental performance, particularly in terms of daylight availability, and practical feasibility related to installation and maintenance. Based on this evaluation, a spacing of 30 cm was identified as the most appropriate configuration, since it established a balance between performance and constructability. This refinement allowed for the effective integration of modular elements into the façade system and reinforced the overall sustainability goals of the design.

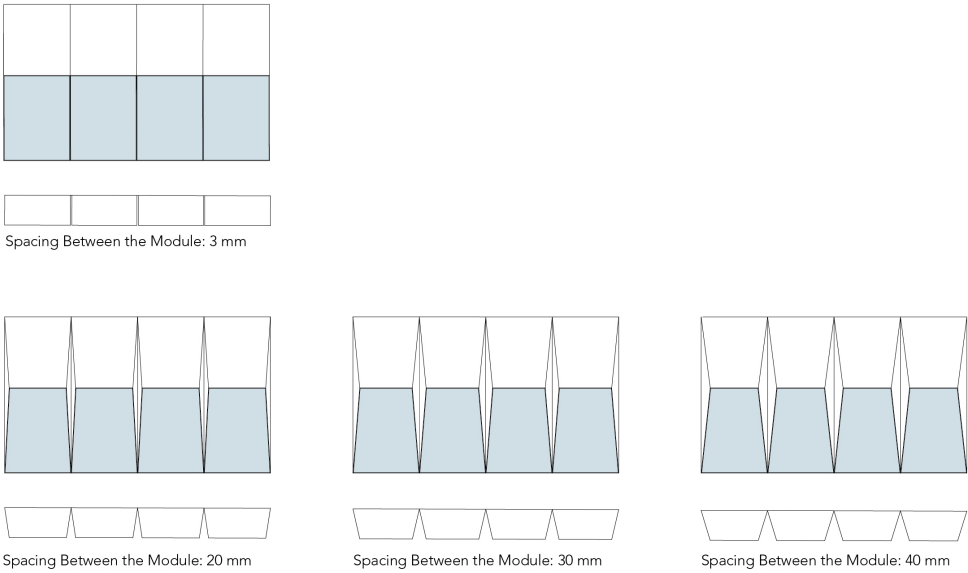


Figure 7.2.2. Spacing between module options

The evaluation established key design constraints for façade modules: window height ratio limited to 55–95%, façade distance set at 0.30–0.65 m on the south-east and 0.30–0.55 m on the north-west sides, and module spacing optimized at 30 cm. These constraints were applied to the shoebox cases to ensure a balance between daylight performance, construction feasibility, visual comfort, and architectural expression. Building on these defined boundaries, the following chapter develops alternative scenarios that enable a comparative study of different façade strategies.

**7.3 S1-1 (South-East, 45th Floor)**

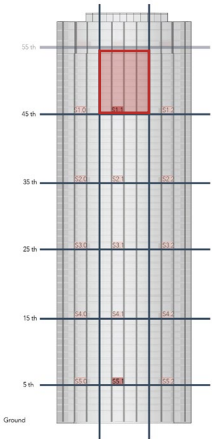


Figure 7.3 S1-1 study area

The S1-1 scenario concentrated on the southeast façade at the 45th level, where orientation and substantial exposure to direct sunlight markedly affected daylight analyses. This configuration, marked by substantial direct sunlight, resulted in heightened ASE values, highlighting the inherent challenge of balancing daylight accessibility with visual comfort on the upper floors of the tower. In addition, this scenario emphasized the sensitivity of the façade design to orientation-specific conditions.

Furthermore, daylight analyses will first be carried out on the S1-1 shoebox model, and later these results will be applied and tested at the façade scale within the designated 10-floor zone.(Figure 7.3)

### 7.3.1.Regular Facade

#### 7.3.1.1. F01 Scenario: Baseline from Optimization

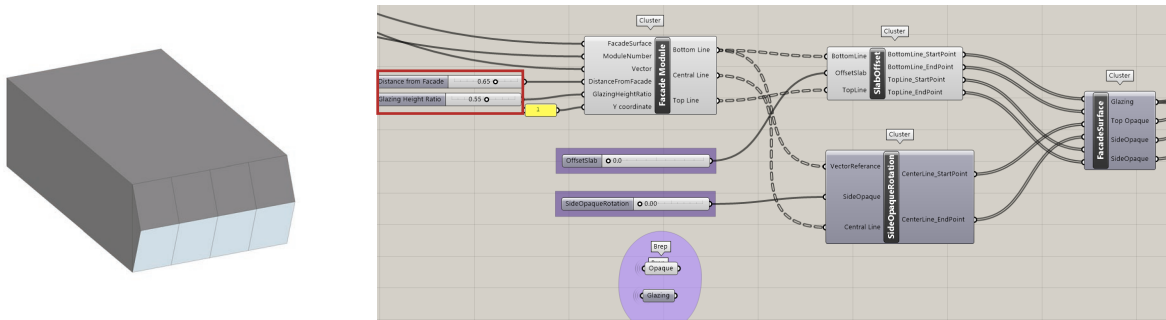


Figure 7.3.1.1.1. F01 Shoebox (S1-1) and Grasshopper Parameters

The F01 scenario was defined directly from the optimization results presented in the previous chapter. Based on the applied construction and comfort limitations, the configuration identified as generation 3, solution 37 (0.65 m distance from façade and 55% window height ratio) was adopted as the baseline (Figure 7.3.1.1.1.). This Excel-based output served as the reference point for the development of new façade modules through shoebox models.

#### 7.3.1.2. F02 Scenario:Distance between Modules

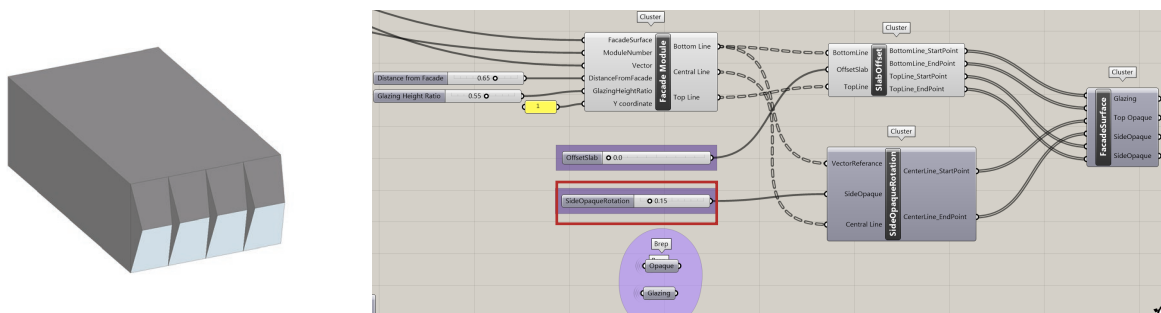


Figure 7.3.1.2.2. F02 Shoebox (S1-1) and Grasshopper Parameters

According to the design limits (Section 7.2.2), modules need to be spaced by 30 cm. To evaluate the impact of the 30 cm separation on daylight distribution, the F02 scenarios were analyzed. (Figure 7.3.1.2.2). A sDA of 72.5% and an ASE of 14% were obtained in the F01 scenario, whereas a sDA of 64% and an ASE of 12% were obtained in the F02 scenario. (Figure 7.3.1.2.3)

F01 increased the amount of daylight available, but it also increased the risk of glare annually. A better balance between daylight performance, visual comfort, and maintenance needs was achieved by F02, on the other hand, which ensured adequate daylight autonomy while limiting excessive sunlight exposure.

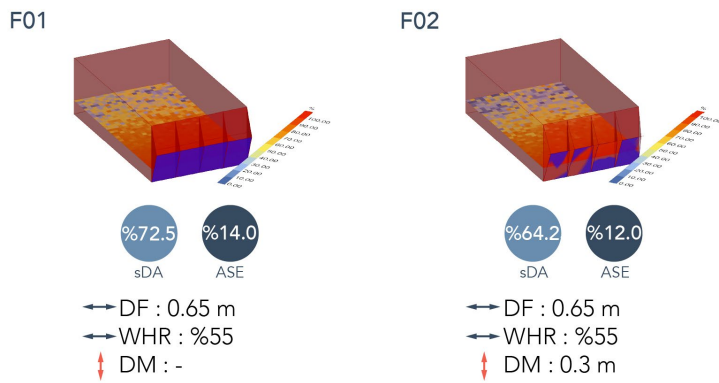
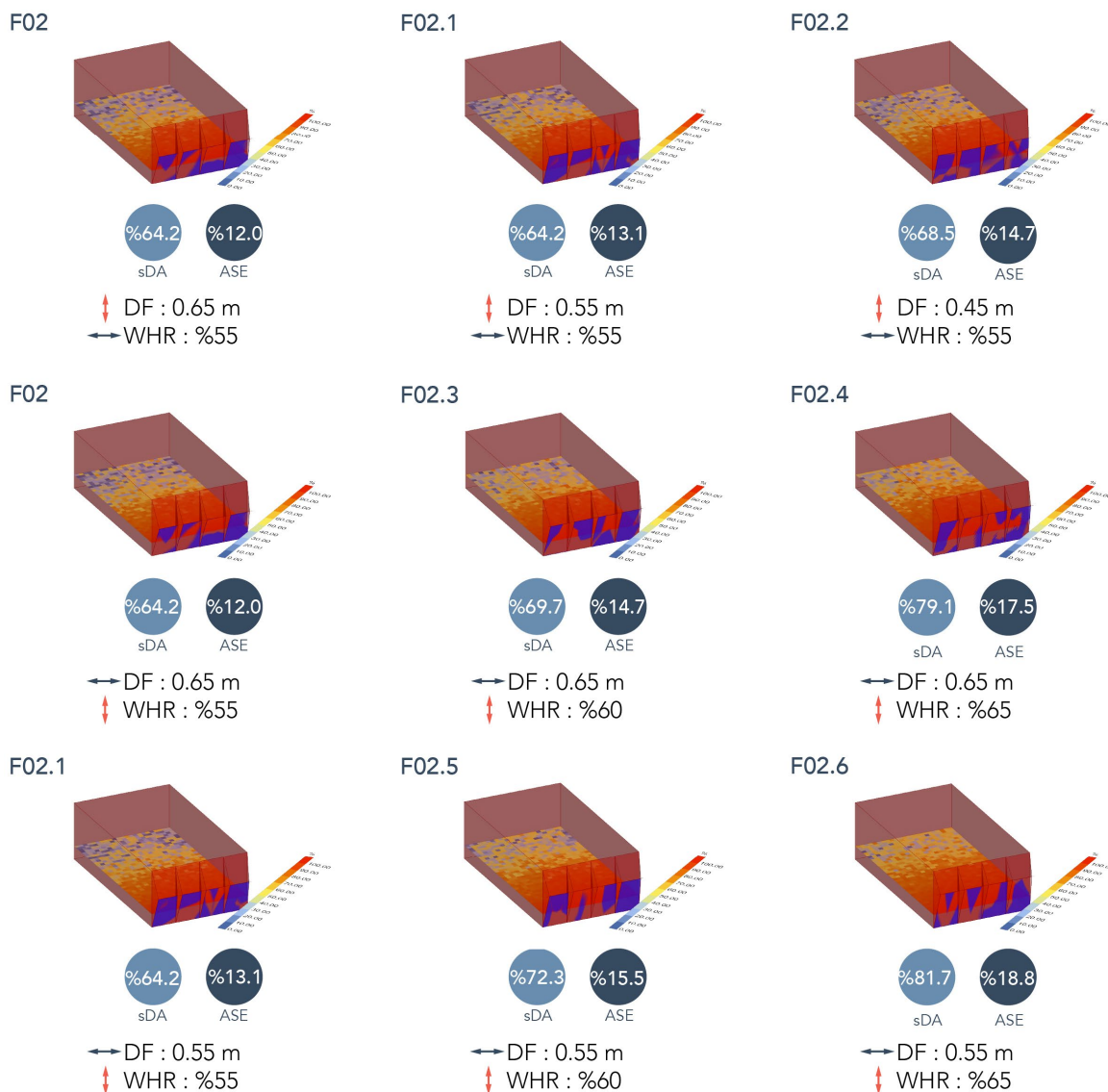


Figure 7.3.1.2.3. F01 and F02 (S1-1) Parameters and Daylight Results

However, applying this solution uniformly across the façade risked producing monotony. For this reason, F02 was treated as a reference scenario from which further variations were generated by adjusting the façade offset (0.65 m, 0.55 m, 0.45 m) and window height ratio (55%, 60%, 65%), resulting in 9 alternatives (F02.1–F02.8)

With the window height ratio fixed at %55, distance from the façade was varied to compare scenarios F02, F02.1, and F02.2. Conversely, when the distance from the



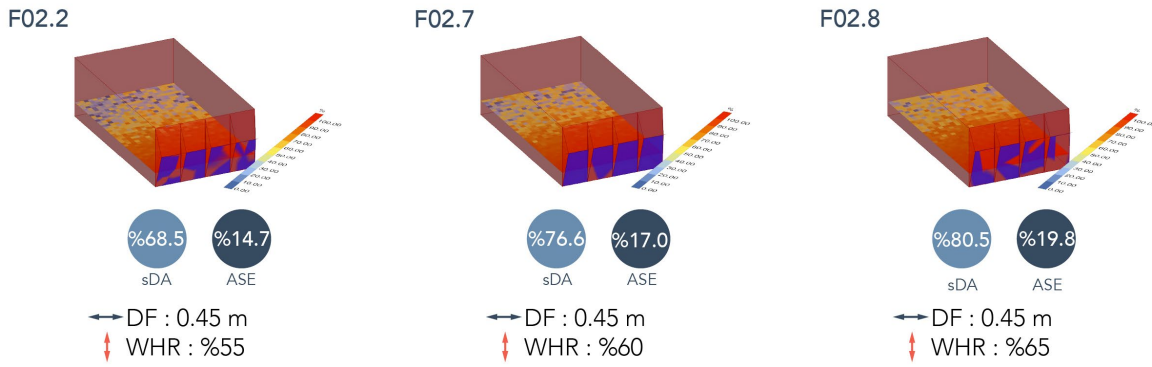


Figure 7.3.1.2.4. F02 Generation's (S1-1) Parameters and Daylight Results

façade was fixed at 0.65 m, the glazing height ratio was adjusted, allowing comparisons between F02, F02.3, and F02.4. Similarly, with the distance set at 0.55 m, changes in glazing height ratio generated comparisons among F02.1, F02.5, and F02.6. Finally, when the distance from the façade was fixed at 0.45 m, variations in window height ratio were tested through the comparison of F02.2, F02.7, and F02.8. (Figure 7.3.1.2.4.)

Daylight analyses for these alternatives showed sDA values ranging from 64% (F02) to 80.5% (F02.8), while ASE values between 12% and 19%. These results demonstrate how controlled parametric variation can mitigate uniformity while maintaining a balance between environmental performance and architectural expression. Through this process, nine module variations were generated, aimed at breaking façade monotony and offering alternative design possibilities. These variations are intended to support a balance between environmental performance and architectural diversity.

### 7.3.1.3 Facade Development

The regular façade typology was conceived as one of the most direct strategies for translating the outcomes of the shoebox analyses into façade-scale applications.

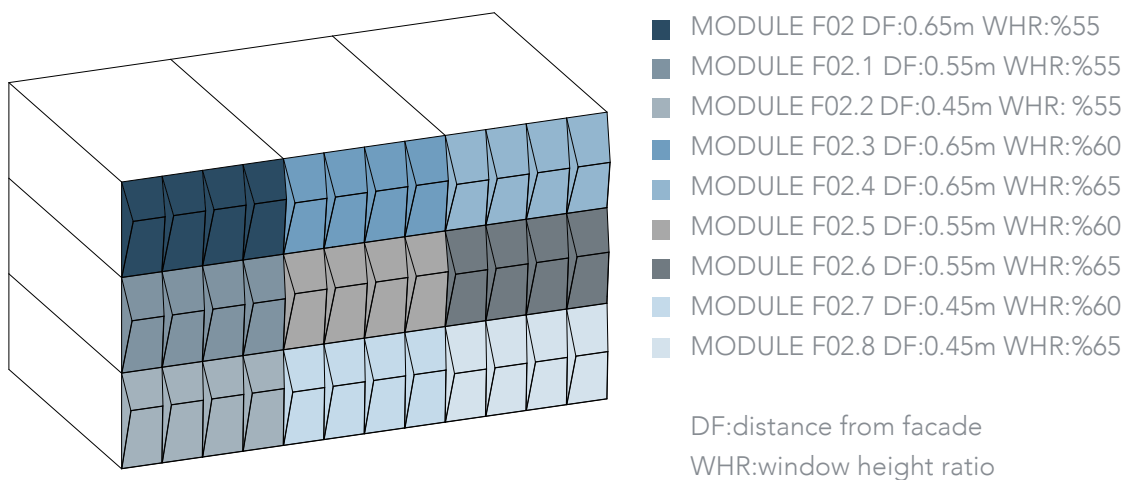


Figure 7.3.1.3.1. Regular Facade Modules (S1-1)

Based on the F02 scenario, 9 module variations were organized by combining different values of distance from façade and window height ratio. In this arrangement, module changes were made after the combination of 4 modules that formed a single room size rather than after each 1.45 m module. This method created a more controlled rhythm, minimized needless fluctuations, and made the façade visible through wider transitions. At the same time, the modules' repetition strengthened a sense of continuity and order, and the methodical arrangement made production and assembly procedures easier. (Figure 7.3.1.3.1).

Despite these advantages, the limited range of window height ratios defined for daylight performance restricted the expressive potential of the façade. As a result, the intended movement could not be fully perceived, which stands out as the main weakness of this typology. Although minor parametric variations helped to soften monotony, they were insufficient to create a stronger architectural identity or convey façade dynamics with clarity.

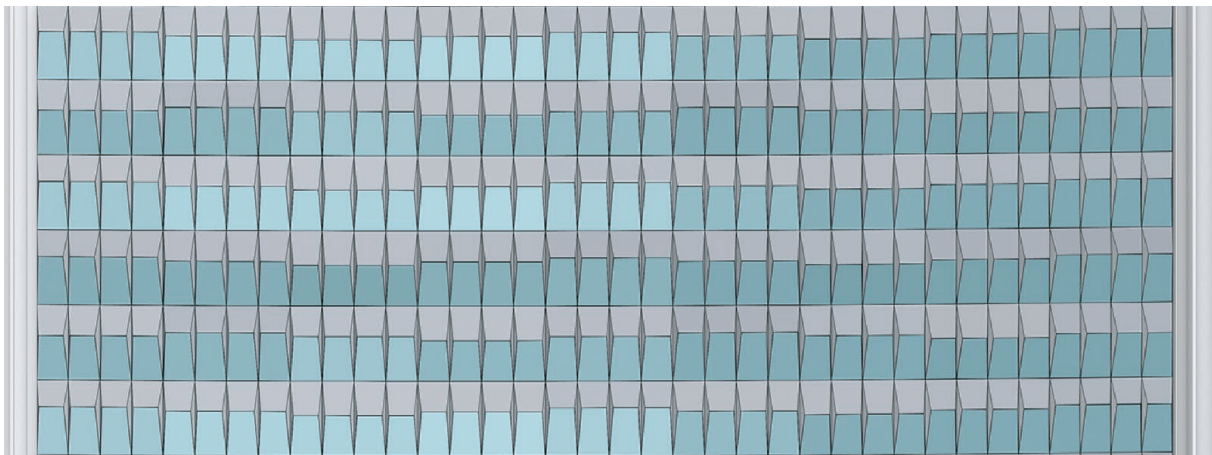


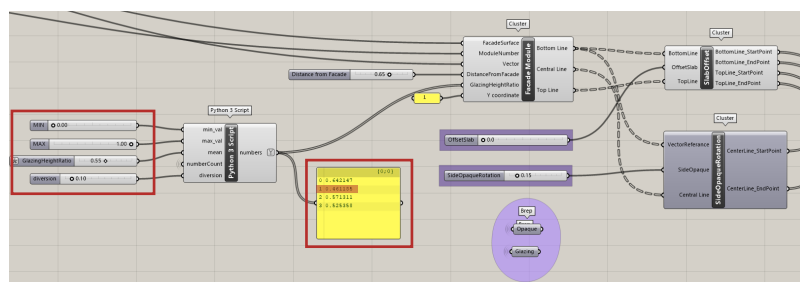
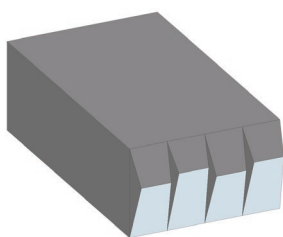
Figure 7.3.1.3.2. Regular Facade View (S1-1)

In conclusion, the regular façade typology illustrates how controlled parameter variation can create order and scale while only partially mitigating uniformity. (Figure 7.3.1.3.2)

## 7.3.2. Random Facade

### 7.3.2.1. F03 Scenario: Randomization

In the F03 scenario, the modules were kept at a fixed distance of 0.65 m from the façade, consistent with the measurement used in F01 and F02.



7.3.2.1.1. F03 Shoebox (S1-1) and Grasshopper Parameters

The window height ratios were generated by introducing diversions through a Python script in Grasshopper. In this process, a diversion value between 0.10 and 0.15 was applied to the predefined window height ratio, and each adjustment of this parameter produced a new set of modules randomly. While this approach created modules slightly different from one another, adding visual variation and movement to the façade, the small deviations also raised concerns for modular production. In addition, each diversion produced a different window height ratio, resulting in a high degree of randomness that risked weakening the architectural coherence of the design.

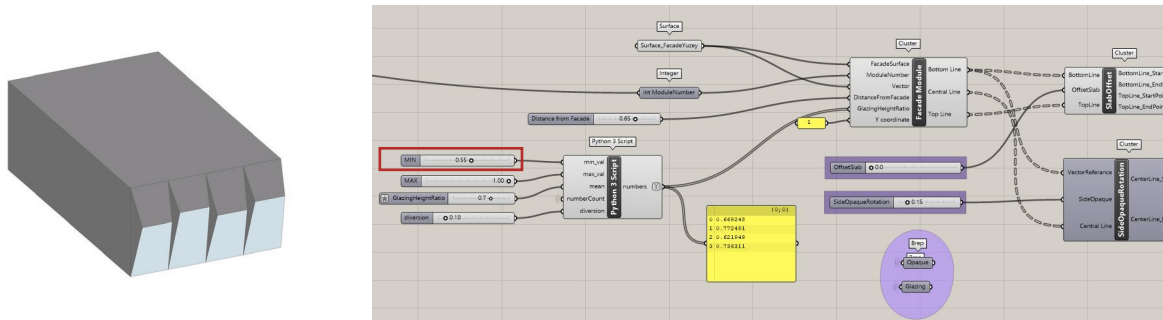


Figure 7.3.2.1.2. F03.1 Shoebox (S1-1) and Grasshopper Parameters

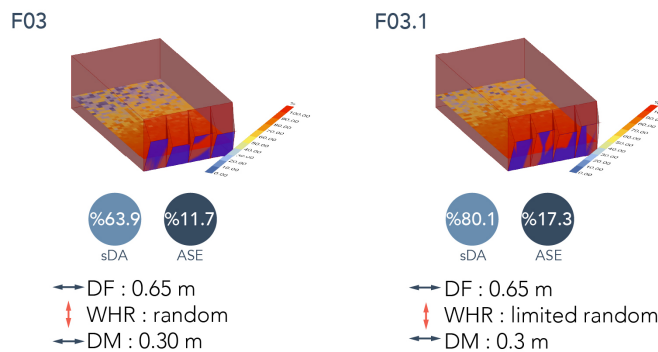


Figure 7.3.1.2.3. F03 and F03.1 (S1-1) Parameters and Daylight Result

The first problem encountered in F03 was that some of the randomly generated window height ratios fell below the predefined threshold of 55% (Figure 7.3.1.2.1). This occurred because the random range in the Python code was kept between 0 and 1, which allowed values lower than the required minimum. To address this, the parameter range was adjusted in the F03.1 scenario, setting the minimum value to 0.55, and daylight analyses were carried out again. (Figure 7.3.1.2.2.)

Since the F03 scenario did not meet visual comfort requirements, only the modules generated in F03.1 were considered valid for façade design. Each random generation produced a different set of modules; therefore, the daylight analysis for this scenario was interpreted as a representative average case rather than definitive performance data. The values reflect the outcomes of the tested iterations, acknowledging that different randomizations can result in slight variations in daylight performance. (Figure 7.3.1.2.3.) Nonetheless, because the level of diversion in the code was constrained to the 0.10–0.15 range, changes in the window height ratio remained relatively minor, preventing significant fluctuations in the results.

### 7.3.2.2 Facade Development

The random façade typology was developed as a strategy to move beyond systematic repetition of the shoebox-derived modules, aiming instead to introduce diversity and dynamism to the building envelope. Based on the F03 scenario, each module was designed independently, with its proportions and dimensions varied, and then distributed across the façade in a randomized manner. (Figure 7.3.2.2.1) This process generated a pixelated and unpredictable visual effect that strengthened the architectural identity of the building.

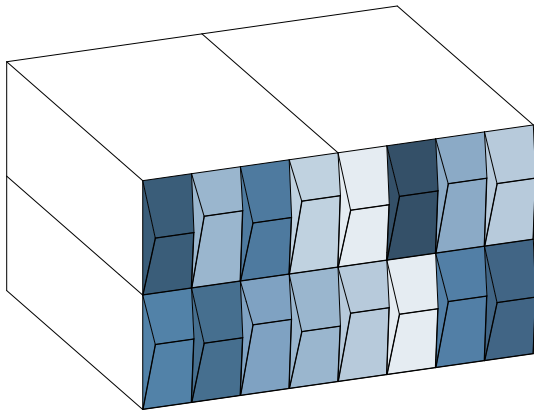


Figure 7.3.2.2.1 Random Facade Modules

The defining characteristic of this typology is its emphasis on variety and movement, which allows the façade to stand apart from monotonous compositions. Within the urban context, such a façade becomes a striking and expressive element. However, this approach also introduced technical constraints. Because every module differs, opportunities for standardization in production and assembly are reduced, making the process more complex and costly. The efficiency of serial production in the regular typology is largely lost, which is a significant disadvantage in application. Performance-wise, fully randomized placement occasionally resulted in window height ratios below the visual comfort threshold. This was addressed by the F03.1 sub-scenario, which set a minimum window height ratio of 55% to maintain user comfort without sacrificing randomness.

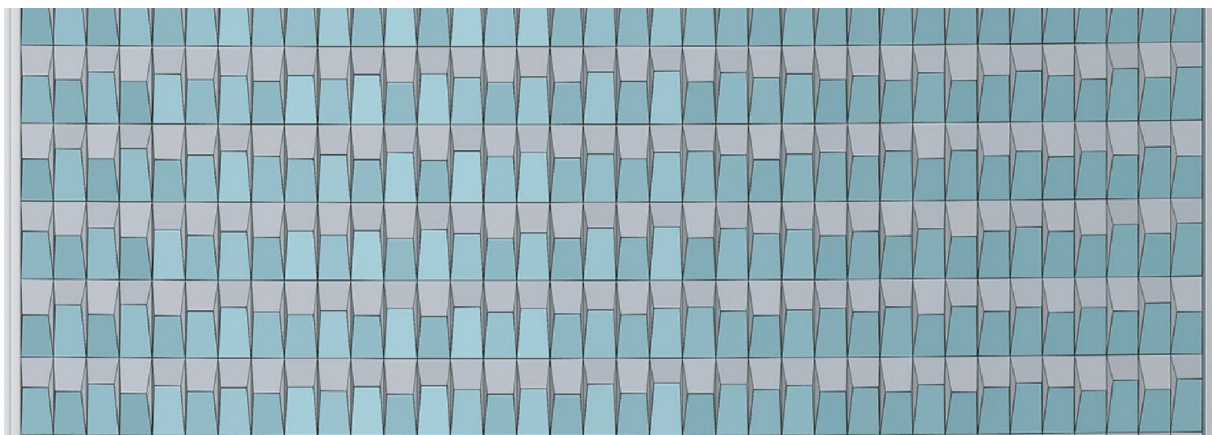


Figure 7.3.2.2.2. Random Facade View (S1-1)

In overall, the random façade typology provides a powerful architectural expression and visual dynamism, but it is more difficult to execute during production and installation due to its lack of standardization.

### 7.3.3 Wave Façade

#### 7.3.3.1 F04 Scenario : Variable Glazing Height

In the F04 scenario, façade modules were generated by fixing the distance from façade at 0.55 m while varying the window height ratio within the 55–65% range (55%, 60%, 65%). The window height ratio range was generated in Grasshopper through a Python script. (Figure 7.3.3.1.1)

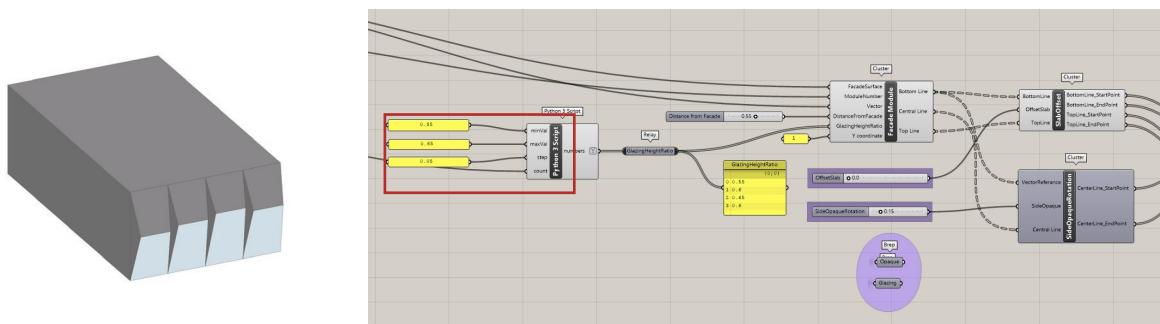


Figure 7.3.3.1.1 F04 Shoebox (S1-1) and Grasshopper Parameters

In a standard shoebox configuration, which consists of four modules each 1.45 m wide, the window heights would normally follow the sequence 55%, 60%, 65%, 55%. To test the potential for greater control and modularity in the façade composition, the script was modified so that the sequence was reversed starting from the fourth module, producing an alternative order of 55%, 60%, 65%, 60%.

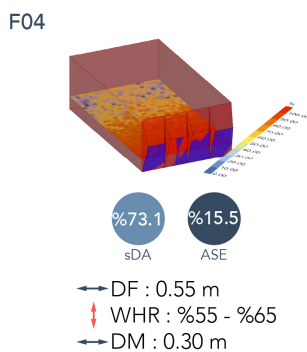


Figure 7.3.3.1.2 F04 (S1-1) Parameters and Daylight

This method allowed an assessment of whether controlled variation could provide visual richness without compromising modular production. The daylight analyses of F04 indicated an sDA of 73% and an ASE of 15%. (Figure 7.3.3.1.2) While daylight autonomy has been successfully improved, the ASE value is above the 10% threshold, necessitating the integration of additional solar control strategies to ensure compliance with visual comfort criteria, according to the LEED perspective. Based on these discoveries, the F04 parametric framework served as the basis for creating the F05 scenario, which is covered in the section that follows.

### 7.3.3.2 F05 Scenario: Flexible Range and F05 Generations

The development of F05 emerged from the need to expand the design exploration beyond the limitations of the previous scenarios. F05 aimed to examine the simultaneous modification of both distance from the façade and window height ratio, while F01 through F04 tested variables individually or in controlled combinations.

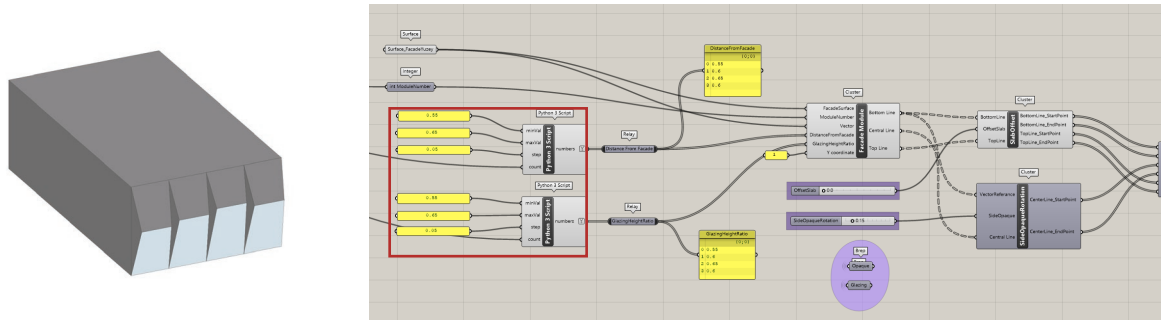


Figure 7.3.3.2.1 F05 Shoebox (S1-1) and Grasshopper Parameters

This approach was guided by two main goals. The first was to expand the design space by generating diverse façade morphologies within specific parameter ranges, helping to avoid repetitive or overly uniform outcomes. The second was to define clearer module dimensions that would simplify the production process while still achieving a façade expression that feels as varied and dynamic as a randomized composition.

In the F05 scenario, both distance from façade and window height ratio were varied within a range of 55–65% (55%, 60%, 65%), using the same Python script applied in F04. (Figure 7.3.3.2.1) Based on this setup, three modules were generated: the first combined a distance from façade of 55% with a window height ratio of 55%, the second increased both values to 60%, and the third reached 65% for both parameters. When these modules were applied to form a shoebox, the daylight analysis showed an sDA of 72.5% and an ASE of 15.11%. (Figure 7.3.3.2.2.) This indicates that the scenario meets LEED requirements for daylight autonomy, but the ASE value remains above the 10% threshold. For this reason, the use of blinds or other solar control strategies was assumed to ensure visual comfort.

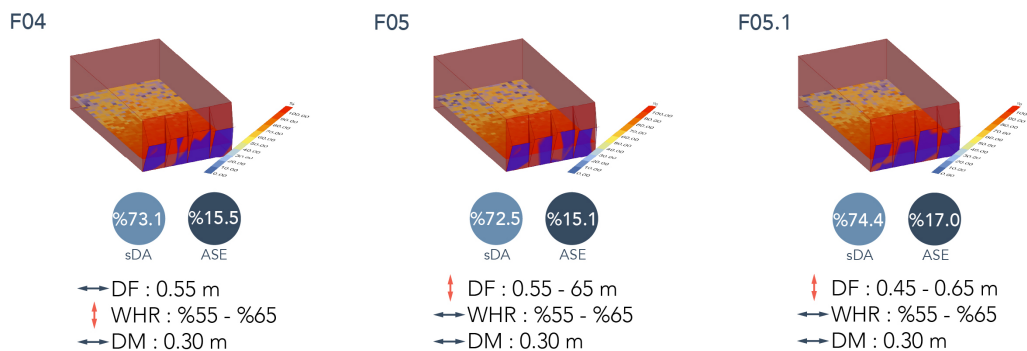


Figure 7.3.3.2.2. F04 and F05, F05.1 (S1-1) Parameters and Daylight Result

Further explore alternatives, the window height ratio range was kept constant while the distance from façade was adjusted to a lower range of 45–55%. This variation, defined as F05.1, produced three modules: the first combined a distance from façade of 45% with a window height ratio of 55%, the second increased these values to 50% and 60%, and the third reached 55% and 65% respectively.

Daylight analysis of F05.1 showed an sDA of 74% and an ASE of 17%. (Figure 7.3.3.2.2) From a LEED perspective, both scenarios satisfy the minimum requirement for daylight autonomy; however, ASE values remain above the 10% threshold. For this reason, the integration of blinds as solar control strategies is necessary to achieve compliance with visual comfort criteria.

The evaluation of F05 and F05.1 shows that, despite the reduction in distance from façade, similar results were obtained with respect to LEED performance criteria.

The window height ratio was kept within the 55–65% range to maintain sDA and ASE performance and to ensure that ASE did not exceed the 20% limit, while the maximum distance from façade was restricted to 0.65 m for feasibility reasons. Testing the 45–55% range for distance from façade allowed an assessment of performance under the same window height values with reduced depth. These findings highlight the potential of parametric flexibility to generate alternative façade solutions while staying within both performance and constructability limits.”

### 7.3.3.3 Facade Development

The wave façade typology was developed by organizing the shoebox-derived modules in a more controlled and rhythmic manner. This approach builds on the F05 scenario, particularly the modules F05.1 and F05.2. In this configuration, the window height ratio was kept constant within the range of 55–65%, while only the distance from façade was varied. (Figure 7.3.3.3.1.) By applying successive offsets in the arrangement of modules, the façade surface acquired a wave composition. In addition to improving the façade’s visual articulation, this flowing pattern created dynamic light and shadow effects that gave the building a more expressive personality.

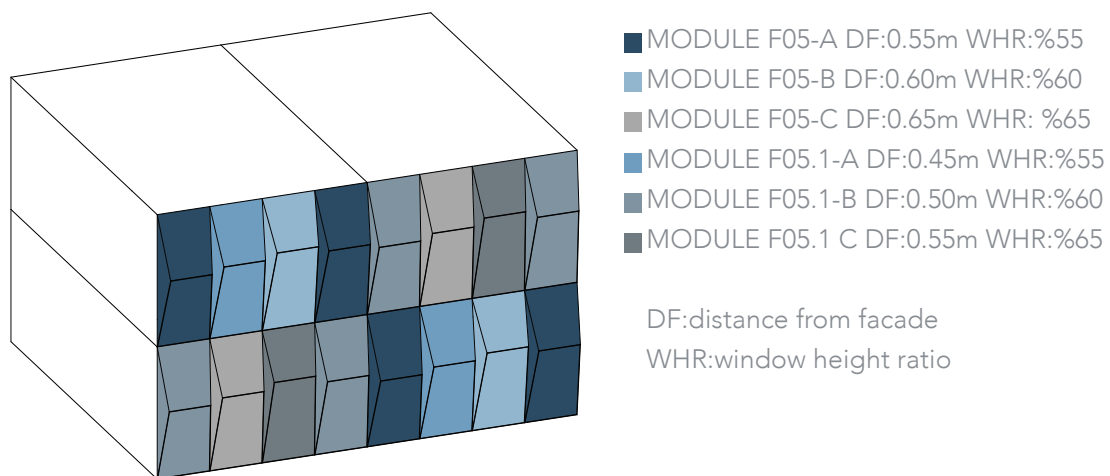


Figure 7.3.3.3.1. Wave Facade Modules (S1-1)

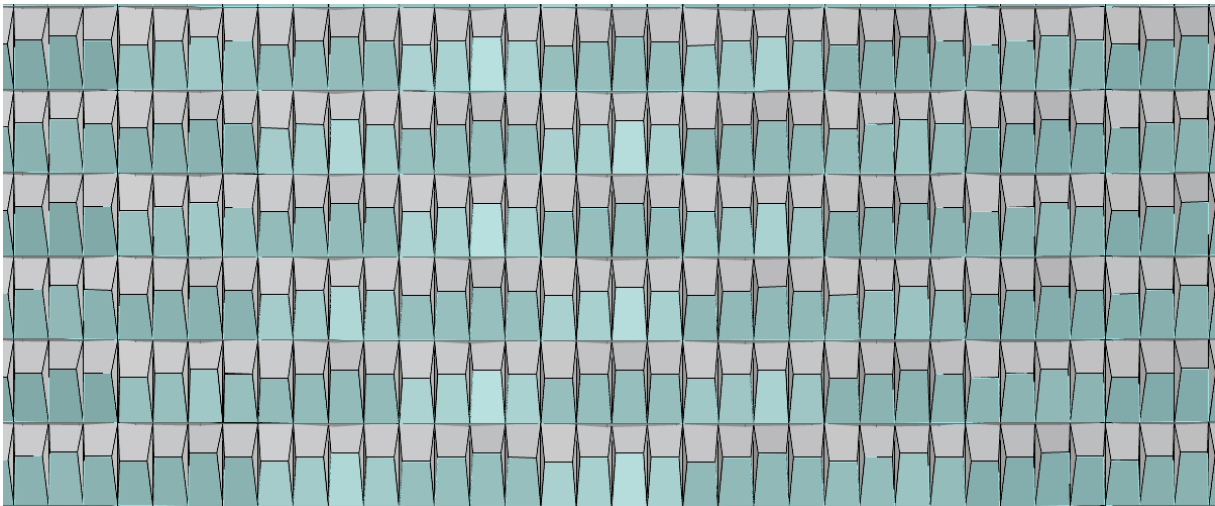


Figure 7.3.3.3.2. Wave Facade View (S1-1)

## 7.4 S5-1 (South-West, 5th Floor)

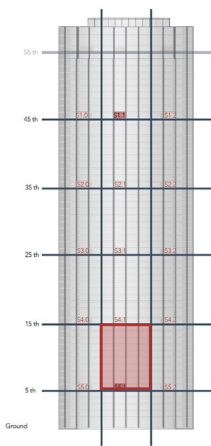


Figure 7.4 S1-1 study area

The southeast façade of the case study tower is examined in the S5-1 scenario. (Figure 7.4) This level is significantly impacted by shading from adjacent buildings, which significantly lowers daylight availability compared to the upper floors. As a result, sDA values were consistently lower in daylight analyses for this level than for the upper levels. In order to improve daylight autonomy and reduce dependency on artificial lighting, the design approach placed a high priority on optimizing window height ratios within practical construction constraints, all the while adhering to technical and maintenance specifications.

### 7.4.1 Regular Façade

#### 7.4.1.1 F01 Scenario: Baseline from Optimization

The F01 scenario was derived directly from the optimization results presented in the design limitation chapter. (7.2.1.) The selected arrangement achieved a 70% window height ratio with a 0.65 m façade offset. (Figure 7.4.1.1.1.) This configuration served as the initial reference point for evaluating performance on the shaded southeast

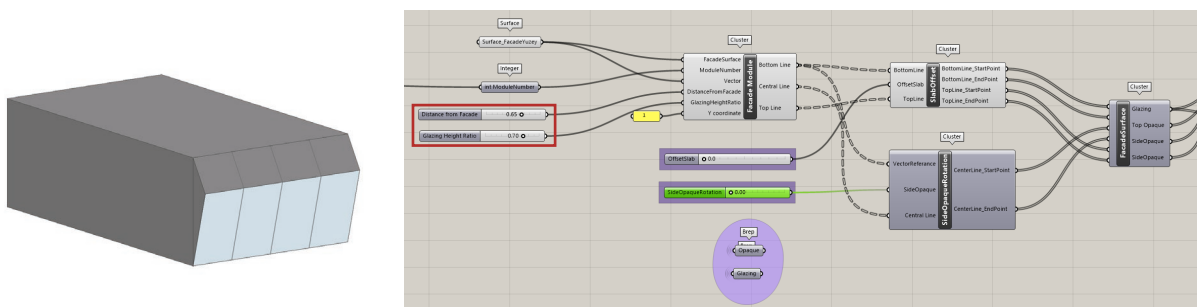


Figure 7.4.1.1.1 F01 Shoebox (S5-1) and Grasshopper Parameters

façade, where maximizing daylight intake was a critical design priority. By establishing this setup as a baseline, subsequent variations were systematically compared to highlight the impact of different parametric adjustments on daylight availability and visual comfort.

### 7.4.1.2 F02 Scenario: Spacing Between Modules

Spacing between modules was changed to guarantee accessibility and maintenance viability in accordance with the design guidelines (Section 7.2.2). In the F02 scenario, adjacent modules were spaced 0.30 meters apart. (Figure 7.4.1.2.1).

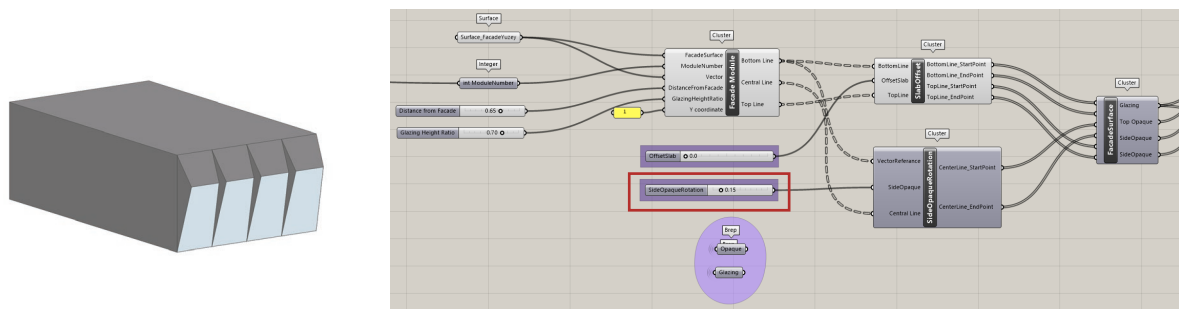


Figure 7.4.1.2.1. F02 Shoebox (S5-1) and F02 Grasshopper Parameters

Daylight simulations for the baseline scenario (F01) achieved an sDA of 62.17% and an ASE of 17.5%. Although the ASE value exceeded the 10% threshold recommended by LEED for visual comfort, this configuration was selected as the starting point because it maximized daylight autonomy in shaded areas and provided a solid basis for further adjustments. In comparison, the F02 scenario, which introduced tighter module spacing, resulted in an sDA of 56.41% and an ASE of 15.11%. While daylight autonomy decreased compared to F01, the reduction in ASE enhanced visual comfort, emphasizing the trade-off between performance optimization and glare control. This comparison established the foundation for exploring additional parametric variations in subsequent scenarios. (Figure 7.4.1.2.2. )

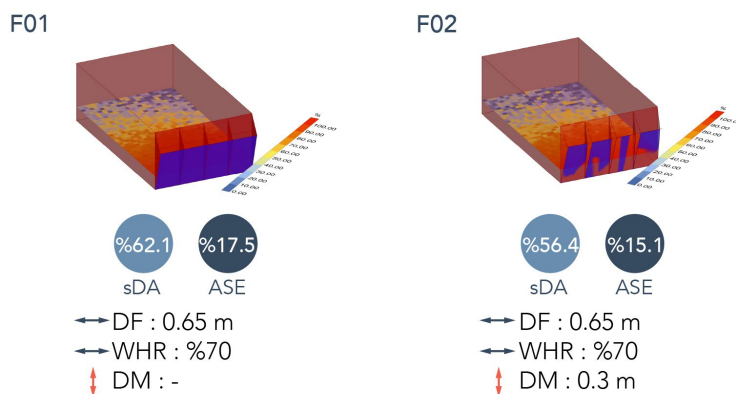
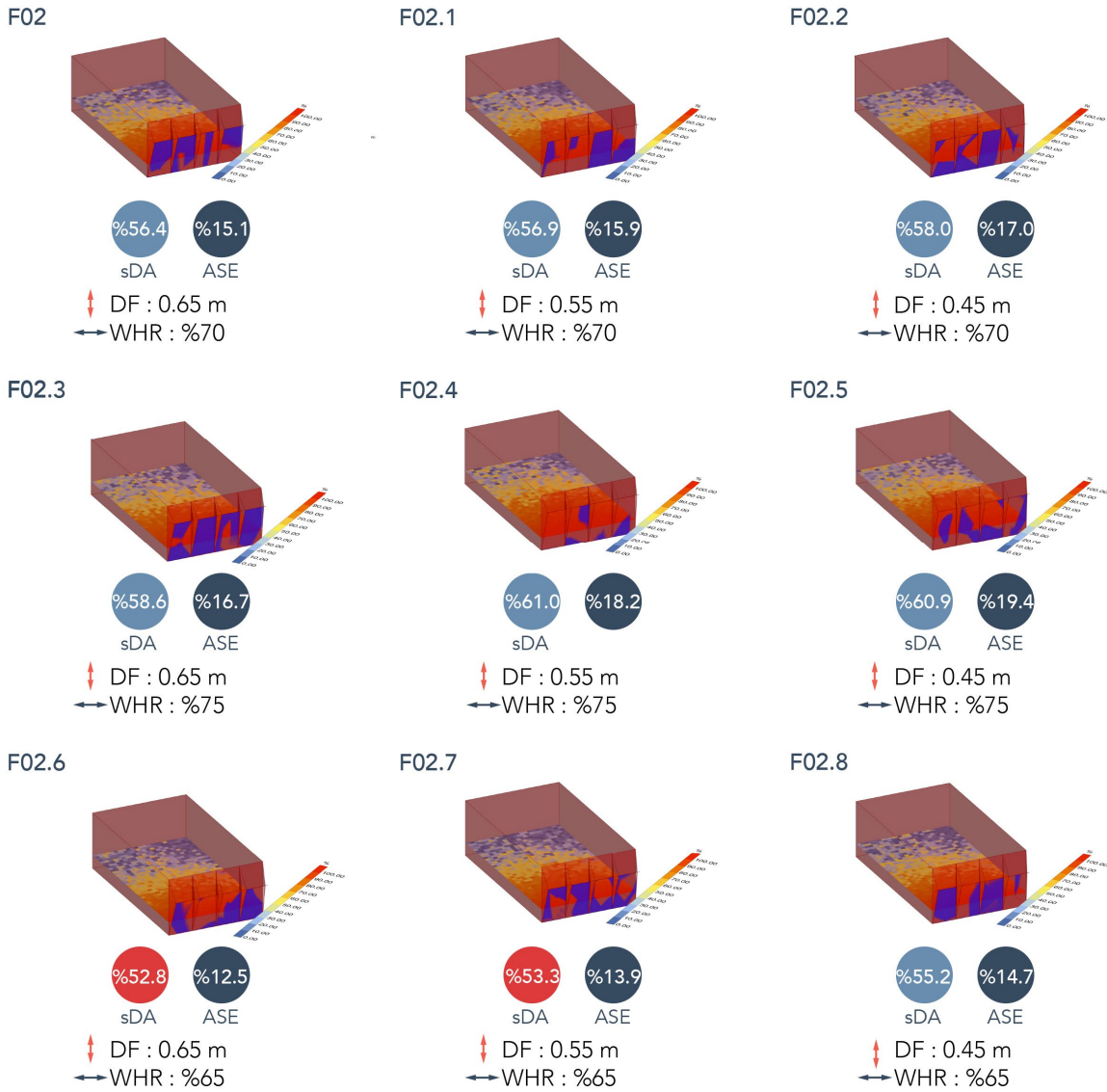


Figure 7.4.1.2.2. F01 and F02 (S5-1) Parameters and Daylight Result

However, applying this solution uniformly across the façade risked producing monotony. For this reason, F02 was treated as a reference scenario, from which further variations were generated by adjusting the façade offset (0.65 m, 0.55 m, 0.45 m) and the window height ratio (65%, 70%, 75%), resulting in 9 alternatives (F02–F02.8).

When the window height ratio (WHR) was set to 70%, the distance from the façade was varied between 0.45 m and 0.65 m (F02, F02.1, F02.2). A shorter distance improved daylight autonomy, with sDA rising from 56.41% to 58.04%, but it also increased annual sunlight exposure, as ASE grew from 15.11% to 17.07%. A similar trend was observed when the WHR was fixed at 75% (F02.3–F02.5): reducing the distance from the façade enhanced sDA, increasing it from 58.69% to 60.97%, while ASE also rose from 16.74% to 19.46%. This highlights the trade-off between greater daylight access and higher glare risk. At a WHR of 65% (F02.6–F02.8), the results followed the same pattern, with reduced distance leading to higher sDA (from 52.82% to 55.21%) but slightly greater ASE (from 12.50% to 14.78%). Finally, when the distance from the façade was kept constant at 0.45 m, comparisons among F02.2, F02.5, and F02.8 showed that increasing the WHR consistently improved daylight autonomy, which rose from 55.21% to 60.97%, but at the cost of higher sunlight exposure, as ASE increased from 14.78% to 19.46%. (Figure 7.4.1.2.3)



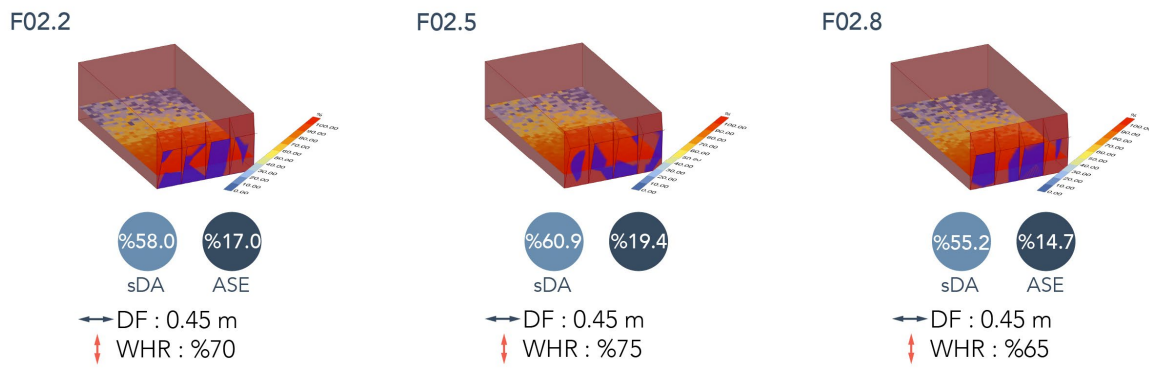


Figure 7.4.1.2.3 F02 (S5-1) Parameters and Daylight Result

sDA values ranged from 52.82% (F02.6) to 61.08% (F02.4), whereas ASE varied from 12.5% (F02.6) to 19.46% (F02.5). The results show that larger window sizes and closer proximity to the facade improve daylight autonomy but also raise the risk of direct sunlight exposure. They highlight the need to balance sunlight gain with glare control, especially in shaded areas like lower tower levels. Modules with sDA below 55% indicated insufficient daylight in shaded lower floors and were excluded from facade applications, ensuring that only effective configurations guide the design process.

### 7.4.1.3 Façade Development

The regular façade typology was developed by reapplying the same system described in the S1-1 scenario (7.3.1.3), this time adapted to the shoebox results of S5-1. As in the previous case, 6 module variations derived from the F02 scenario were transferred to façade scale (Figure 7.4.1.3.1.), organized through parametric combinations of window height ratio and distance from façade. Compared with the S1-1 scenario, where the strategy relied on reducing window heights to limit glare from direct sunlight, the shaded conditions at S5-1 shifted the priority to maximizing window height to capture daylight. This contrast explains why window height ratios in S5-1 are generally higher, though glare control still required careful balance. In summary, the regular façade typology for S5-1 demonstrates how controlled parameter variation can generate order and scale.

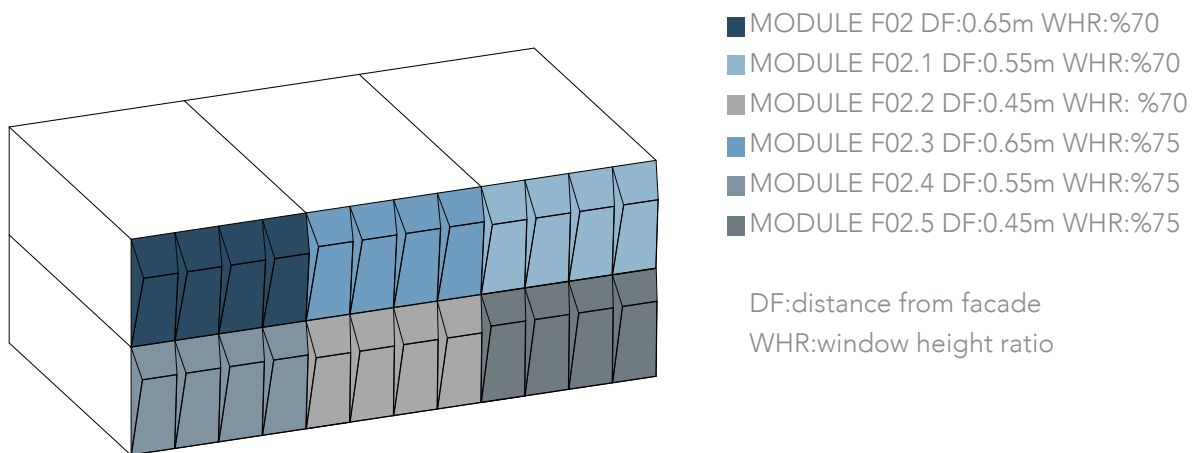


Figure 7.4.1.3.1. Regular Façade Modules (S5-1)

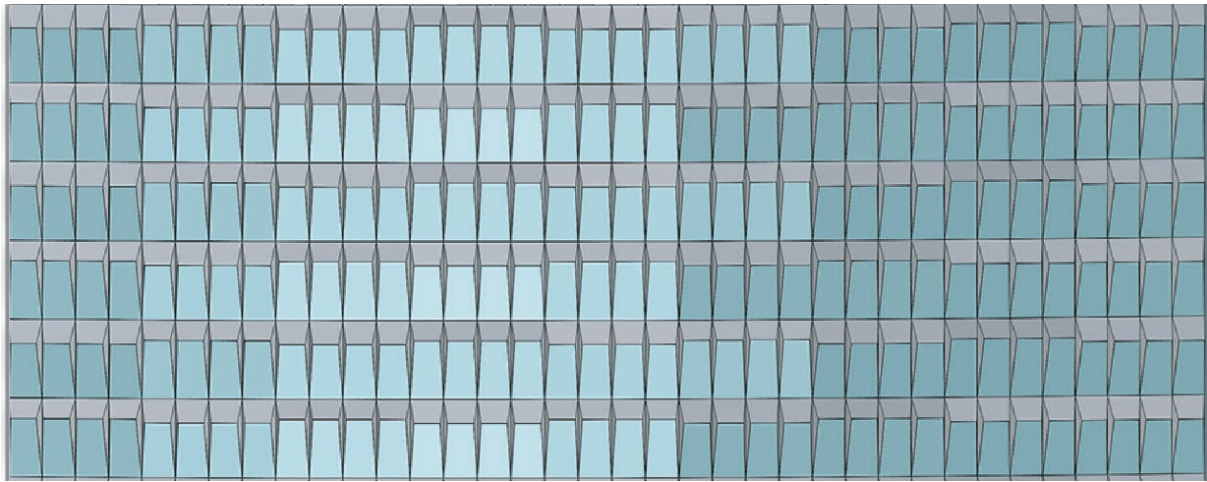


Figure 7.4.1.3.2. Regular Façade View (S5-1)

## 7.4.2 Random Façade

### 7.4.2.1 F03 Scenario: Randomization

In the F03 scenario, the modules were kept at a fixed distance from the façade of 0.65 m, consistent with the measurements used in the regular façade scenarios. The window height ratios were randomized through a Python script in Grasshopper. In this case, the initial setup defined the window height ratio at 65%, with diversions ranging between 0.1 and 0.15. As a result, none of the tested outcomes dropped below the 55% threshold for window height ratio. However, since in the S1-1 scenario the risk of falling below 55% had been encountered, the Python code here was also adjusted to enforce a minimum value of 0.55. (Figure 7.4.2.1.1.)

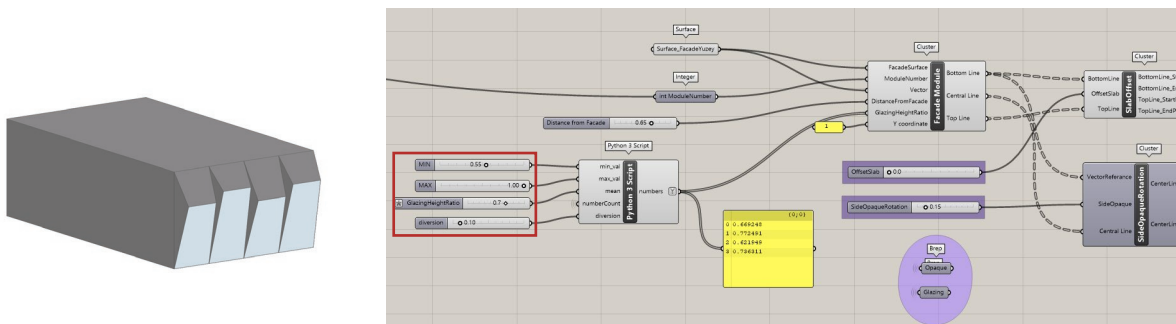


Figure 7.4.2.1.1. F03.1 Shoebbox (S5-1) and Grasshopper Parameters

In the base F03 run, the sDA value was close to the LEED v4 limit of 55%, which prompted further testing through F03.1 and F03.2. In F03.1, the sDA value fell below 55% while the diversion was kept at 0.10. (Figure 7.4.2.1.2).

In F03.2, the diversion was increased to 0.15, generating new modules, and each adjustment of the diversion value produced different module sets. Under these conditions, the random façade for S5-1 could not reliably guarantee compliance with daylight requirements. If this strategy were to be pursued, shoebbox analyses would need to be repeated for the entire façade to verify performance, but in a high-rise building this approach is not considered practical.

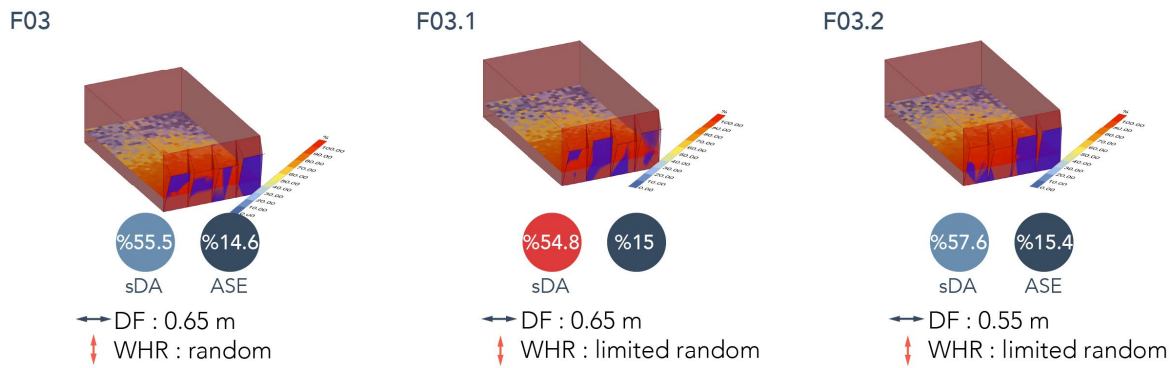


Figure 7.4.2.1.2. F03, F03.1 and F03.2 (S5-1) Parameters and Daylight Result

### 7.4.2.2 Façade Development

Although the shoebox analyses indicated that the random façade strategy could not consistently meet daylight requirements for S5-1, a brief outline of how such a façade might be composed is useful. In principle, modules created with random proportions would be spread across the façade to produce a pixelated and lively surface. This uneven pattern could enhance the architectural identity by breaking predictability and monotony. However, needing to individually fabricate each module would raise production complexity and cost.

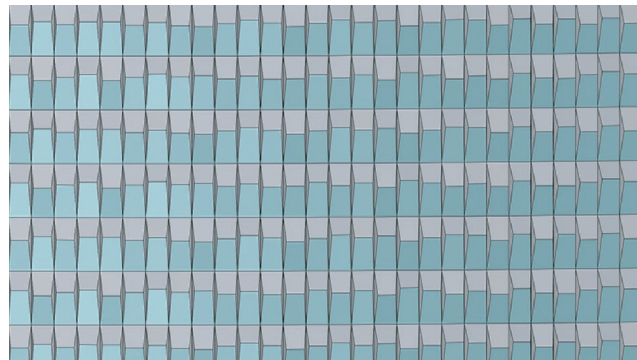
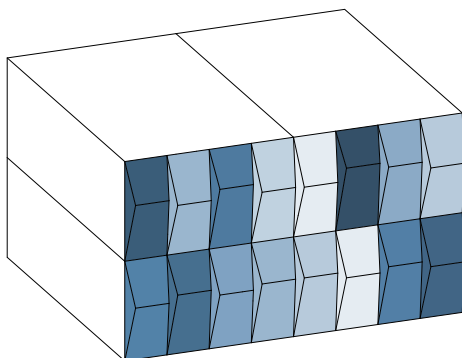


Figure 7.4.2.2.1. Random Façade Modules (S5-1) Figure 7.4.2.2.2. Random Façade View (S5-1)

Despite these potential qualities, the shoebox results underline that for S5-1 the random façade is not a viable option, as it cannot reliably ensure compliance with daylight requirements. In high-rise applications, testing every possible random variation across the entire façade is not practical. Therefore, within this study the random façade is described only as a conceptual possibility rather than a strategy for implementation.

### 7.4.3 Wave Façade

#### 7.4.3.1 F04 Scenario: Variable Window Height

In the adapted version of the method described in S1-1 (see Section 7.3.3.1) for S5-1, the façade offset was fixed at 0.55 m, while the window height ratio was varied within the 65–75% range (65%, 70%, 75%). Sequential arrangements were generated using a Python-based script, and a reversed sequence was also tested in order to maintain controlled variation among the modules. (Figure 7.4.3.1.1.)

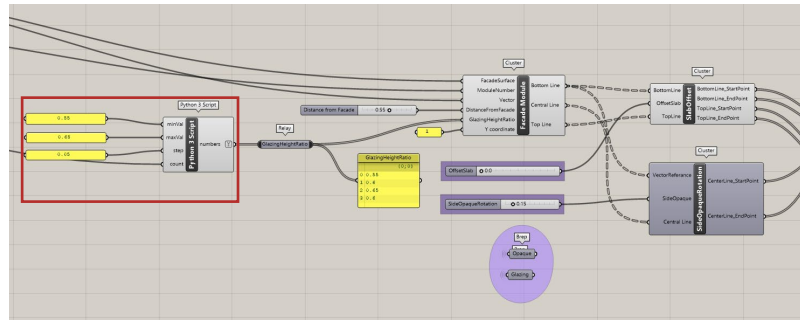
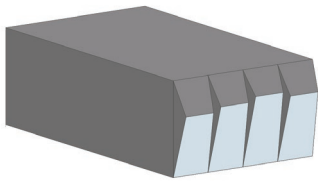


Figure 7.4.3.1.1 F04 Shoebox (S5-1) and Grasshopper Parameters

Daylight analysis resulted in 56.52% sDA and 15.93% ASE. (Figure 7.4.3.1.2.) While the outcome approached an acceptable threshold in terms of sDA, the ASE value exceeded the 10% limit, making the integration of additional shading measures as blinds necessary under LEED requirements. Although the performance improvement was limited, this scenario showed the potential to enhance visual diversity while keeping modular constructability.

F04

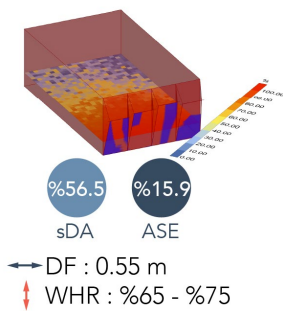


Figure 7.4.3.1.2 F04 (S5-1) Parameters and Daylight Result

### 7.4.3.2 F05 Scenario: Flexible Range and F05 Generations

The F05 scenario expanded the method introduced in S1-1 by combining variations in distance from facade and window height ratio to explore a wider morphological spectrum (see Section 7.3.3.2). In this case, the façade offset was defined within the range of 0.55–0.65 m, while the window height ratio was maintained at 65–75%. (Figure 7.4.3.2.1.)

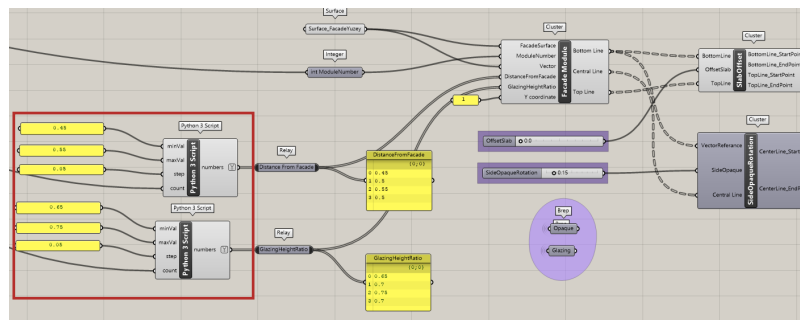
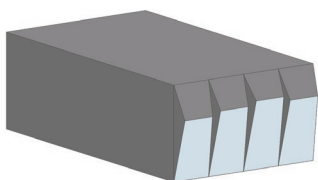


Figure 7.4.3.2.1. F05 Shoebox (S5-1) and Grasshopper Parameters

Daylight analysis for F05 showed 56.73% sDA and 15.54% ASE. Although daylight autonomy stayed above the 55% threshold, the ASE value went over the LEED guide-

line of 10%, which means additional shading strategies, like a blind system, are needed for visual comfort. To investigate the effect of further variations, two sub-scenarios were developed. In F05.1, the distance from facade was decreased to 0.45–0.55 m, while maintaining the glazing ratio at 65–75%. This alteration yielded 57.28% sDA and 16.85% ASE, signifying a minor increase in daylight autonomy alongside an increase in excessive sun exposure. Conversely, F05.2 entailed a significant reduction of façade depth to 0.30–0.40 m, while preserving the identical window ratio. This configuration attained 53.36% sDA and 18.48% ASE, with daylight autonomy was lower than the required 55% threshold and ASE at critical levels. (Figure 7.4.3.1.2.) Consequently, this step not only tested the potential for parametric variation but also identified the limit beyond which façade depth should not be reduced in future designs.

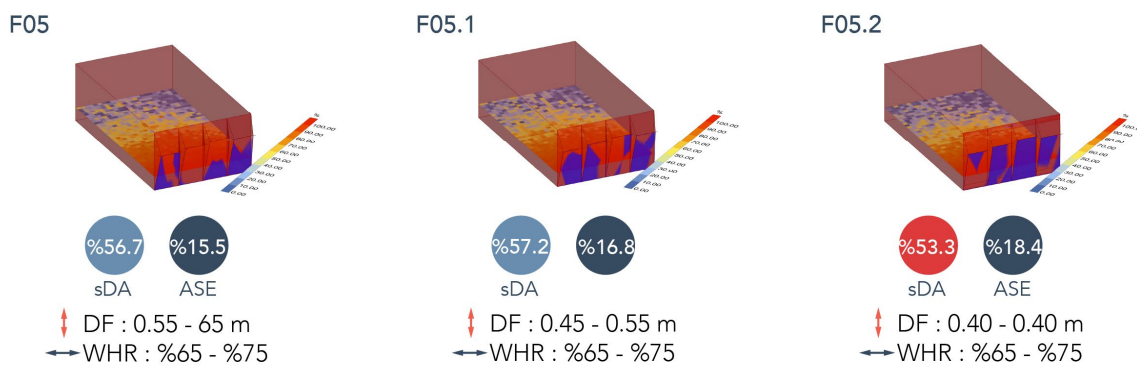


Figure 7.4.3.2.2 F04 and F05, F05.1 (S5-1) Parameters and Daylight Result

### 7.4.3.3 Façade Development

The wave façade typology for S5-1 was developed by arranging the shoebox-based modules in a rhythmic sequence, building on the outcomes of the F05 scenarios. In this design, the window height ratio was kept between 65% and 75%, while the façade offset gradually shifted in increments from 0.45 to 0.65 meters (Figure 7.4.3.3.1). This controlled variation produced an undulating surface that enhanced the façade’s expression and generated dynamic patterns of light and shadow throughout the day.

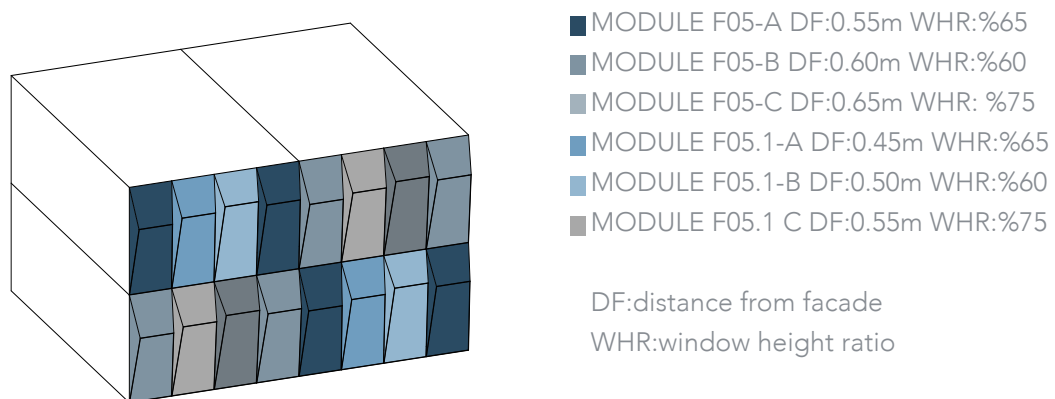


Figure 7.4.3.3.1. Wave Facade Modules (S5-1)

Unlike the randomness explored in other typologies, the wave approach in S5-1 established diversity within a systematic framework, ensuring order without monotony. The façade balanced modular constructability with architectural expression, softening the building’s verticality through a horizontal rhythm. From an urban perspective, this strategy reinforced the building’s identity and contributed to its perceptual distinctiveness..

The wave façade in S5-1 demonstrated both benefits and drawbacks in terms of performance. Daylight analysis showed that daylight autonomy stayed above the 55% threshold, but ASE values routinely exceeded the 10% limit, highlighting the need for additional shading to satisfy LEED visual comfort standards. This revealed the point at which daylight quality is compromised by façade depth reductions, while also showing how the wave façade can combine architectural richness and parametric flexibility.

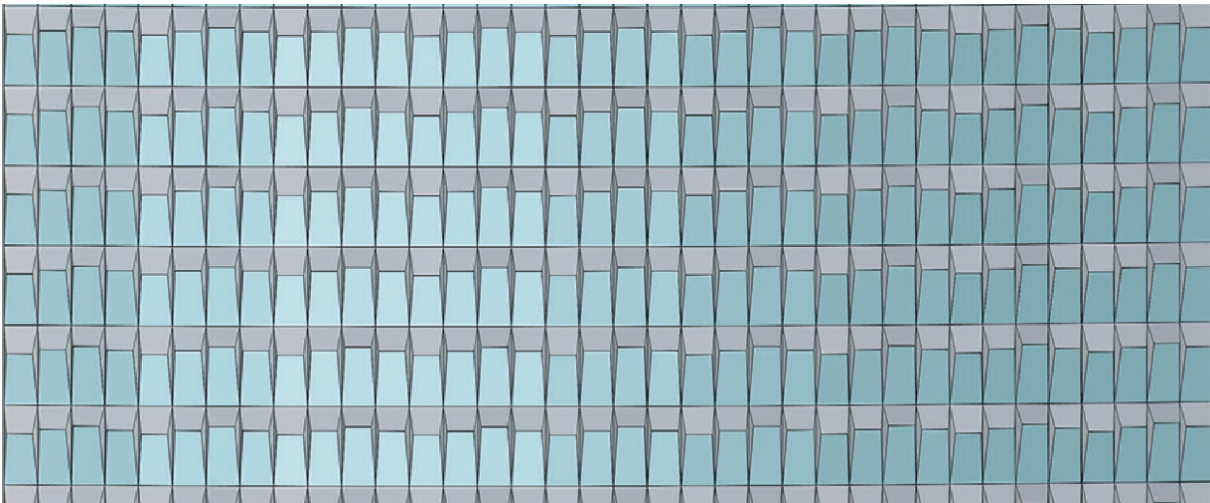


Figure 7.4.3.3.2. Wave Facade View (S5-1)

**7.5 N1-1(North-East, 45th Floor) & N5-1 (North-East, 5th Floor)**

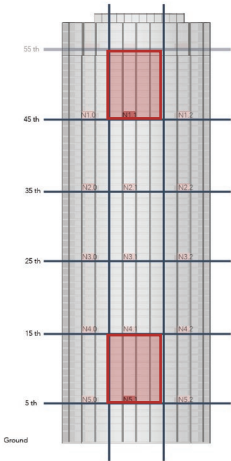


Figure 7.3. North-west selected facade shoebox

The north-east façade of the tower is one of the orientations that receives the least direct sunlight. Based on the environmental analyses carried out earlier in the study, this façade remains shaded for long periods in winter and is only partially exposed to morning sun in summer. These softer daylight conditions lower the risk of glare and overheating compared to the southern façades, but they also require careful design to ensure consistent daylight quality inside the building. In this context, the N1-1 shoebox represents the 45th floor, while the N5-1 shoebox corresponds to the 5th floor, capturing the vertical variation in daylight performance across the tower. (Figure 7.3. )





proved daylight access but also raised glare risk. The effect was stronger at higher window ratios and in favorable orientations, while more modest at lower ratios. Nevertheless, all configurations complied with LEED v4 requirements, ensuring sufficient daylight performance without exceeding glare thresholds.

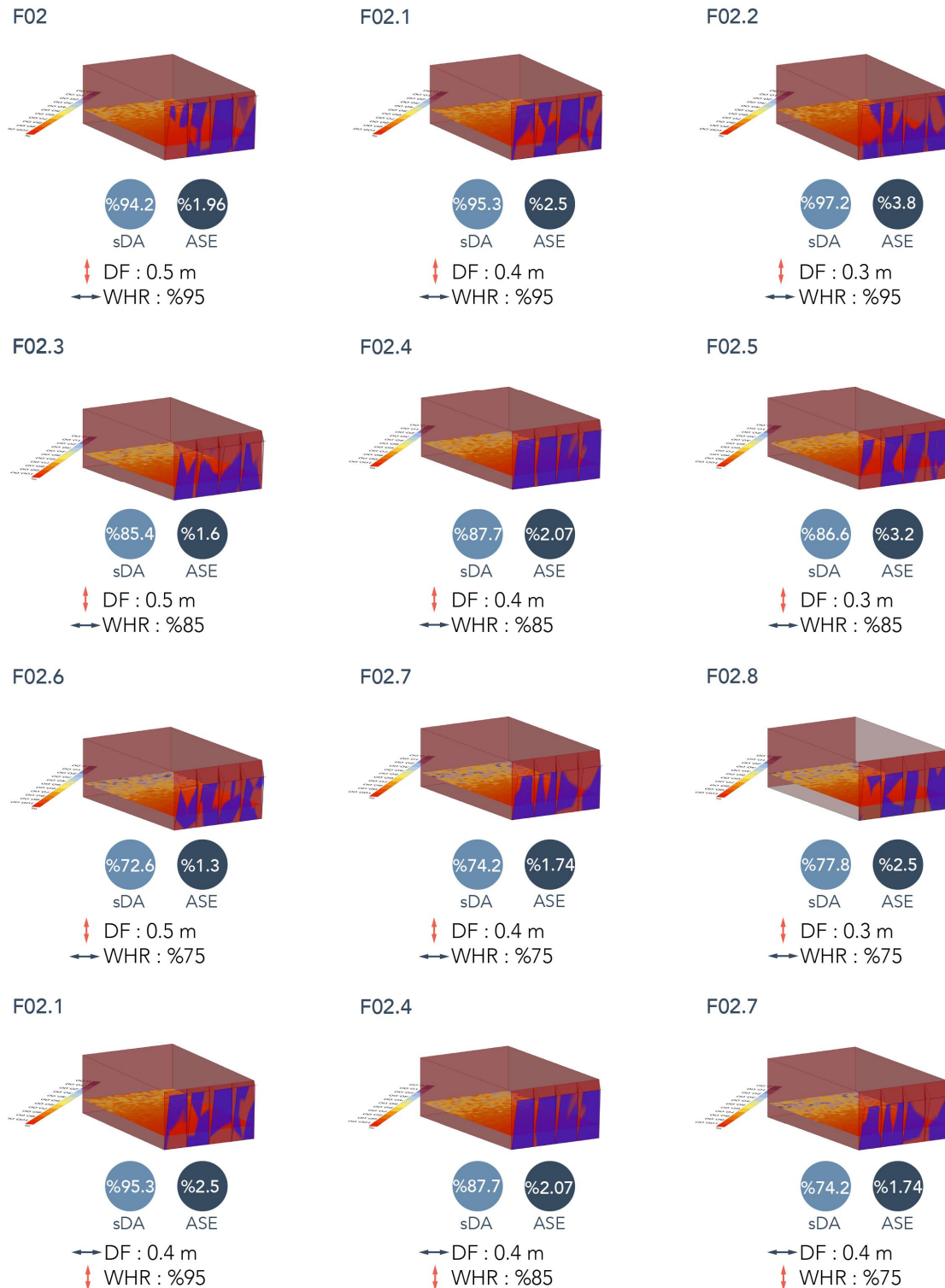


Figure 7.5.1.2.2. F02 Generation's (N1-1) Parameters and Daylight Result

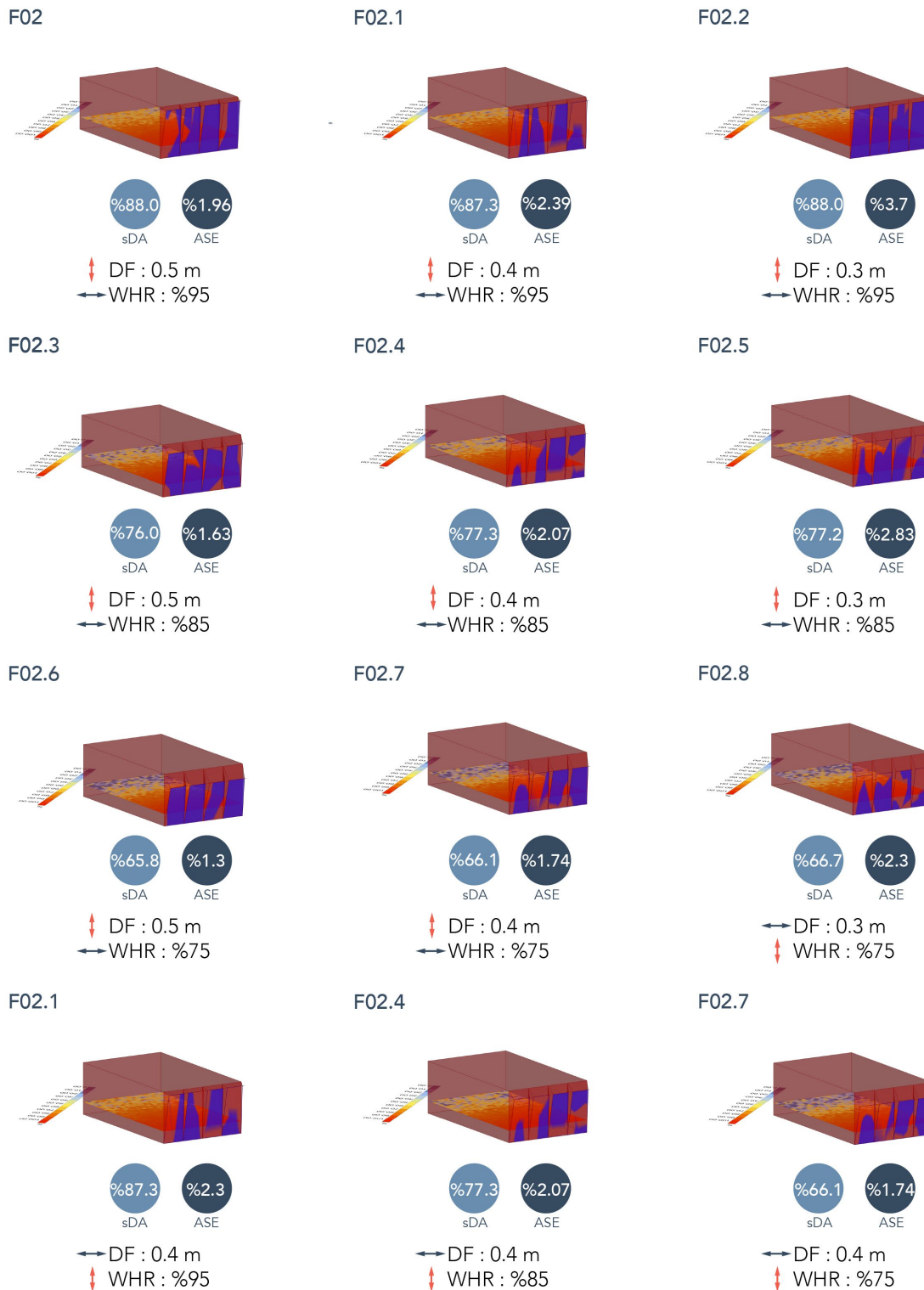


Figure 7.5.1.2.3. F02 Generation's (N5-1) Parameters and Daylight Result

Through this process, 9 module variations were generated, aimed at breaking façade monotony and offering alternative design possibilities. These variations balanced environmental performance with architectural diversity, showing that different results could arise from the same parameters depending on the shoebox position.

### 7.5.1.3 Facade Development

The regular façade typology was developed from the 9 variations produced in the F02 scenario. A systematic set of modules was derived by combining façade distances of 0.30 m, 0.40 m, and 0.50 m with window height ratios of 95%, 85%, and 75%. These modules were then organized in a systematic sequence to create a façade composition that balanced order with subtle variation. (Figure 7.5.1.3.1.)

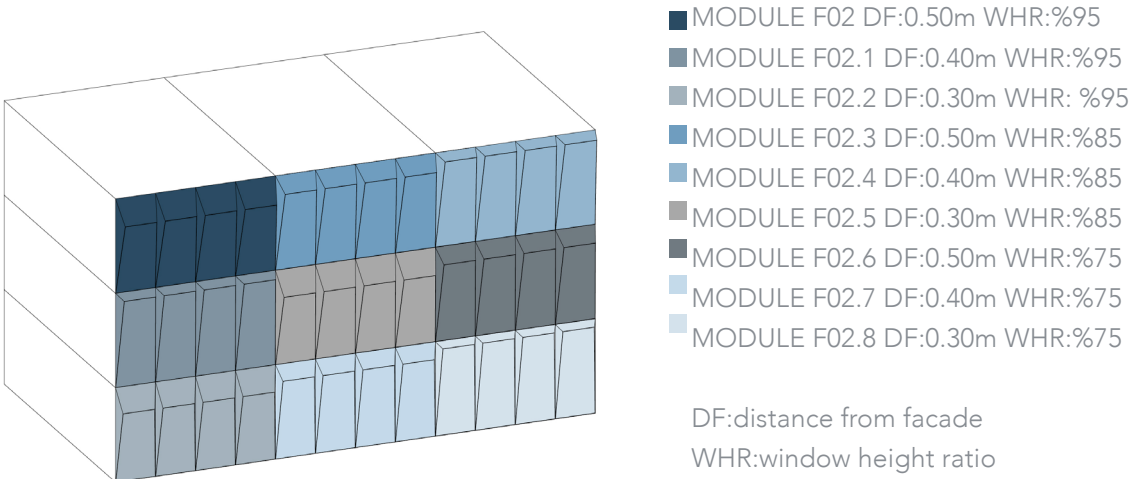


Figure 7.5.1.3.1.Regular Facade Modules (N1-1 & N5-1)

Instead of alternating the modules every 1.45 m, the rhythm was defined at larger intervals to avoid excessive fluctuation and to establish a more legible façade order. In this way, broader transitions became perceptible, reducing the risk of irregularity while still preventing monotony.

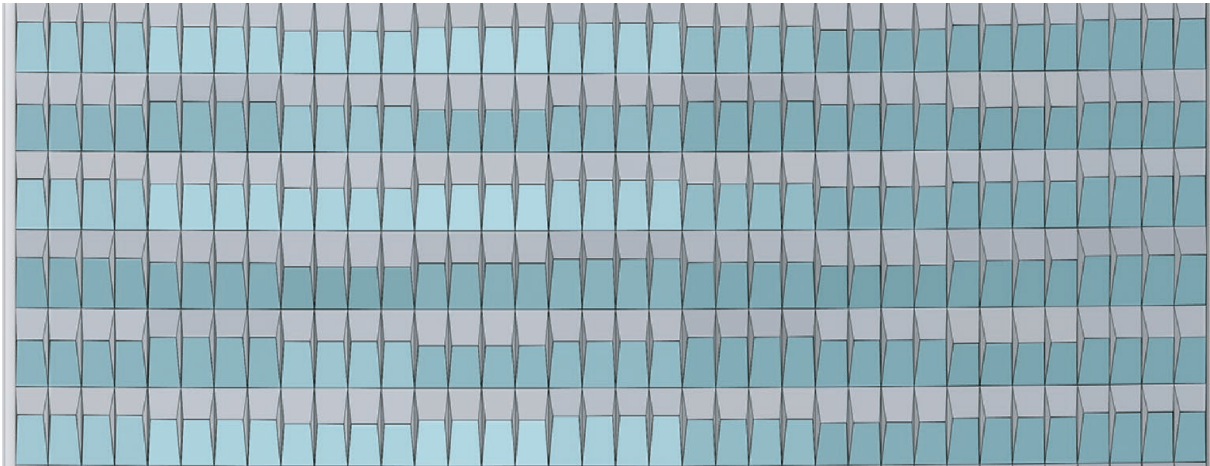


Figure 7.5.1.3.2.Regular Facade View (N1-1 & N5-1)

This typology succeeded in performance due to the constant daylight outcomes of the F02 variations, with both N1-1 and N5-1 reliably satisfying LEED standards. Regulated repetition enabled modular manufacturing and streamlined assembly, whereas parametric modifications provided sufficient variation to prevent monotony.



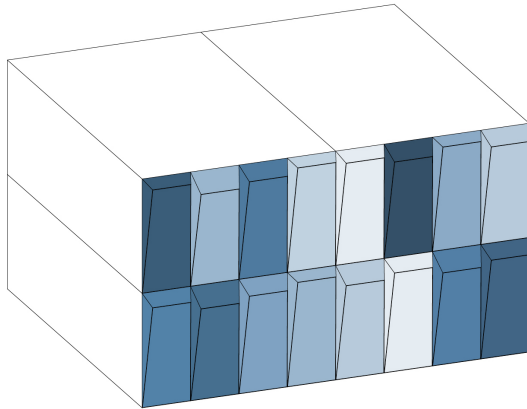


Figure 7.5.2.2.1. Random Facade Modules

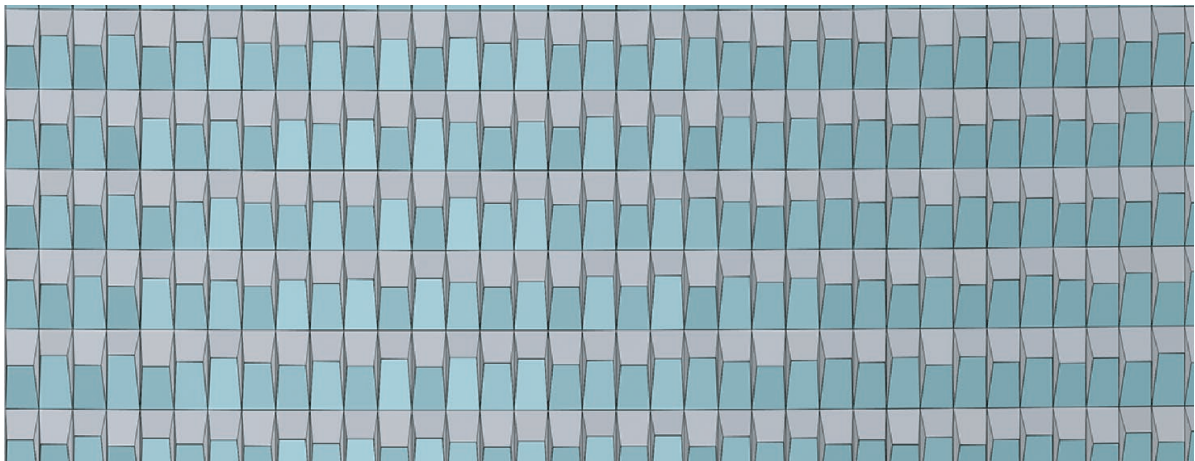


Figure 7.5.2.2.2. Random Facade

Architecturally, this approach created a more dynamic façade expression compared to the regular typology. The pixelated diversity strengthened the visual identity of the building and prevented monotony, yet at the cost of reduced efficiency. Therefore, the random façade is more suitable as a partial strategy rather than a uniform solution for the entire façade.

### 7.5.3 Wave Facade

#### 7.5.3.1 F04 Scenario : Variable Glazing Height

When the façade depth was fixed at 0.40 m, the impact of varying the window height ratio between 75–85% and 85–95% was tested through scenarios F04 and F04.1. (Figure 7.5.3.1.1.)

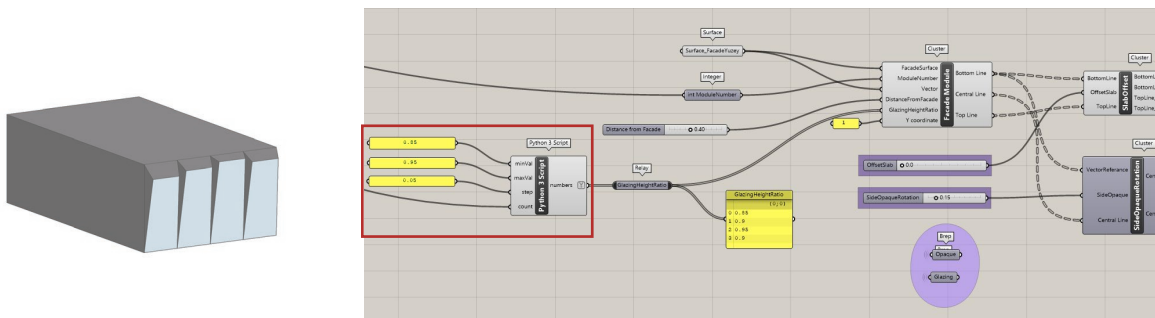


Figure 7.5.3.1.1. F04 Shoebox (N1-1 & N5-1) Grasshopper Parameters

In the N1-1 series, increasing the window height ratio improved daylight autonomy from 82.28% to 94.02%, while ASE rose only marginally from 1.96% to 2.28%. (Figure 7.5.3.1.2.) A similar tendency was seen in the N5-1 case, where sDA increased from 72.39% to 83.04%, accompanied by a modest ASE growth from 1.96% to 2.28%. (Figure 7.5.3.1.3.) Despite the rise in ASE, both cases stay within the LEED visual comfort threshold, indicating that the chosen façade depth works well. However, the results also indicate that additional adjustments to the façade offset might achieve a better balance, preserving daylight access while minimizing glare risk.

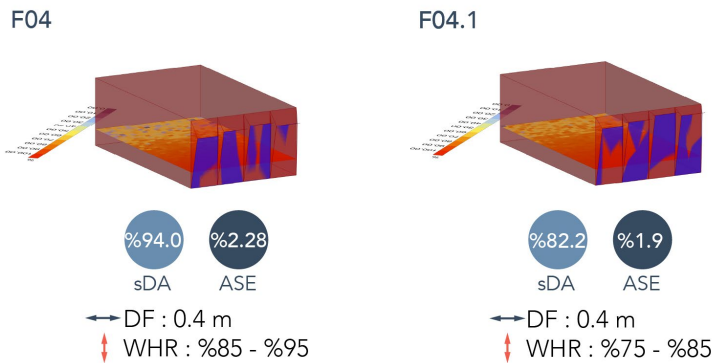


Figure 7.5.3.1.2. F04 and F04.1 (N1-1) Parameters and Daylight Result

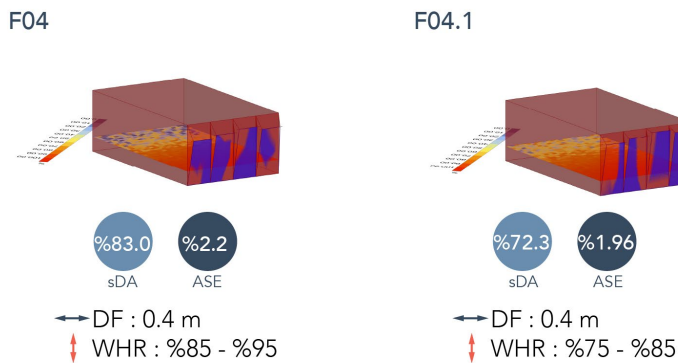


Figure 7.5.3.1.3. F04 and F04.1 (N5-1) Parameters and Daylight Result

### 7.5.3.2 F05 Scenario: Flexible Range and F05 Generations

In the F05 scenario, with the distance from façade set between 0.30–0.40 m and the window height ratio fixed at 75–85%, the performance outcomes varied between orientations. (Figure 7.5.3.2.1.)

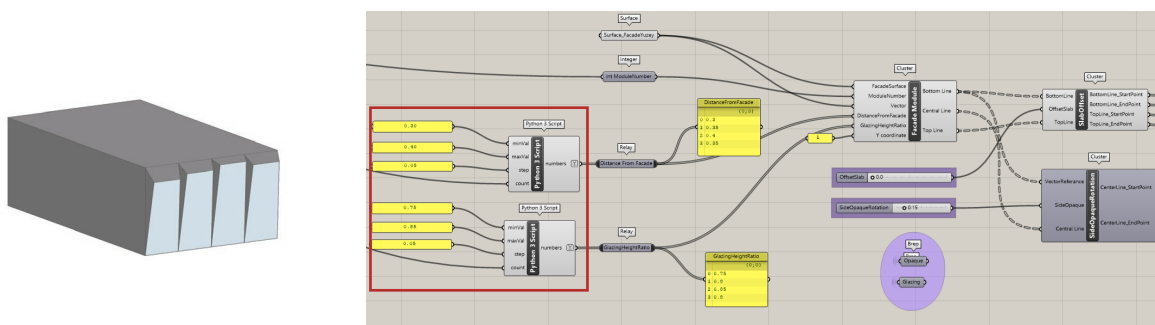


Figure 7.5.3.2.1. F05 Shoebox (N1-1 & N5-1) Grasshopper Parameters

In the N1-1 case, sDA reached 81.73% with an ASE of 2.17%, demonstrating effective daylight access with minimal glare. (Figure 7.5.3.2.2.) By comparison, N5-1 achieved a lower sDA of 73.80%, while ASE remained unchanged at 2.17%,(Figure 7.5.3.2.3.) emphasizing the role of orientation in shaping daylight performance even when glare conditions are stable.

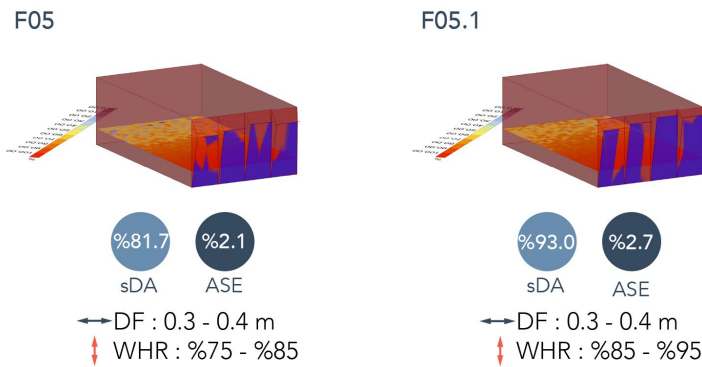


Figure 7.5.3.2.2. F05 and F05.1 (N1-1) Parameters and Daylight Result

Scenario F05.1, which tested a façade distance of 0.30–0.40 m with a window height ratio of 85–95%, showed stronger daylight outcomes. In N1-1, sDA rose to 93.04%, accompanied by a slight ASE increase to 2.72%, suggesting greater daylight penetration with only marginal glare risk. (Figure 7.5.3.2.2.) In N5-1, sDA was lower at 84.89% and ASE measured 2.61% (Figure 7.5.3.2.3.), indicating reduced daylight access compared to N1-1 but still within acceptable comfort limits.

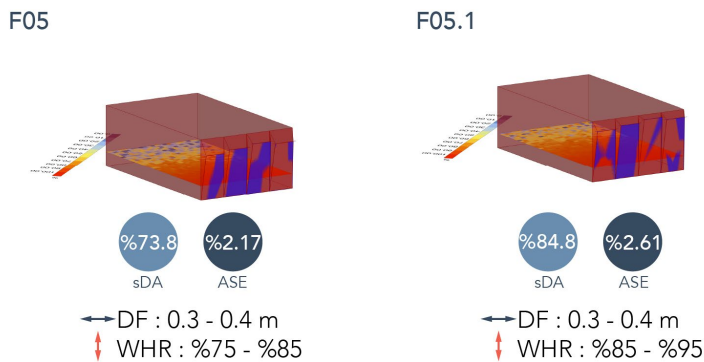


Figure 7.5.3.2.3. F05 and F05.1 (N5-1) Parameters and Daylight Result

This scenario confirmed that increasing glazing height while keeping façade depth constant can substantially improve daylight performance without surpassing glare thresholds. These consistent results confirmed the stability of the parametric framework. Since sDA values in N5-1 showed significant improvement compared to F05, this scenario was introduced to test how daylight performance would change if façade distance was increased.

### 7.5.3.3 Facade Development

The wave façade typology was developed from scenarios F05 and F05.1. Comparative analysis showed that the daylight performance of these scenarios was favorable,

making them suitable for further application. To reinforce the perception of façade movement, modules from F05 and F05.1 were prioritized for the final design. When arranged sequentially, these modules generated a continuous wave-like rhythm across the façade (Figure 7.5.3.3.1).

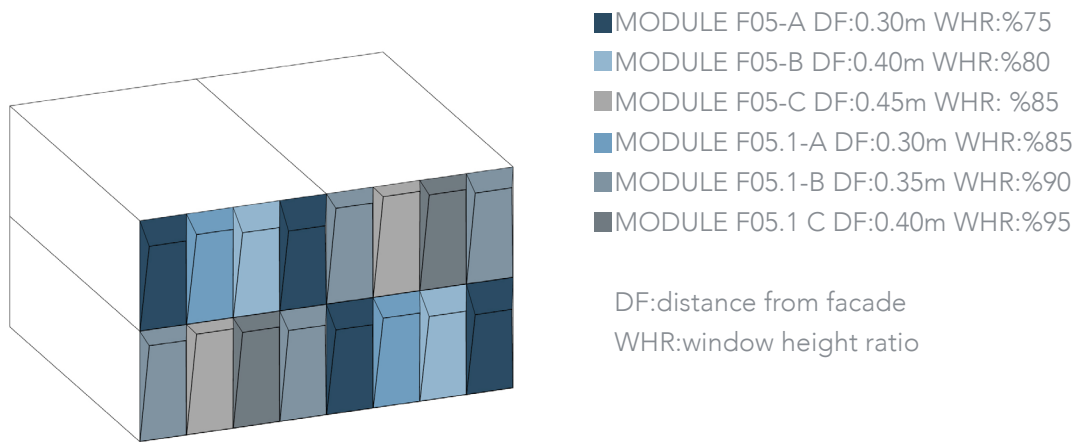


Figure 7.5.3.3.1 Wave Facade Modules (N1-1 & N5-1)

This controlled alternation introduced horizontal movement and softened the tower’s verticality, enriching its architectural presence while ensuring smoother transitions across the surface. The resulting composition maintained order yet achieved variety, distinguishing it from the strict regularity of the regular façade and the unpredictability of the random façade. Beyond compliance, the wave façade offered a structured yet dynamic solution, combining controlled modular variation with architectural expression. This balance of environmental efficiency, feasibility, and design character positioned the wave façade as the most resilient strategy among the tested typologies. (Figure 7.5.3.3.2.)

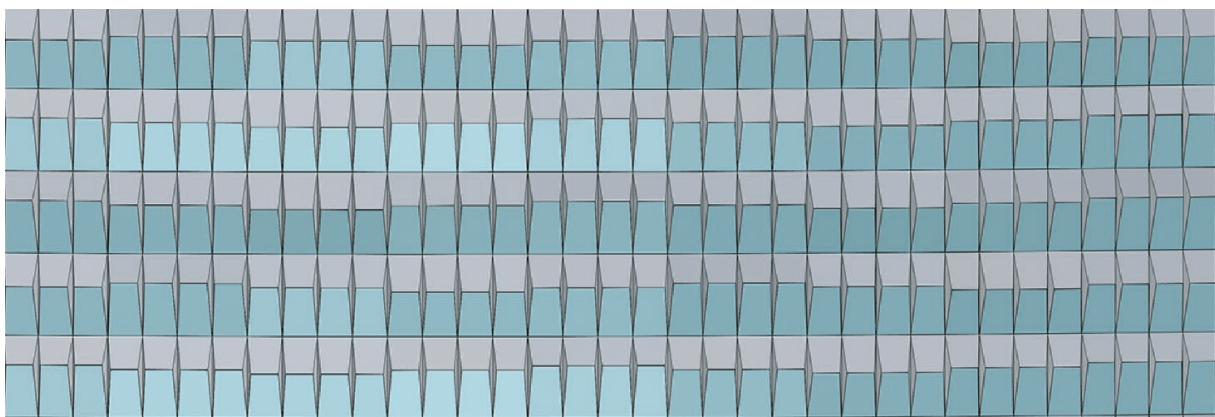


Figure 7.5.3.3.2. Wave Facade View (N1-1 & N5-1)

## 7.6. Comparative Evaluation

### 7.6.1 Structural Integration

The integration of façade modules with the structural frame played a decisive role in the development of all typologies. Two principal approaches were explored: concealing the structural grid behind the modules to emphasize surface continuity, and

aligning the modules with the columns to reinforce rhythm, hierarchy, and scale within the façade composition. This interplay between structure and envelope not only influenced the visual outcome but also shaped how the building would be perceived in relation to its urban context.

In the regular façade, this relationship determined the balance between simplicity and articulation. When the structure was concealed, the façade read as a homogeneous surface defined primarily by modular repetition. While this strategy enhanced continuity and clarity, it risked monotony at the scale of a high-rise, as the limited window height variations were insufficient to sustain visual richness. Conversely, when the modules were positioned between the vertical structural columns, the continuity of axes introduced rhythm and proportion. This approach established hierarchy, improved perceptual quality, and reinforced a clear sense of scale, while maintaining consistency with the architectural identity of the existing tower. In this way, the façade could simultaneously achieve clarity of expression and spatial depth. (Figure 7.6.1.1.)

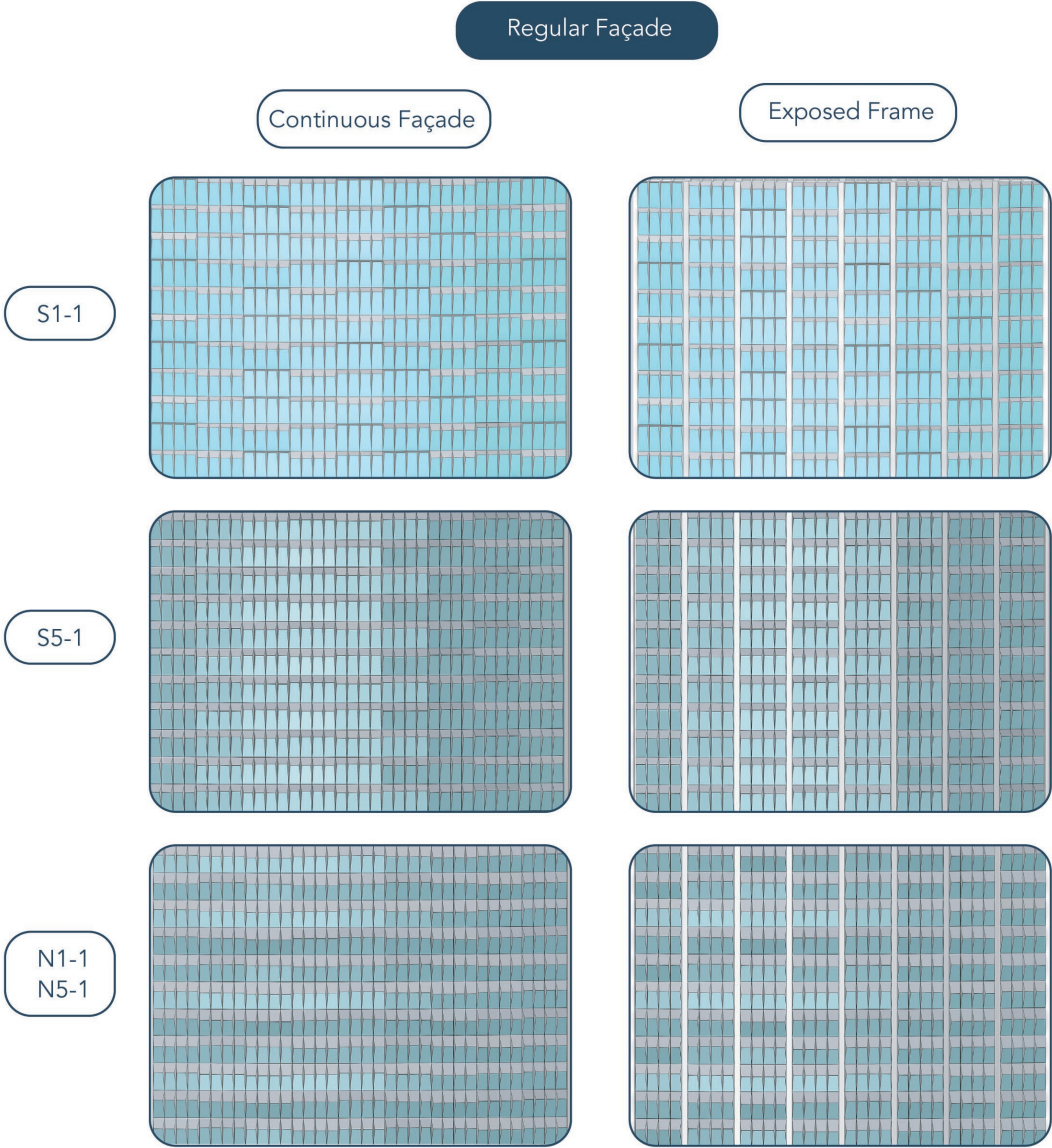


Figure 7.6.1.1. Regular façade alternatives: continuous vs. exposed frame

In the random façade, the structural frame provided a degree of order to an otherwise unpredictable system. Concealing the structure left the façade to be perceived only through the irregular diversity of its modules, which emphasized dynamism but also risked fragmentation and weakened legibility. Exposing the vertical columns, however, introduced rhythm and scale that moderated the randomness. This clarified the composition without undermining its expressive character, allowing the façade to retain dynamism while improving architectural coherence. As a result, the tension between order and variation became a key design driver, balancing expressiveness with readability. (Figure 7.6.1.2. )

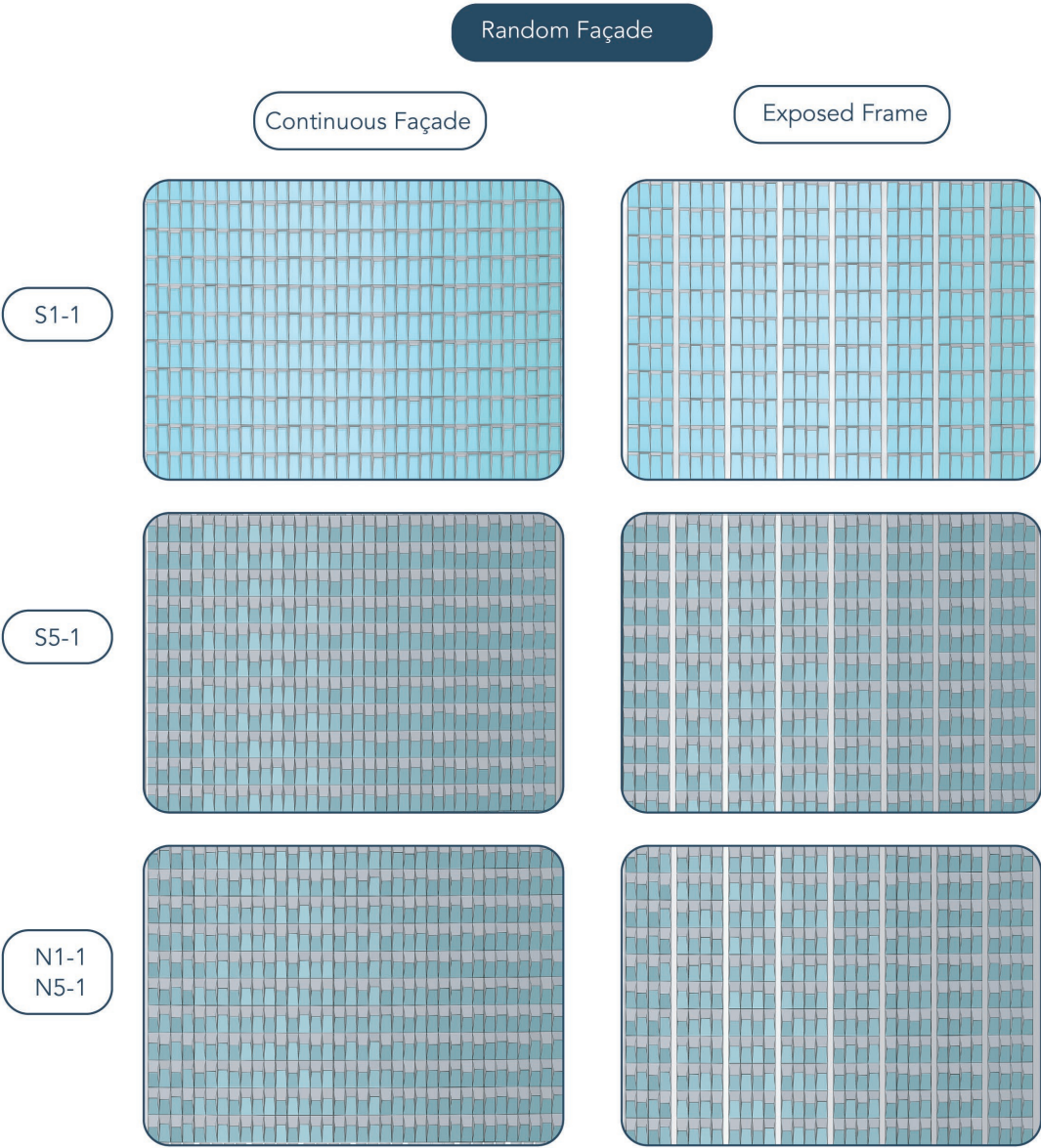


Figure 7.6.1.2. Random façade alternatives: continuous vs. exposed frame

In the wave façade, the extent to which the flowing pattern could be perceived was strongly influenced by structural integration. With the frame concealed, the undulating rhythm unfolded continuously across the surface, strengthening cohesion but sometimes diminishing the sense of scale on the tall tower. When the modules were

aligned with the structural grid, the vertical axes counterbalanced the horizontal wave. Although this reduced the continuity of the flowing pattern, it clarified proportions and hierarchy, enhancing legibility while maintaining the expressive quality of the design. Ultimately, this integration demonstrated that the exposed frame offered a more balanced relationship between dynamism, clarity, and architectural identity. (Figure 7.6.1.3.)

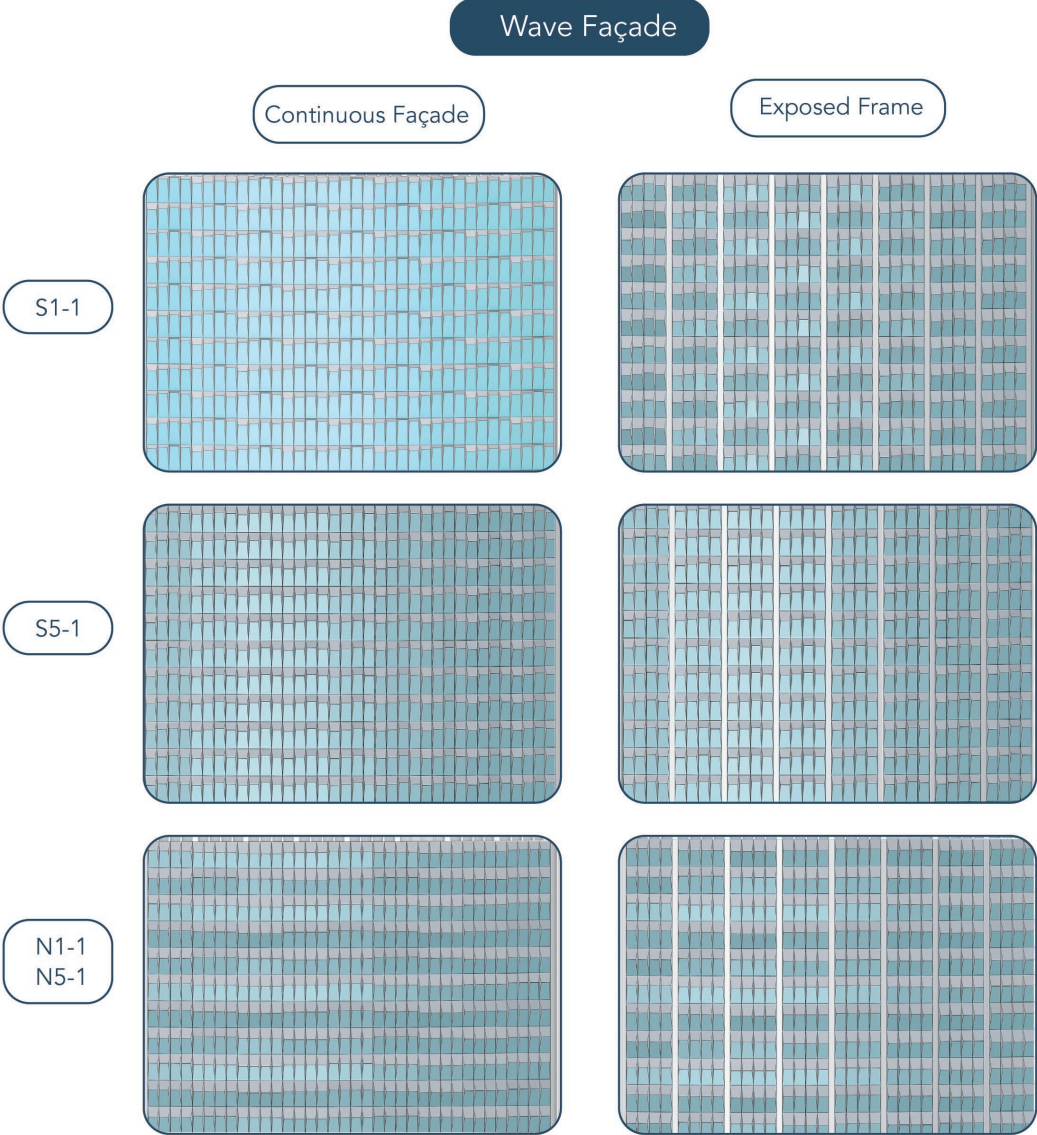


Figure 7.6.1.3. Wave façade alternatives: continuous vs. exposed frame

Taken together, these observations indicate that concealing the structure emphasized cohesion but risked monotony in the regular façade, fragmentation in the random façade, and loss of scale in the wave façade. Exposing the structural frame, on the other hand, consistently reinforced rhythm, hierarchy, and scale, offering a stronger balance between environmental performance and architectural expression. For these reasons, the final design adopts the exposed structural frame as the preferred strategy, ensuring coherence with the existing tower while enhancing its spatial and visual qualities.

## 7.6.2. Façade Typologies

This section compares the three types of facades: Regular, Random, and Wave. It does this by using the results of shoebox simulations, parametric variants, and applications at the facade scale. There are three key factors for the assessment: performance and comfort, feasibility and constructability, and architectural expression. (Figure 7.6.2.)

	Regular	Random	Wave
Performance & Comfort	<ul style="list-style-type: none"> <li>+ Stable daylight performance</li> <li>+ sDA mostly in 55–75% range</li> <li>- ASE between 10–20%, requires blinds</li> <li>- At lower floors of southeast risk of sDA &lt;55%</li> </ul>	<ul style="list-style-type: none"> <li>+ Visual diversity occasionally improves sDA</li> <li>- High ASE on southeast, some cases exceed LEED limit, required blinds</li> <li>- Inconsistent</li> </ul>	<ul style="list-style-type: none"> <li>+ Balanced daylight performance</li> <li>+ Wave arrangement keeps sDA at acceptable level</li> <li>- ASE consistently &gt;10%, required blinds</li> </ul>
Feasibility & Constructability	<ul style="list-style-type: none"> <li>+ Easy serial production</li> <li>+ Modular repetition</li> <li>+ Lower cost</li> <li>- Limited flexibility</li> </ul>	<ul style="list-style-type: none"> <li>+ Strong parametric diversity</li> <li>- Loss of standardization</li> <li>- Complex production and assembly</li> <li>- Higher cost</li> </ul>	<ul style="list-style-type: none"> <li>+ Modular system preserved</li> <li>+ Controlled parametric variation</li> <li>+ Moderate cost</li> </ul>
Architectural Expression	<ul style="list-style-type: none"> <li>+ Order, simplicity, readable rhythm</li> <li>- High risk of monotony</li> <li>- Limited parametric variation insufficient for identity</li> </ul>	<ul style="list-style-type: none"> <li>+ Strong dynamism, expressive identity</li> <li>+ Breaks monotony</li> <li>- Risk of chaotic perception</li> <li>- Weakened sense of coherence</li> </ul>	<ul style="list-style-type: none"> <li>+ Strong architectural expression</li> <li>+ Wave rhythm softens verticality</li> <li>+ Balance of order and diversity</li> <li>- Complex façade arrangement</li> </ul>

Figure 7.6.2. Comparison Table

The Regular façade achieved stable daylight performance, with sDA values typically falling within the 55–75% range. ASE levels frequently exceeded LEED criteria, necessitating the incorporation of shading solutions as blinds. Its strength lies in the efficiency of serial production, modular repetition, and lower costs. Nevertheless, the limited scope for parametric variation and the risk of visual monotony constrain its architectural identity, resulting in a façade that conveys order and rhythm but lacks distinctiveness.

The Random façade generated strong visual diversity and, in some instances, improved daylight autonomy. At the same time, its inconsistent outcomes and elevated ASE levels on southeast orientations presented challenges for meeting visual comfort standards. While the variety produced by randomization enriches architectural expression and creates a dynamic identity, the absence of standardization complicates production, increases costs, and reduces overall feasibility. This restricts its application at the scale of a high-rise tower, even if it offers potential for striking localized interventions.

The Wave façade provided the most balanced performance, combining modular constructability with controlled variation. Its rhythmic expression made the skyscraper

appear less vertical and architecturally more refined, while maintaining a consistent appearance across all levels. This typology requires more detailed planning and moderate costs to be feasible. However, it relies on a restricted number of recurring module families, which facilitates unitized production and ensures that the architecture remains both rich in expression and technically viable.

Orientation-specific daylight conditions further differentiate the typologies. On the southeast upper façade (S1-1), direct solar exposure intensified ASE, making glare control critical. Regular and Wave configurations provided more stable outcomes, although shading remained necessary. On the southeast lower façade (S5-1), overshadowing by neighboring buildings limited daylight, leading the design to prioritize increasing sDA while managing glare. Larger window height ratios were more effective on the Regular and Wave façades, whereas Random strategies had difficulty reaching acceptable performance levels. On the north façades (N1-1 and N5-1), gentler daylight conditions resulted in very high sDA and low ASE values across all typologies. These results indicate that although the north façades are more forgiving, parametric variation continues to shape the balance between daylight quality and architectural expression.

Taken together, the comparison demonstrates that each typology addresses environmental and architectural demands in different ways. Regular façades can seem monotonous, but they emphasize ease of construction and cost effectiveness. Although they frequently lack practicality and performance reliability, random façades encourage expressive diversity. Wave façades, on the other hand, offer architectural dynamism, technical viability, and consistent environmental benefits, thereby striking a balance.

## **7.7 Selection of the Wave Façade Typology**

The comparative analysis identified the Wave façade as the most suitable typology for the case study tower. The system demonstrated reliable daylight performance across different orientations, showing flexibility for both sun-exposed and shaded façades. On the south-east façade, which faced more intense sunlight, shading devices helped meet visual comfort standards without disrupting the architectural rhythm of the undulating modules. Beyond just performance metrics, the Wave façade established a unique architectural identity. Its horizontal modules counterbalance the tower's vertical emphasis, boosting its presence in the urban context and softening how its scale is perceived. The decision also took constructability into account: using a limited set of recurring modules allows for efficient production within a unitized system without sacrificing visual complexity.

In conclusion, while each façade strategy demonstrated specific advantages, the Wave façade offered the most comprehensive response. By integrating environmental performance, constructability, and architectural expression within a single parametric framework, it emerged as the most resilient solution for the high-rise envelope of the case study tower.



# ***CHAPTER VIII***

System Integration for Tour  
Montparnasse Façade Retrofit

## 8.1 Introduction

This chapter examines the transition from conceptual façade evaluation to the development of a technically and spatially coherent retrofit strategy for Tour Montparnasse. Building on the comparative assessment of alternative façade typologies, the focus shifts toward two interrelated aspects: the integration of façade performance within office space planning, and the feasibility of adopting a modular, prefabricated façade approach in alignment with the building's existing structural framework.

The discussion first addresses the spatial organization of office interiors in relation to daylight availability, demonstrating how façade design directly influences functional distribution within the floorplate. It then introduces the Schüco Parametric System as a case study that illustrates the principles of modularity, digital integration, and prefabrication in contemporary façade construction. Finally, these references are tested through detailed adaptations to the Tour Montparnasse, where horizontal and vertical sections explore the compatibility of parametric and prefabricated façade logics with the composite structural framework of the tower.

By connecting environmental performance, systemic façade design, and technical adaptation, the chapter establishes the basis for a high-performance and buildable retrofit strategy.

## 8.2. Office Floor Plan Integration

Beyond the optimization of daylight performance at the façade level, the spatial organization of the office floor plan was also evaluated. For this purpose, a representative layout was developed to examine the distribution and hierarchical structuring of interior spaces. In this scheme, primary workstations are arranged along the façade within a 6 m deep daylight core. This configuration is intended to maximize access to natural light and external views, thereby enhancing user comfort. Such an approach is supported by international guidelines, including CIBSE LG10 and the BCO Guide to Specification, both of which identify the first 6 m from the façade as the optimal zone for primary workspaces due to superior daylight availability (CIBSE 2014; BCO 2024).

Immediately behind this core, in the zone spanning 6–9 m from the façade, collaborative areas and small meeting rooms are located. The resulting lighting conditions provide a balanced visual environment, supporting both the functional and social requirements of contemporary office spaces. Deeper within the floorplate, between 9–18 m from the façade, enclosed meeting rooms, service areas, and circulation are positioned. These spaces rely largely on borrowed daylight from perimeter zones and are supplemented with artificial lighting systems as necessary (CIBSE 2014; BCO 2024).

This spatial strategy demonstrates that environmental performance and functional hierarchy are closely interlinked. Variations in daylight quality across different depths of the floorplate enable the allocation of functions according to their lighting needs,

thereby establishing a coherent relationship between architectural design and user comfort. In this way, scientifically informed and regulation-compliant spatial solutions are achieved for modern office environments (CIBSE 2014; BCO 2024). 8.4 Integration with Schüco Parametric Façade System

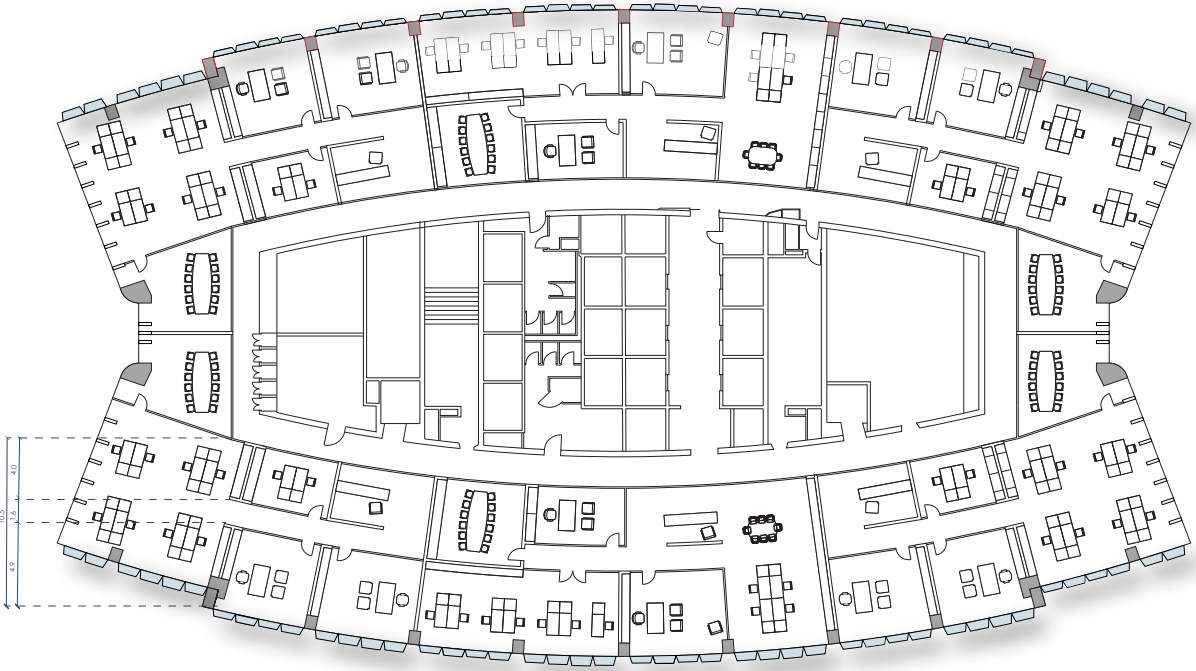


Figure 8.2.1. Typical Office Floor Plan

### 8.3. Schüco Parametric System Overview

The Schüco Parametric System, based on free-form geometries through a modular construction principle (Schüco International KG 2014). Its design is based on an adaptable tubular frame structure that allows rectangular and triangular base modules to be combined at varying angles. (Figure 8.3.1.) In this way, both faceted and smoothly curved surfaces can be realized while maintaining a controlled assembly logic.

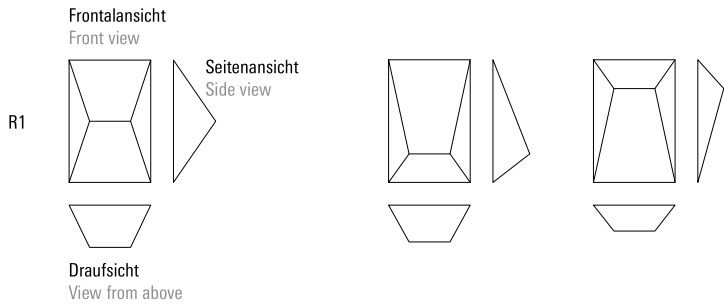


Figure 8.3.1. Schüco Selected Basic Modules

The system is integrated within Schüco's digital design and production environment. Project geometry can be directly used in fabrication, minimizing tolerance problems and guaranteeing that elements are produced according to the specified requirements. This approach highlights the role of digital continuity between design and production in handling complex façade geometries.

Prefabrication represents an important aspect of the system. Modules are produced under workshop conditions, with controlled quality, and later mounted onto a supporting substructure on site. This method reduces installation complexity and allows for precise coordination between design intent and execution. The supporting tubular frame can adapt its configuration to suit straight or curved contours, while project-specific modifications are possible when required by structural or architectural constraints.



*Figure 8.3.2. Well thought-out system details enable reliable fabrication*



*Figure 8.3.3. Unit Prefabrication and Installation of the units on the steel*

At the modular level, the system integrates several components such as frame profiles, glazing panels, opaque aluminium elements, sealing profiles, and bonding layers into coordinated assemblies. These elements are designed to balance thermal, structural, and weatherproofing requirements within the system logic. Beyond transparent glazing, opaque aluminium panels and optionally interior blinds can also be incorporated, broadening the façade's potential functional and environmental performance.

Technical details offered within the system, such as concealed drainage, ventilation at regular intervals, or additional mechanical fixings in high-rise applications, are aimed at ensuring durability and safety under variable environmental conditions. While this study does not focus on proprietary detailing, the general principles of prefabrication, modular logic, and parametric adaptability were relevant as a reference framework for our design adaptation.



Figure 8.3.4. Schüco System Component

## 8.4. Adaptation to Tour Montparnasse

In this thesis, the Schüco Parametric System has been studied primarily as a reference for how prefabricated unitized façades with adaptable geometries can be implemented in retrofit scenarios. Specifically, its modular logic informed the development of a façade solution for the Tour Montparnasse renovation.

The existing structure of the tower, consisting of a reinforced concrete core, a perimeter steel frame of columns and beams, and composite slabs formed by steel beams with concrete decks, provided the necessary anchoring points for attaching façade modules. Building on the principle of a tubular support frame, new façade units have been designed to connect through steel brackets fixed at slab edges.



Figure 8.4.1. Montparnasse construction site

The adaptation of the Schüco Parametric System to the Tour Montparnasse was developed through an anchoring strategy that responds to the existing steel structural framework. The tower is organized around a central steel core with a perimeter of steel columns supporting composite floor slabs made of profiled steel decking with concrete topping. The façade modules are fixed to the concrete layer of these slabs using steel connection brackets.

Around the steel columns, a layered enclosure system was designed to provide fire safety, thermal insulation, and interior finishing. The sequence of materials includes a vapor barrier, 5 cm of rockwool insulation (Knauf Smartwall C1), drywall (2 × 12 mm), and an internal gypsum plaster finish (3 + 2 mm). On the exterior side, AQUAPAN-EL® Cement Board ensures robustness and fire resistance while providing a suitable substrate for the façade system.

The Schüco unitized façade integrates two types of infill: double-glazed Low-E argon-filled panels (6-16-6) for transparent areas and aluminium spandrel panels with mineral wool insulation for opaque zones. These infill elements are first mounted onto tube frame profiles, then inserted into the unit frame, which is ultimately secured to the slab-mounted brackets. Accessories such as glass spacers, bonding adhesives, and rebate insulation ensure airtightness, water tightness, and structural performance of the glazing.

From a performance perspective, the Schüco Parametric System is characterized as a highly insulated aluminium façade system. The brochure specifies U-values ranging between 0.15–0.25 W/(m<sup>2</sup>K) for opaque spandrel panels (Schüco Parametric System Brochure, p.16). For transparent units, the use of Low-E coated, argon-filled double glazing allows U-values to be reduced to 1.0–1.3 W/(m<sup>2</sup>K) (Schüco Parametric System Brochure, p.49). Fire-stopping barriers at floor junctions further guarantee safety by preventing vertical fire spread while maintaining insulation continuity.

Beyond the unitized façade modules, the design also incorporates a secondary layer of single glazing on the interior side of the building envelope. This additional glazing is fixed directly to the concrete surface of the composite slabs, establishing a clear boundary between the internal environment and the external façade modules. Its role extends beyond that of a simple partition: it contributes significantly to acoustic insulation and occupant comfort, while at the same time forming an intermediate cavity that accommodates motorized blinds and allows for maintenance access. By separating the façade modules from the interior finishes in this way, the system strengthens the layered construction principle adopted in the renovation and ensures a more coherent integration between the building's envelope and its interior spaces.

The floor construction is based on a composite slab system, consisting of reinforced concrete poured onto steel beams and supported by profiled steel decking. On top of this slab, the interior finish is completed with a layer of Luxury Vinyl Tile (LVT) flooring, which provides both durability and ease of maintenance.

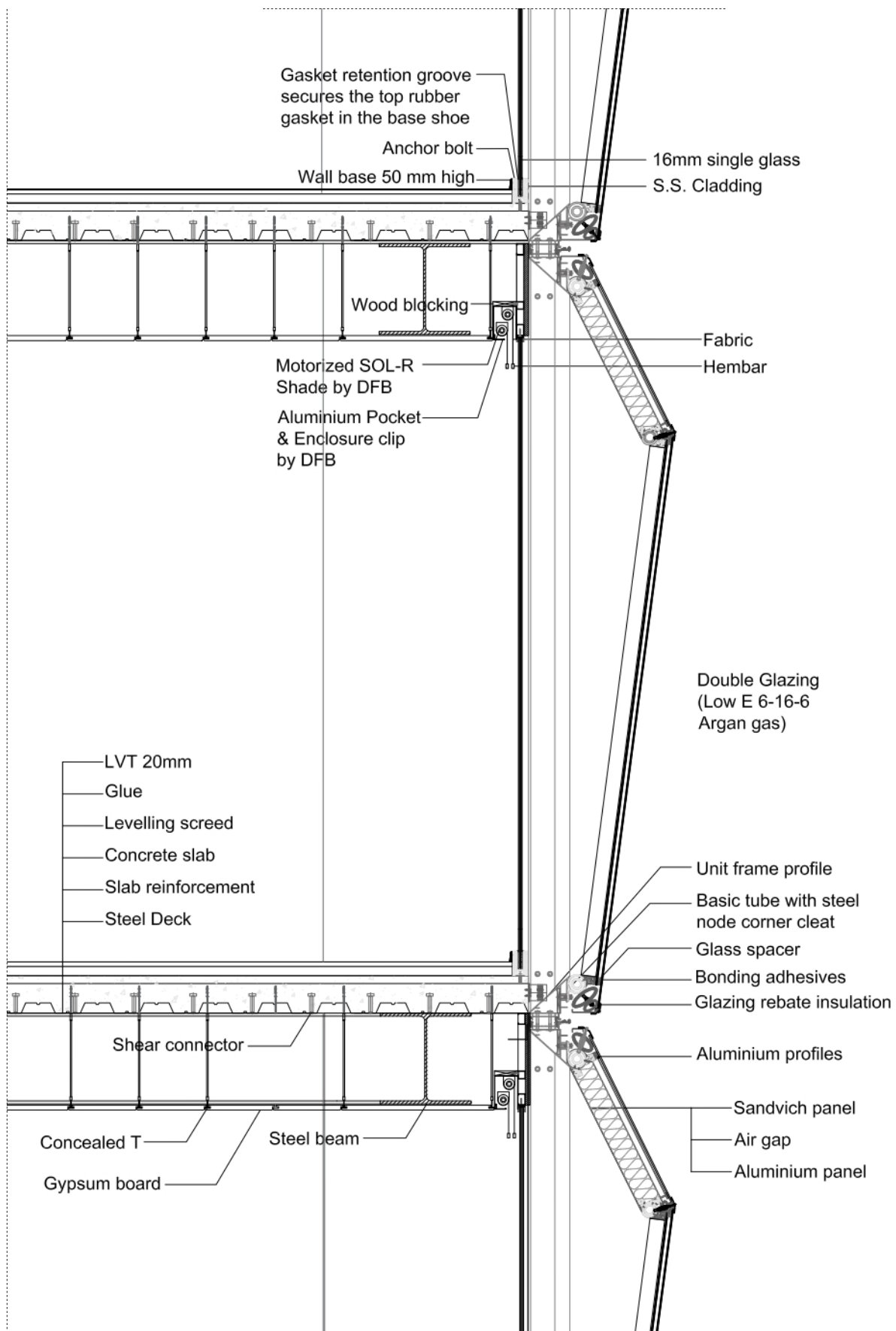


Figure 8.4.1. 1:25 Vertical Section Drawing

Similarly, the interior ceiling is resolved through a suspended system anchored to the concrete slab above by means of concealed T-bar profiles. This structure supports the installation of gypsum board panels, which serve as the visible finish while also allowing for the integration of building services within the plenum.

In order to ensure structural feasibility and limit spatial intrusion into the interior, the distance of the façade modules from the slab edge was restricted not to exceed 0.65 m. This constraint reflects both structural considerations, as larger cantilevering depths would induce higher stresses on the anchoring brackets, and architectural requirements, ensuring that usable interior space is preserved and maintenance accessibility is maintained.

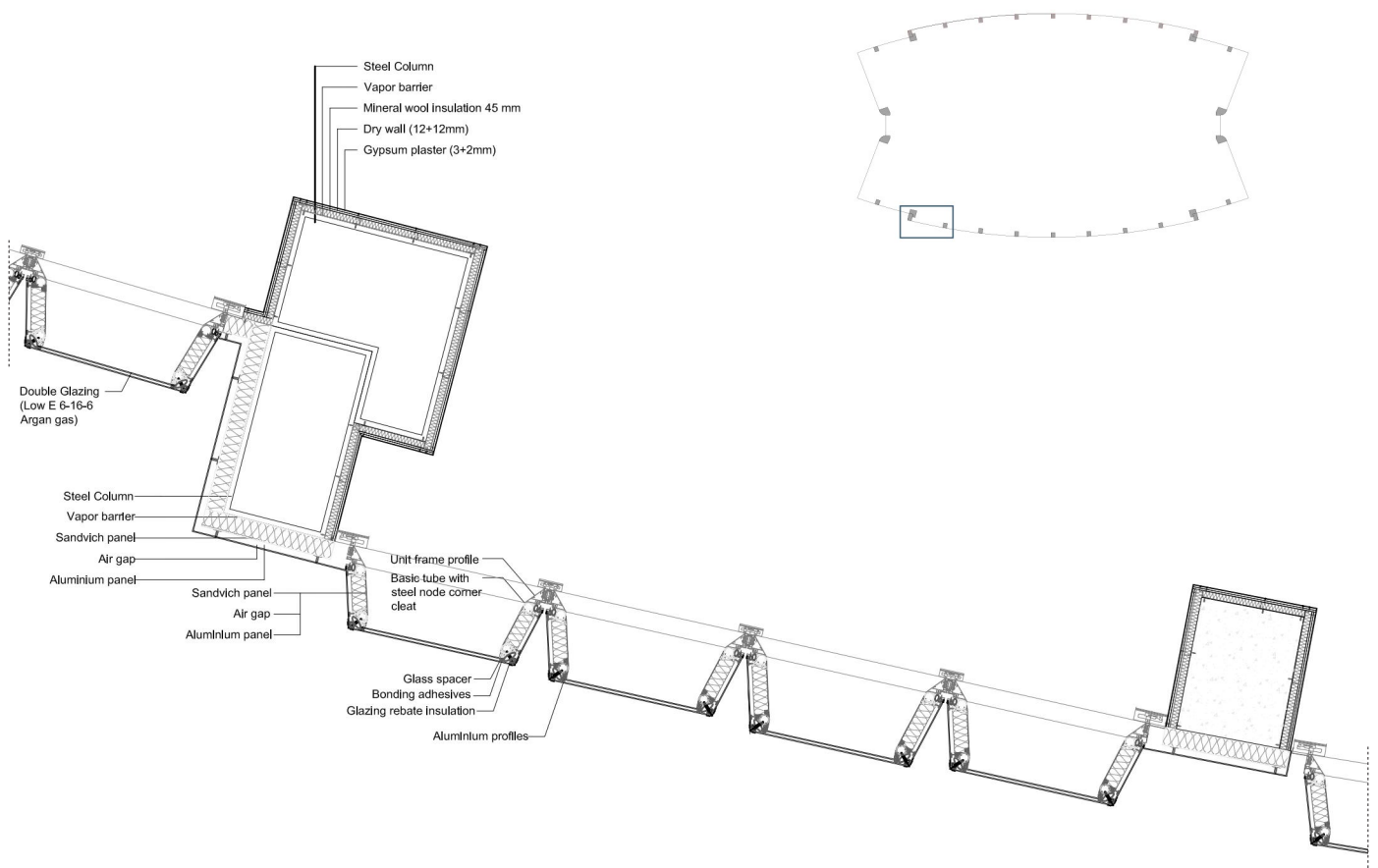


Figure 8.4.2. 1:50 Horizontal Section Drawing

## 8.5. Conclusion

This chapter has shown that the retrofit of Tour Montparnasse can bring together environmental performance, modular façade technology, and interior organization within a single coherent strategy. The study began by examining the link between daylight performance and the arrangement of office spaces, demonstrating that the allocation of functions across the floorplate is directly shaped by façade design. The identification of daylight cores and secondary areas created a spatial framework consistent with international standards, highlighting the close relationship between environmental and architectural parameters.

Building on this foundation, the Schüco Parametric System was explored as a reference case to illustrate the potential of modularity, parametric design, and prefabrication. Its digital workflow and modular assembly logic provide a way to manage geometric variation while ensuring practical buildability. These principles informed the adaptation for Tour Montparnasse, where questions of technical feasibility and spatial coherence were tested against the existing structural system.

In the adaptation process, façade units were anchored to the composite slabs with steel brackets, while layered solutions around the columns addressed fire safety, insulation, and interior finishes. Transparent areas were designed with Low-E double glazing, while opaque zones used aluminium spandrel panels with mineral wool insulation. On the interior, a secondary layer of single glazing enhanced acoustic comfort, solar control, and maintenance access, reinforcing the layered construction approach.

The façade modules were limited to a maximum offset of 0.65 m from the slab edge, a constraint that ensured structural reliability while protecting usable floor space. Prefabricated assembly methods and integrated detailing for fire-stopping, drainage, and airtightness further strengthened the retrofit strategy.

In summary, the chapter demonstrates that a parametric, prefabricated façade system can be successfully adapted to an existing high-rise. Beyond technical feasibility, the approach is capable of improving spatial quality and environmental performance. The Tour Montparnasse case illustrates how modular façade systems can balance structural limits, user comfort, and architectural identity, offering a replicable model for the sustainable retrofit of high-rise buildings.

# ***CHAPTER IX***

Discussion and Conclusion

## 9.1 General Discussion

The study focused on redesigning Tour Montparnasse through performance-based parametric design because its outdated design and poor urban integration with Parisian architecture needed improvement. The research developed a method which merges environmental performance with architectural expression and construction feasibility through the integration of shoebox simulations with evolutionary optimization and Wallacei and façade typology analysis.

The comparative analysis revealed that façade geometry is not only a technical device to control daylight but also a critical determinant of urban identity. The three façade types Regular and Random and Wave presented distinct relationships between their technical performance and their architectural impact. The Regular façade achieved high efficiency and standardization but failed to create unique architectural features. The Random façade design created strong architectural identity yet presented challenges for manufacturing and construction expenses and future maintenance requirements for maintenance. Among the alternatives, the Wave façade proved to be the most balanced solution: it enhanced daylight autonomy, reduced excessive solar exposure, and introduced a rhythmic expression that helped ease the rigid verticality of the tower.

The research demonstrated that parametric workflows operate as design decision-making instruments. The designers maintained complete design freedom through their architectural choices because Grasshopper and Honeybee and Wallacei operated as a continuous system to assess LEED daylighting standards. The connection between data-driven insights and design qualities allowed designers to study optimization as a design tool which directs architectural development instead of imposing particular forms.

## 9.2 Advantages and Limitations

The research achieves its main strength through its complete and unified research approach. The study advances past performance-based research through its combination of environmental simulation with parametric variation and optimization methods and industrial partnership. The research combines quantitative performance indicators with architectural identity and practical implementation feasibility to develop a sustainable retrofit strategy which adapts to local conditions and maintains architectural value. The research method which studies multiple factors strengthens its value for academic studies and professional applications.

Multiple restrictions exist within this research framework which need acknowledgment. The research conducted environmental analysis through daylight performance assessment but it did not thoroughly investigate energy usage and thermal comfort and acoustic conditions and user satisfaction which require additional study. The Schüco integration process stopped at digital detailing without progressing to physical testing or on-site verification which would have delivered more concrete evidence. The detailed examination of the Montparnasse Tower as a case study

produced valuable insights about this complex high-profile complex project but restricted the general applicability of the research findings. The proposed framework requires modifications to work across different locations because it needs to consider local climate conditions and cultural elements and regulatory requirements.

### **9.3 Future Development**

Future research should expand the performance criteria to include energy demand, thermal comfort, and life-cycle analysis, thereby offering a more comprehensive sustainability assessment. Hybrid configurations that combine the vibrancy of Random typologies with the order of Regular strategies could also be explored, extending design diversity while maintaining feasibility. Physical prototyping and mock-ups serve as critical tools to evaluate assembly tolerances and maintenance approaches and durability performance. The application of machine learning tools enables parametric exploration to proceed faster which produces optimized solutions that meet performance requirements and cost constraints and architectural needs.

### **9.4 Final Remark**

The research demonstrates how Tour Montparnasse retrofitting becomes more effective through the combination of performance evaluation with architectural design elements and construction practicality. The research established that parametric methods function as design tools which maintain architectural freedom while improving environmental quality through their ability to handle façade geometry as both technical and cultural elements.

The Wave façade typology represents the most balanced solution because it unites performance requirements with construction principles and architectural characteristics to create sustainable buildings that match their surroundings. The research methodology presents a repeatable approach although it faces restrictions when trying to expand its analysis to include environmental and user-focused assessment criteria.

The research presents a method to transform high-rise building retrofits in modern urban areas through its analysis of the Montparnasse case study. The research presents a method to transform future building retrofits by combining computational optimization with façade typology studies and design feasibility assessments which will lead to integrated strategies that unite performance optimization with architectural value and urban character.

# ***CHAPTER X***

Referances and List of Figures

# References

1. Pietrzak, J. "High-Rise Buildings in Europe: Development in the 20th and 21st Centuries." Faculty of Architecture, Warsaw University of Technology, 2013
2. Hollister N., "The History of European Skyscraper", CTBUH Journal, Issue II, pp. 52-55, 2013. Accessed at <http://skyscrapercenter.com>.
3. "The Special Nature of the European Skyscraper" CTBUH Journal, Issue II, PP. 19-29 (2013). Accessed at <http://skyscrapercenter.com>.
4. Ilgın, H. Emre. A Study on Tall Buildings and Aerodynamic Modifications Against Wind Excitation. Master's thesis, Middle East Technical University, 2006.
5. Fakhari, Maral, and Hasan Ünver. "Evaluation and Comparison of Construction Technologies for High-Rise Buildings." *ESOGÜ Mühendislik ve Mimarlık Fakültesi Dergisi* 31, no. 4 (2023): 1013-1027.
6. Polat, Murat. "Innovation and Technological Advancements in High-Rise Buildings: In Search of Enabling the Most Flexible Space in Architecture." Paper presented at ISAS 2018-Winter, 2nd International Symposium on Innovative Approaches in Scientific Studies, Samsun, Turkey, November 30-December 2, 2018.
7. Tour Maine Montparnasse Real Estate Project. PC 11 Etude d'impact: PC 11-c: Update of the Non-Technical Summary of November 2018 of the Renovation Project of the Montparnasse Tower (PC 75 115 18 V 042) and the CIT Tower with Additions Relating to the CIT Tower. March 11, 2020. Ref. 4931289.
8. Colin Marshall, "A Defense of the Ugliest Building in Paris," *The New Yorker*, August 21, 2023, <https://www.newyorker.com/culture/cultural-comment/a-defense-of-the-ugliest-building-in-paris>
9. Velho, Mariana Caye. *The Montparnasse Tower: Analysis of a Renovation Project*. January 2021.
10. Paris." *Parametric Architecture*, March 3, 2023. <https://parametric-architecture.com/skyscraper-ban-reinstated-amidst-tour-triangle-controversy-in-paris/>
11. *HuffPost France*. "La Tour Montparnasse fête ses 40 ans, 40 ans de désamour." June 18, 2013. *HuffPost France*.
12. Andreu, Sylvie, and Michèle Leloup. *La Tour Montparnasse 1973-2013: Je t'aime... moi non plus*. Paris: Éditions de la Martinière, 2013.
13. VELUX Group. "Daylight Requirements in Building Codes." VELUX. Accessed September 26, 2025. <https://www.velux.com/what-we-do/research-and-knowledge/>

deic-basic-book/daylight/daylight-requirements-in-building-codes#section1.9.4

14.Ladybug Tools. "Modeling Zone Geometry." Honeybee Wiki. Accessed September 26, 2025. <https://docs.ladybug.tools/honeybee-wiki/single-zone-model/modeling-zone-geometry>

15.U.S. Green Building Council. "EQ Credit: Daylight." USGBC. Accessed September 26, 2025. <https://www.usgbc.org/credits/healthcare/v4-draft/eqc-0>

16.Ladybug Tools. "Daylighting." Honeybee Wiki (GitHub Repository). Accessed September 26, 2025. <https://github.com/ladybug-tools/honeybee-wiki/blob/master/Daylighting.md>

17.Cove.Tool. "Shoebox Model." cove.tool Help Center. Accessed September 26, 2025. <https://help.covetool.com/en/articles/5790051-shoebox-model>

18.Massachusetts Institute of Technology. "Lecture Slides 1." 4.401 Environmental Technologies in Buildings, Fall 2018. MIT OpenCourseWare. Accessed September 26, 2025. <https://ocw.mit.edu/courses/4-401-environmental-technologies-in-buildings-fall-2018/pages/lecture-slides-1/>

19.U.S. Green Building Council. LEED Reference Guide for Building Design and Construction. Washington, DC: U.S. Green Building Council, 2016.

20.Wallacei. "Learn." Wallacei. Accessed September 26, 2025. <https://www.wallacei.com/learn>

21. Skidmore, Owings & Merrill (SOM). "BBVA Bancomer Operations Center." <https://www.som.com/projects/bbva-bancomer-operations-center/>

22.Skidmore, Owings & Merrill (SOM). "Manhattan Loft Gardens." <https://www.som.com/projects/manhattan-loft-gardens/>

23.Smith + Gill. "Zhongzhou Holdings Financial Center." [https://smithgill.com/work/zhongzhou\\_holdings\\_financial\\_center/](https://smithgill.com/work/zhongzhou_holdings_financial_center/)

24.Skidmore, Owings & Merrill (SOM). "Beijing Greenland Center." <https://www.som.com/projects/beijing-greenland-center/>

25.BCO (British Council for Offices). 2024. Guide to Specification. London: BCO.

26.CIBSE (Chartered Institution of Building Services Engineers). 2014. Lighting Guide 10: Daylighting—A Guide for Designers. London: CIBSE.

27. Schüco International KG. Schüco Parametric System. Bielefeld: Schüco International KG, 2014.

# List of Figures

Figure 2.1.1 - Home Insurance Building, Chicago, Postcard, 1912

Figure 2.1.2 - Monadnock Building, Chicago, Postcard, 1912.

Figure 2.1.3 - Empire State Building, NY by Boyan Georgiev Creative, 2023

Figure 2.2: Frankfurt cityscape showing integration of modern skyscrapers with historic urban fabric (Igor Flak, 2019).

Figure 2.3.1 - L'Avenue des Maisons-Tours. Auguste Perret. Perspective de Jacques Lambert, L'illustration, 12 de agosto de 1922. Bibliothèque Forney, Paris (Abram, 1994, p. 321)

Figure 2.3.2 - Quecq d'Henripret, Jacques. "Tour Montparnasse, Paris (15th arrondissement), general view." 1980. Mémoire. Ministry of Culture.

Figure 2.3.3 - Panorama of La Défense, seen from the Henri IV Pavilion in Saint-Germain-en-Laye (photo: R. Brunet, July 2010)

Figure 2.3.4 - Halbe, Roland. Photograph of Tours Duo

Figure 2.3.5.1 - Henry, Steven. Photograph of Tour Montparnasse. Skyscraper Center

Figure 2.3.5.2 - Montparnasse Tower from the Tossan slab

Figure 2.4.2 :The Montparnasse Tower (left) with the Panthéon in the foreground.

The image illustrates how the tower disrupts the historic Parisian skyline, overshadowing iconic landmarks. Photograph by Etienne Laurent / Getty.

Figure 3.1.1 – Grasshopper setup for Sun Path and Direct Sun Hours simulation, showing solar exposure on the façades.

Figure 3.1.2 – Grasshopper setup for Solar Radiation Gain, calculating incident solar energy on the façades.

Figure 3.2.1. Direct Sun Hours analysis across different façades of Tour Montparnasse using Ladybug in Grasshopper.

Figure 3.2.2. Sunpath diagrams for Tour Montparnasse, illustrating annual, summer, and winter sun positions.

3.2.3 Solar radiation analysis of Tour Montparnasse façades, showing annual radiation distribution in kWh/m<sup>2</sup>.

Figure 3.2.4.1 Wind speed variations in Paris throughout the year, ranging from 0 to 18 m/s.

Figure 3.2.4.2 Wind rose diagram for Paris, showing wind directions, speeds, and frequencies.

Figure 3.2.5. Temperature variation heatmap for Paris, illustrating seasonal differences.

Figure 3.2.6.1 Shadow analysis diagrams for Tour Montparnasse during winter solstice (December 21).

Figure 3.2.6.2 Comparative shadow analysis showing seasonal variations between summer and winter

3.2.6.3 Shadow analysis diagrams for Tour Montparnasse during summer solstice (June 21).

Figure 4.1: BBVA Bancomer Operations Center façade system showing modular glass curtain wall with vertical aluminum louvers calibrated for solar orientation, enhancing daylight performance and sustainability.

Figure 4.2: Manhattan Loft Gardens façade articulation with serrated glass and GRC cladding in a triangulated geometry, integrating Juliet balconies and sky gardens as

sustainable design elements.

Figure 4.3: Shenzhen Zhongzhou Holdings Financial Center showcasing rectilinear glazed façade with insulated units, designed to balance transparency, thermal efficiency, and mixed-use urban integration

Figure 4.4: Beijing Greenland Center parametric façade modules with prismatic trapezoidal geometry, optimized through digital modeling to enhance self-shading, energy efficiency, and architectural dynamism.

Figure 5.1: Parametric façade workflow integrating building geometry, daylight analysis, and optimization with Wallacei

Figure 5.3.1. Grasshopper definition for geometry and material setup. This configuration established the baseline for evaluating alternative façade strategies in subsequent analyses.

Figure 5.3.2. Grasshopper workflow for glazing and external shading parameterization.

Figure 5.3.3. Integration of EPW climate and weather data in Grasshopper

Figure 5.3.4: Setup of daylight simulation in Grasshopper, showing (top) the definition of analysis grids and (bottom) the assembly of the HB Model integrating geometry, glazing, shading, and weather data.

Figure 5.3.5. Visualization of daylight performance metrics (sDA and ASE) in Grasshopper

Figure 5.4.1: Daylight performance of the original Montparnasse façade (baseline case), showing sDA and ASE results for Southeast and Northwest façades at the 6th and 35th floors

Figure 5.4.2: Shoebox test model in Grasshopper showing variations of vertical fins with different angles and depths. (Grasshopper model illustrating the application of vertical fin systems tested at 10°,

Figure 5.4.3 Shoebox test model in Grasshopper illustrating horizontal overhang strategies.

(Overhang depths tested at 40 cm, 50 cm, 75 cm, 1 m, and 1.5 m.) 30°, 45°, 60°, and 90°.)

Figure 5.4.4. Shoebox test model in Grasshopper combining vertical fins and horizontal overhangs.

(Hybrid strategy integrating both shading devices to evaluate combined performance.)

Figure 5.4.5: Shoebox test model in Grasshopper showing symmetric and asymmetric combinations of vertical and horizontal shading devices.

Figure 5.4.6 Shoebox test model of horizontal brise-soleil case study with varying depths and angles.

Figure 5.4.7: Shoebox test model in Grasshopper based on the SOM Manhattan Garden reference façade design.

Figure 5.4.8.1: Solar path diagrams for the Montparnasse site on June 21 (Summer Solstice) at 10:00 AM, 1:00 PM, and 5:00 PM.

Figure 5.4.8.2: Angled façade modules (20°, 30°, 40°, and 45°) and daylight simulation results for Southeast façade, 6th floor.

Figure 5.4.8.3: Angled façade modules (20°, 30°, 40°, and 45°) and daylight simulation results for Northwest façade, 6th floor.

Figure 5.4.8.4: Comprehensive shoebox test results for the Southeast and Northwest façades across multiple shading strategies, comparing the limitations of planar and hybrid systems with the superior performance of angled modules.

Figure 5.6.1: Schüco façade reference adapted into the parametric framework, demonstrating the differentiation of opaque shading elements at the top and transparent glazing at the bottom to balance solar control with daylight penetration.

Figure 5.7.1: Integration of data management and geometric operations in Grasshopper, showing the systematic parametric generation of façade modules.

Figure 5.7.2: Parametric workflow linking geometry with environmental analysis (Honeybee daylight simulations), demonstrating the direct connection between form and daylight metrics (sDA, ASE) and establishing iterative performance feedback.

Figure 6.1: Integrated workflow for façade optimization, combining environmental analysis, daylight simulations, evolutionary optimization, and final design refinement

Figure 6.2: Comparison diagram of deterministic optimization, machine learning, and evolutionary optimization approaches.

Figure 6.3.1: Conceptual diagram of the genetic algorithm workflow in Wallacei, illustrating population generation, daylight simulation, evaluation against LEED thresholds, selection, crossover, mutation, and convergence.

Figure 6.3.2: Wallacei setup in Grasshopper, showing the definition of objectives (maximize sDA, minimize ASE) and data connections for evolutionary optimization.

Figure 6.3.3: Wallacei control panel in Grasshopper, displaying the setup of evolutionary optimization parameters.

Figure 6.4.1.1: Simulation workflow showing calculation of daylight performance metrics (sDA and ASE) and their integration into Wallacei optimization. ing geometric parameters to performance metrics (sDA and ASE).

Figure 6.4.1.2: Export of optimization results into structured CSV datasets, enabling traceability and validation of daylight performance.

Figure 6.5: Subdivision strategy of the Montparnasse Tower façade, divided into 15 groups (5 vertical × 3 horizontal) to capture variations in solar exposure, with systematic group naming (e.g., S00–S12 for Southeast, N00–N12 for Northwest).

Figure 6.6.1: Pareto front diagram showing trade-offs between sDA and ASE across optimized solutions.

Figure 6.6.2: Example of Excel verification of Wallacei outputs, validating daylight performance results for façade groups.

Figure 6.7.1.1: Parametric setup in Grasshopper defining the two optimization variables: façade projection distance and window height ratio.

Figure 6.7.1.2: Illustrations façade modules generated by varying projection distance (30 cm–65 cm) and window height ratio (55%–95%), illustrating angular differences in geometry.

Figure 7.1.1. Facade Optimization Workflow

Figure 7.1.2. North-west selected facade shoebox

Figure 7.1.3 South-east selected facade shoebox

Figure 7.2.1. Impact of Window Height Ratio (WHR) on Geometry and User Experience

Figure 7.2.1.1.1. Example Wallacei result (S1-1) before design limitations

Figure 7.2.1.1.2. Example Wallacei result (S1-1) after design limitations  
 Figure 7.2.1.1.3. Filtered Wallacei results for S1-1 after design limitations  
 Figure 7.2.1.2.1. Example Wallacei result (S5-1) before design limitations  
 Figure 7.2.1.2.2. Example Wallacei result (S5-1) after design limitations  
 Figure 7.2.1.2.3. Filtered Wallacei results for S5-1 after design limitations  
 Figure 7.2.1.3.1. Example Wallacei result (N1-1) before design limitations  
 Figure 7.2.1.3.2. Example Wallacei result (N1-1) after design limitations  
 Figure 7.2.1.3.3. Filtered Wallacei results for N1-1 after design limitations  
 Figure 7.2.1.4.1. Example Wallacei result (N5-1) before design limitations  
 Figure 7.2.1.4.2. Example Wallacei result (N5-1) after design limitations  
 Figure 7.2.1.4.3. Filtered Wallacei results for N5-1 after design limitations  
 Figure 7.2.2. Spacing between module options  
 Figure 7.3 Study area (S1-1)  
 Figure 7.3.1.1.1. F01 Shoebox (S1-1) and Grasshopper Parameters  
 Figure 7.3.1.2.2. F02 Shoebox (S1-1) and Grasshopper Parameters  
 Figure 7.3.1.2.3. F01 and F02 (S1-1) Parameters and Daylight Result  
 Figure 7.3.1.2.4. F02 Generation's (S1-1) Parameters and Daylight Results  
 Figure 7.3.1.3.1. Regular Facade Modules (S1-1)  
 Figure 7.3.1.3.2. Regular Facade View (S1-1)  
 Figure 7.3.2.1.1. F03 Shoebox (S1-1) and Grasshopper Parameters  
 Figure 7.3.2.1.2. F03.1 Shoebox (S1-1) and Grasshopper Parameters  
 Figure 7.3.1.2.3. F03 and F03.1 (S1-1) Parameters and Daylight Result  
 Figure 7.3.2.2.1. Random Facade Modules (S1-1)  
 Figure 7.3.2.2.2. Random Facade View (S1-1)  
 Figure 7.3.3.1.1. F04 Shoebox (S1-1) and Grasshopper Parameters  
 Figure 7.3.3.1.2. F04 (S1-1) Parameters and Daylight Result  
 Figure 7.3.3.2.1. F05 Shoebox (S1-1) and Grasshopper Parameters  
 Figure 7.3.3.2.2. F04 and F05, F05.1 (S1-1) Parameters and Daylight Result  
 Figure 7.3.3.3.1. Wave Facade Modules (S1-1)  
 Figure 7.3.3.3.2. Wave Facade View (S1-1)  
 Figure 7.4. Study area (S5-1)  
 Figure 7.4.1.1.1. F01 Shoebox (S5-1) and Grasshopper Parameters  
 Figure 7.4.1.2.1. F02 Shoebox (S5-1) and Grasshopper Parameters  
 Figure 7.4.1.2.2. F01 and F02 (S5-1) Parameters and Daylight Result  
 Figure 7.4.1.2.3. F02 (S5-1) Parameters and Daylight Result  
 Figure 7.4.1.3.1. Regular Facade Modules (S5-1)  
 Figure 7.4.1.3.2. Regular Facade View (S5-1)  
 Figure 7.4.2.1.1. F03.1 Shoebox (S5-1) and Grasshopper Parameters  
 Figure 7.4.2.1.2. F03, F03.1 and F03.2 (S5-1) Parameters and Daylight Result  
 Figure 7.4.2.2.1. Random Facade Modules (S5-1)  
 Figure 7.4.2.2.2. Random Facade View (S5-1)  
 Figure 7.4.3.1.1. F04 Shoebox (S5-1) and Grasshopper Parameters  
 Figure 7.4.3.1.2. F04 (S5-1) Parameters and Daylight Result  
 Figure 7.4.3.2.1. F05 Shoebox (S5-1) and Grasshopper Parameters  
 Figure 7.4.3.2.2. F04 and F05, F05.1 (S5-1) Parameters and Daylight Result

Figure 7.4.3.3.1. Wave Facade Modules (S5-1)  
Figure 7.4.3.3.2. Wave Facade View (S5-1)  
Figure 7.5. North-west selected facade shoebox  
Figure 7.5.1.1.1 F01 Shoebox (N1-1 & N5-1) Grasshopper Parameters  
Figure 7.5.1.1.2. F01 and F02 (N1-1) Parameters and Daylight Result  
Figure 7.5.1.1.3. F01 and F02 (N5-1) Parameters and Daylight Result  
Figure 7.5.1.2.1. F02 Shoebox (N1-1 & N5-1) Figure 7.5.1.2.2. F02 Generation's (N1-1) Parameters and Daylight Result  
Figure 7.5.1.2.2. F02 Generation's (N1-1) Parameters and Daylight Result  
Figure 7.5.1.2.3. F02 Generation's (N5-1) Parameters and Daylight Result  
Figure 7.5.1.3.1. Regular Facade Modules (N1-1 & N5-1)  
Figure 7.5.1.3.2. Regular Facade View (N1-1 & N5-1)  
Figure 7.5.2.1 F03 Shoebox (N1-1 & N5-1) Grasshopper Parameters  
Figure 7.5.2.1.2. F03 (N1-1) Parameters and Daylight Result  
Figure 7.5.2.1.3 F03 (N5-1) Parameters and Daylight Result  
Figure 7.5.2.2.1. Random Facade Modules  
Figure 7.5.2.2.1. Random Facade Modules  
Figure 7.5.3.1.1. F04 Shoebox (N1-1 & N5-1) Grasshopper Parameters  
Figure 7.5.3.1.2. F04 and F04.1 (N1-1) Parameters and Daylight Result  
Figure 7.5.3.1.3. F04.1 (N5-1) Parameters and Daylight Result  
Figure 7.5.3.1.3. F04 and F04.1 (N5-1) Parameters and Daylight Result  
Figure 7.5.3.2.1. F05 Shoebox (N1-1 & N5-1) Grasshopper Parameters  
Figure 7.5.3.2.2. F05 and F05.1 (N1-1) Parameters and Daylight Result  
Figure 7.5.3.2.3. F05 and F05.1 (N5-1) Parameters and Daylight Result  
Figure 7.5.3.3.1 Wave Facade Modules (N1-1 & N5-1)  
Figure 7.5.3.3.2. Wave Facade View (N1-1 & N5-1)  
Figure 7.6.1.1. Regular façade alternatives: continuous vs. exposed frame  
Figure 7.6.1.2. Random façade alternatives: continuous vs. exposed frame  
Figure 7.6.1.3. Wave façade alternatives: continuous vs. exposed frame  
Figure 7.6.2. Compression Table  
Figure 8.2.1. Typical Office Floor Plan  
Figure 8.3.1. Schuco Selected Basic Modules  
Figure 8.4.1.2. Well thought-out system details enable reliable fabrication Figure  
Figure 8.4.1.1:25 Vertical Section Drawing  
Figure 8.4.2.1:50 Horizontal Section Drawing

